

FOR REFERENCE
NOT TO BE TAKEN FROM THIS ROOM

MEMRISTIVE SYSTEMS and
the USE of MEMRISTORS
in MODELING

by

Mustafa GÜNDÜZALP

Submitted to the Faculty of
Engineering for the Degree of
Master of Science in Electrical
Engineering

Bogazici University Library



39001100315673

14

Boğaziçi University

June - 1982

Acknowledgements:

I would like to thank my thesis supervisor, Prof.Dr.İ.Cem Gökner for his help and encouragement during this study. I would also like to thank Yardımcı Doç.Uğur Çilingiroğlu for his discussions of the transistor model.

Yaşamım boyunca bana her yönden destek olan Annem'e ve Babam'a
saygılarımla.....

ABSTRACT

In the past years many developments have been observed and so many devices have been invented. The design of new systems using these devices are becoming more and more important. Moreover nonlinear behaviours of these devices and systems necessitate knowledge of nonlinear circuit theory.

In this thesis, memristor which is introduced as the fourth basic circuit element into nonlinear circuit theory, and memristive systems which are the generalization of memristors into a special class of dynamical systems have been considered. And examples of applications are also given. Finally a new model of bipolar junction transistors is presented and the theoretic proof the model has also been given.

ÖZETÇE

Geçtiğimiz yıllarda Elektrik Mühendisliği Biliminde birçok gelişmeler gözlenmiş; ve birçok yeni devre elemanı icat edilmiştir. Bu elemanlar, yeni sistemlerin tasarımında yaygın olarak kullanılmaya başlanmıştır. Ayrıca bu yeni icat edilen devre elemanlarının birçoğunun davranışları doğrusal değildir. Dolayısıyla bu sistemlerin incelenmesi doğrusal olmayan devre teorisini gündeme getirmektedir.

Bu tezde doğrusal olmayan devre teorisine dördüncü temel eleman olarak giren hafıza-dirençler, bunların bir genellemesi olan hafıza-dirençsel sistemler gözden geçirildi ve uygulama örnekleri sunuldu. Son olarakta bu eleman kullanılarak yeni bir transistor modeli geliştirildi ve modelin ispatı yapıldı.

| | | |
|------|---|-----|
| I- | Introduction. | 1 |
| II- | Memristor | 2 |
| | 1- Definition and Basic Properties. | 2 |
| | 2- An Electromagnetic Interpretation of Memristor Definition. | 8 |
| | 3- Mechanical Analogue of Memristor. | 11 |
| III- | Realization of Memristors. | 16 |
| | 1- Realizability Conditions. | 16 |
| | 2- Mutators | 17 |
| | 3- Active Circuit Realization. | 19 |
| IV- | Memristive Systems. | 24 |
| | 1- Definition of Memristive Systems. | 24 |
| | 2- Generic Properties of Memristive One-Ports. | 26 |
| | 3- A Canonical Model for Memristive One-Ports. | 38 |
| V- | Device Modeling Using Memristors and Examples. | 51 |
| VI- | A Model of the Bipolar Junction Transistor Using Memristors. | 75 |
| | 1- Preliminary Studies. | 75 |
| | 2- Construction of the Model. | 87 |
| | 3- Justification of the Model. | 90 |
| | 4- Remarks on the Model. | 105 |
| VII- | Conclusion. | 107 |
| | References. | 109 |

C H A P T E R I

INTRODUCTION

In the recent years, many new developments have been observed in the field of Electrical Engineering Science, and many new devices have been invented. These devices are becoming more and more important in the design of new systems. The analysis and the synthesis of these systems and the modeling of the newly invented devices bring the tools of nonlinear circuit theory into consideration, since the behaviours of most of these devices are nonlinear.

This thesis is going to deal with the new born, basic, two-terminal element of the nonlinear circuit theory, namely the memristor. In Chapter II, the definition and basic properties of memristors are given. The electromagnetic interpretation of the element and its mechanical analogy is also presented. In Chapter III the realization of the memristor is considered. Though it is postulated as a two terminal basic circuit element, the memristor is realized using mutator, a two-port element, which in turn requires active elements for its realization. In Chapter IV, the memristive systems which are a generalization of the memristor concept are studied. The properties which distinguish them from the other systems are given. Several existing memristive systems such as thermistors, discharge tubes are also presented.

Applications of the memristor to device modeling is the subject of Chapters V and VI. The junction diode model using memristor is the main subject of Chapter V, whereas the model of a bipolar junction transistor presented in Chapter VI is new. First, necessary preliminary studies are carried on and then the model is constructed and justified in Chapter VI.

CHAPTER II

MEMRISTOR

II.1- DEFINITION AND BASIC PROPERTIES

Let's consider four basic electrical variables, namely flux, charge, voltage and current. Out of six possible binary relationships of these four variables five lead to well known relationships. Three of them are the axiomatic definition of

classical circuit element. i.e. They are the

definitions of resistor ($f_R(i,v)=0$), capacitor

($f_C(v,q)=0$) and inductor ($f_L(\psi,i)=0$). The other two are operational i.e.

$$\psi(t) = \int_{-\infty}^t v(\tau) d\tau \quad \text{and} \quad q(t) = \int_{-\infty}^t i(\tau) d\tau.$$

From a logical point of view there is a missing relationship between flux and charge. In 1971 Chua postulated a fourth basic two-terminal circuit element for the completeness of the figure [1].

The name memristor is given to this new circuit element, which is a contraction from "memory resistor". And the proposed symbol is shown in figure II.2. Although we don't have a memristor in the form of a passive physical device yet, there are some active circuit realizations of the device. This will be covered in the chapter III.

Now let's see the basic properties of the memristor.

By definition a memristor is characterized by a relation of the type $g(\psi,q)=0$; it is said to be charge (flux) controlled if this relation can be expressed as a single-valued function of charge q

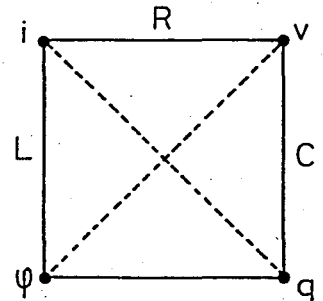


Figure II.1

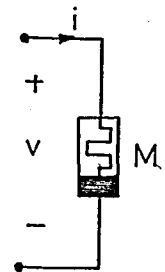


Figure II.2

(flux ψ). Then the voltage (current) developed across the device can be written as

$$v(t) = M(q(t)) i(t) \text{ or } \frac{d\psi(t)}{dt} = \frac{d\psi(q)}{dq} \cdot \frac{dq(t)}{dt} \quad (\text{II.1})$$

$$\left(i(t) = W(\psi(t)) v(t) \text{ or } \frac{dq(t)}{dt} = \frac{dq(\psi)}{d\psi} \cdot \frac{d\psi}{dt} \right) (\text{II.2})$$

Since $M(q)(W(\psi))$ has the unit of resistance (conductance) it's called incremental memristance (mductance). We also see from equation II.1 that the value of the incremental memristance at any time t depends on $q(t)$ and since $q(t) = \int_{-\infty}^t i(t') dt'$, it depends upon the integral of memristor current from $t = -\infty$ to t , we observe that the value of the memristance depends on the complete past history of its current (voltage) and this is why the name memory-resistor is given to the element. Note also that once the voltage of a memristor is specified it behaves like a linear time-varying resistor. In the special case when the ψ - q curve is a straight line the memristor reduces to a linear time-invariant resistor. Hence there is no need of introducing the memristor into linear network theory.

What was said before was that, there was no memristor in the form of a passive physical device. The following theorem may be thought as a criterion for the class of memristors which may be discovered in a pure device form without internal power supply.

Theorem II.1: Passivity Criterion.

A memristor characterized by a differentiable charge-controlled ψ - q curve is passive if and only if, its incremental memristance $M(q)$ is nonnegative i.e. $M(q) \geq 0$.

Proof:

The instantaneous power dissipated by a memristor is given by

$$p(t) = v(t) \cdot i(t) = M(q(t)) (i(t))^2 \quad (\text{II.3})$$

if $M(q(t)) \geq 0$ then $p(t) \geq 0$ and memristor is obviously passive.

Suppose there is a point q_0 on ψ - q curve such that $M(q_0) < 0$. Then the differentiability of the ψ - q curve implies that there exists an $\epsilon > 0$ such that $M(q_0 + \Delta q) < 0$, $|\Delta q| < \epsilon$. Now if we drive the memristor with a current source $i(t)$ which is zero for $t \leq t_0$ and such that $q(t) = q_0 + \Delta q(t)$ for $t \geq t_0$, then since for this current $M(q_0 + \Delta q) < 0$ and since $p(t) = M(q(t))i(t) \leq 0$ and $\int_{-\infty}^t p(\tau) d\tau < 0$ for sufficiently large t , then memristor is active. Hence the conclusion follows.

This criterion shows that only memristors which have monotonically increasing ψ - q curves can exist in the form of a passive device.

Theorem II.2: Closure Theorem.

A one-port containing only memristors is equivalent to a memristor.

Proof:

Let i_j, v_j, q_j and ψ_j denote the current voltage, charge and flux-linkage of the j 'th memristor. Where $j=1, \dots, b$ and i and v denote the port current and voltages. We can write $(n-1)$ linearly independent Kirchhoff current law equations where n is the total number of nodes and b is the total number of memristors. More explicitly KCL eq's are

$$a_{j0}i + \sum_{k=1}^b a_{jk}i_k = 0 \quad j=1,2,\dots, n-1 \quad (II.4)$$

Similarly we can write $(b-n+2)$ linearly independent Kirchhoff voltage law equations.

$$\beta_{j0}v + \sum_{k=1}^b \beta_{jk}v_k = 0 \quad j=1,2,\dots, b-n+2 \quad (II.5)$$

where a_{jk}, β_{jk} are either 1, -1, or 0.

Now let's integrate these equations with respect to time

$$a_{j0} \int_{-\infty}^t i(t') dt' + \int_{-\infty}^t \left(\sum_{k=1}^b a_{jk} i_k(t') \right) dt' = 0 \quad \text{to obtain}$$

$$a_{j0}q + \sum_{k=1}^b a_{jk}q_k = Q_j \quad j=1,2,\dots, n-1 \quad (II.6)$$

and
$$\beta_{j0} \int_{-\infty}^t v(t') dt' + \int_{-\infty}^t \left(\sum_{k=1}^b \beta_{jk} v_k(t') \right) dt' = 0 \quad \text{to obtain}$$

$$\beta_{j0}\psi + \sum_{k=1}^b \beta_{jk}\psi_k = \Phi_j \quad j=1,2,\dots, b-n+2 \quad (\text{II.7})$$

if we also assume that memristors are charge-controlled then

$$\beta_{j0}\psi + \sum_{k=1}^b \beta_{jk}\psi_k(q_k) = \Phi_j \quad (\text{II.8})$$

These equations (II.6) and (II.8) constitute a system of (b+1) independent nonlinear functional equation in (b+2) unknowns, solving for ψ we obtain a relation $f(q, \psi) = 0$

Theorem II.3: Existence and Uniqueness Theorem.

Any network containing only memristors with positive incremental memristances has one, and only one solution. The proof of the theorem will not be given here. See [11] .

Theorem II.4: Principle of Stationary Action (Coaction).

A vector $\underline{q}_L = \underline{Q}_L$ ($\underline{\psi}_J = \underline{\Phi}_J$) is a solution of a network N containing only charge-controlled (flux-controlled) memristor, if and only if it is a stationary point of the total action $R(\underline{q}_L)$ associated with N. i.e. the gradient of $R(\underline{q}_L)$ ($\hat{R}(\underline{\psi}_J)$) evaluated at \underline{Q}_L ($\underline{\Phi}_J$) is zero.

$$\left. \frac{\partial R(\underline{q}_L)}{\partial \underline{q}_L} \right|_{\underline{q}_L = \underline{Q}_L} = 0 \quad \left(\left. \frac{\partial \hat{R}(\underline{\psi}_J)}{\partial \underline{\psi}_J} \right|_{\underline{\psi}_J = \underline{\Phi}_J} = 0 \right) \quad (\text{II.9})$$

Before the proof of the theorem let's define the necessary concept

Definition II.1:

The action (coaction) associated with a charge (flux-controlled) memristor is defined to be the integral

$$A(q) = \int_0^q \psi(x) dx \quad \left(\hat{A}(\psi) = \int_0^\psi q(x) dx \right) \quad (\text{II.10})$$

Let's now consider a pure memristor network N containing n nodes and b branches. Let \mathcal{T} be a tree and \mathcal{L} its associated cotree Let's label the branches consecutively starting with the tree elements and define.

$$\underline{\psi} = (\psi_1, \psi_2, \dots, \psi_b)^t, \quad \underline{q} = (q_1, q_2, \dots, q_b)^t$$

$$\underline{\psi}_{\sim j} = (\psi_1, \psi_2, \dots, \psi_{n-1})^t \text{ and } \underline{q}_{\sim \ell} = (q_n, \dots, q_b)^t$$

We know also that $\underline{\psi}_j$ or $\underline{q}_{\sim \ell}$ constitutes a complete set of variables in the sense that $\underline{\psi} = D^t \underline{\psi}_j$ and $\underline{q} = B^t \underline{q}_{\sim \ell}$ where D and B are the fundamental cut-set matrix and the fundamental loop matrix, respectively.

Definition II.2:

Total action (coaction) associated with a network containing only charge-controlled (flux-controlled) memristors is defined to be the scalar function

$$\mathcal{R}(\underline{q}_{\sim \ell}) = A_0(B^t \underline{q}_{\sim \ell}) \left(\hat{\mathcal{R}}(\underline{\psi}_j) = \hat{A}_0(D^t \underline{\psi}_j) \right) \quad (II.11)$$

$$A = A(\underline{q}) = \sum_{j=1}^b A_j(q_j) = \sum_{j=1}^b \int_0^{q_j} \psi_j(q_j) dq_j \quad (II.12)$$

$$\left(\hat{A} = \hat{A}(\underline{\psi}) = \sum_{j=1}^b \hat{A}_j(\psi_j) = \sum_{j=1}^b \int_0^{\psi_j} q_j(\psi_j) d\psi_j \right)$$

and o denotes the composition operation. Now we have the mathematical tools to prove the theorem.

Proof of Theorem II.4:

$$\frac{\partial \mathcal{R}(\underline{q}_{\sim \ell})}{\partial \underline{q}_{\sim \ell}} = \frac{\partial A_0(B^t \underline{q}_{\sim \ell})}{\partial \underline{q}_{\sim \ell}} = B \frac{\partial A(\underline{q})}{\partial \underline{q}} \Big|_{\underline{q} = B^t \underline{q}_{\sim \ell}} = B \underline{\psi}_0(B^t \underline{q}_{\sim \ell}) \quad (II.13)$$

But as $B \underline{\psi}_0(B^t \underline{q}_{\sim \ell})$ is nothing but KVL in terms of \mathcal{L} , any vector \underline{Q} is a solution of N if, and only if it is a stationary point of $\mathcal{R}(\underline{q}_{\sim \ell})$.

The above theorems are concerned with the networks composed of only memristors. Now a more general theorem for networks containing resistors, capacitors, inductors and memristors will be given. In most cases the governing equations of this kind of networks take the form of a system of m-first order nonlinear differential equation in the form

$\dot{\underline{x}} = f(\underline{x}, t)$ where \underline{x} is an $m \times 1$ vector whose components are called state variables. The number m is called the "order of complexity" and is equal to the maximum number of independent initial conditions that can be specified arbitrarily.

Theorem II.5: Order of Complexity:

Let N be a network containing resistors, inductors, capacitor, memristors, independent voltage sources and independent current sources. An upper bound for the order of complexity m of N is given by

$$m = (b_L + b_C + b_M) - (n_M + n_{CE} + n_{LM}) - (\hat{n}_M + \hat{n}_{LJ} + \hat{n}_{CM}) \quad (II.14)$$

where b_L, b_C, b_M are total number of inductors, capacitors and memristors respectively ; n_M is the number of independent loops containing only memristors, n_{CE} is the number of independent loops containing only capacitors and voltage sources, n_{LM} is the number of independent loops containing only inductors and memristors, \hat{n}_M is the number of independent cut sets containing only memristors, \hat{n}_{LJ} is the number of independent cut sets containing only inductors and current sources, \hat{n}_{CM} is the number of independent cut sets containing only capacitors and memristors.

Proof:

The order of complexity of an RLC network is given by $m = (b_L + b_C) - (n_{CE}) - (\hat{n}_{LJ})$. For an RLC-Memristor network with $n_M = n_{LM} = \hat{n}_M = \hat{n}_{CM} = 0$ each memristor introduces a new state variable and we have $m = (b_L + b_C + b_M) - n_{CE} - \hat{n}_{LJ}$.

Observe next that a constraint among the state variables occurs whenever an independent loop consisting of elements corresponding to those specified in the definition of n_M and n_{LM} is present in the network. And similarly there will be a constraint among the state variables whenever an independent cut-set consisting of the elements corresponding to those specified in the definition of \hat{n}_M and \hat{n}_{CM} is present in the network. Since each constraint removes one degree of freedom the order complexity must be reduced by one.

II.2- AN ELECTROMAGNETIC INTERPRETATION OF MEMRISTOR DEFINITION.

We know that the circuit theory is a special case of electromagnetic field theory. Particularly the three classical circuit elements (resistor, capacitor, inductor) can be given a good electromagnetic interpretation in terms of the quasi-static expansion of Maxwell equations. Now we will give an electromagnetic field interpretation of memristor analogous to that of other basic circuit elements. First, Let's write down the Maxwell equations.

$$\text{Curl } \vec{E} = - \frac{\partial \vec{B}}{\partial t} \quad (\text{II.15})$$

$$\text{Curl } \vec{H} = \vec{J} + \frac{\partial \vec{D}}{\partial t} \quad (\text{II.16})$$

where \vec{E} , \vec{H} are the electric and magnetic field intensity, \vec{D} , \vec{B} are the magnetic field density and \vec{J} is the current density.

Defining $\tau = \alpha t$ as the family time where α is called the time-rate parameter, the Maxwell equations become

$$\text{Curl } \vec{E} = -\alpha \frac{\partial \vec{B}}{\partial \tau} \quad (\text{II.17})$$

$$\text{Curl } \vec{H} = \vec{J} + \alpha \frac{\partial \vec{B}}{\partial \tau} \quad (\text{II.18})$$

\vec{E} , \vec{H} , \vec{D} , \vec{B} and \vec{J} in these equations are functions of both the position (x, y, z) and of α, τ . Let's expand the vector quantities in power series in α and substitute them into the equations. Upon equating the coefficients of α^n obtain the n^{th} order Maxwell's equations where $n=0, 1, 2, \dots$

For example if $\vec{E} = \alpha^n \vec{E}_n + \alpha^{n-1} \vec{E}_{n-1} + \dots + \alpha \vec{E}_1 + \vec{E}_0$, then zero, first, second order Maxwell equations can be written as follows.

Zero-order Maxwell equations:

$$\text{Curl } \vec{E}_0 = \vec{0} \quad (\text{II.19})$$

$$\text{Curl } \vec{H}_0 = \vec{J}_0 \quad (\text{II.20})$$

First-order Maxwell equations :

$$\text{Curl } \vec{E}_1 = - \frac{\partial \vec{B}_0}{\partial \tau} \quad (\text{II.21})$$

$$\text{Curl } \vec{H}_1 = \vec{J}_1 + \frac{\partial \vec{D}_0}{\partial \tau} \quad (\text{II.22})$$

Second-order Maxwell equations :

$$\text{Curl } \vec{E}_2 = - \frac{\partial \vec{B}_1}{\partial \tau} \quad (\text{II.23})$$

$$\text{Curl } \vec{H}_2 = \vec{J}_2 + \frac{\partial \vec{D}_1}{\partial \tau} \quad (\text{II.24})$$

and so on.

Many electromagnetic phenomena and systems can be analyzed satisfactorily by using only the zero-order and first order Maxwell equations. The corresponding solutions are called quasi-static Maxwell equations [2]. For example a resistor can be identified as an electromagnetic system whose first-order fields are negligible as compared with the zero-order fields. So the resistor is interpreted as an instantaneous relationship between \vec{E}_0 and \vec{H}_0 . When only the first-order magnetic field is negligible the electromagnetic system can be interpreted as an inductor in series with a resistor. Similarly when only the first-order electric field is negligible the system can be interpreted as a capacitor in parallel with a resistor. But the case that both first-order fields are not negligible has been omitted in the studies as having no correspondance in circuit theory.

It is suggested, that this case is precisely the one that gives rise to the characterization of a memristor. Under appropriate conditions the instantaneous value of the first-order electric flux-density \vec{D}_1 (surface integral of \vec{D}_1 is proportional to $q(t)$) is related to the instantaneous value of the first-order magnetic flux-density \vec{B}_1 (surface integral of \vec{B}_1 is proportional to $\varphi(t)$). This would be the case if we postulate the existence of a two-terminal device with the following properties. a) zero-order fields are negligible as compared to first-order fields. i.e. $\vec{J} \approx \vec{J}_1$, $\vec{E} \approx \vec{E}_1$, $\vec{H} \approx \vec{H}_1$, $\vec{B} \approx \vec{B}_1$, $\vec{D} \approx \vec{D}_1$.

b) The material from which the device is made is nonlinear. More generally we have the following nonlinear relationships

$$\vec{J}_1 = \mathcal{J}(\vec{E}_1) \quad (\text{II.25})$$

$$\vec{B}_1 = \mathcal{B}(\vec{H}_1) \quad (\text{II.26})$$

$$\vec{D}_1 = \mathcal{D}(\vec{E}_1) \quad (\text{II.27})$$

where $\mathcal{J}(\cdot)$, $\mathcal{B}(\cdot)$, $\mathcal{D}(\cdot)$ are one-to-one continuous functions from \mathbb{R}^3 to \mathbb{R}^3 . Under these assumptions the equations II.22 and II.25 can be combined to give.

$$\text{Curl } \vec{H}_1 = \mathcal{J}(\vec{E}_1) \quad (\text{II.28})$$

Observe that II.28 does not contain any time derivative. Hence, under any specified boundary condition appropriate for the device, \vec{E}_1 is related to \vec{H}_1 by a functional relation namely

$$\vec{E}_1 = f(\vec{H}_1) \quad (\text{II.29})$$

if we substitute into $\vec{D}_1 = \mathcal{D}(\vec{E}_1)$ and using $\vec{B}_1 = \mathcal{B}(\vec{H}_1)$

we obtain

$$\vec{D}_1 = \mathcal{D} \circ f \circ [\mathcal{B}^{-1}(\vec{B}_1)] = g(\vec{B}_1) \quad (\text{II.30})$$

This specifies the instantaneous relationship between \vec{D}_1 and \vec{B}_1 which can be interpreted as the quasi-static representation of the memristor in terms of electromagnetic quantities. If we summarize the above interpretation of the memristor, the physical mechanism characterizing the device must come from the instantaneous interaction between the first-order electric field and the first-order magnetic field. We see from the interpretation that the physical memristor device must essentially be an ac. device otherwise its associated dc electromagnetic fields give rise to nonnegligible zero-order fields. This is consistent with the circuit-theoretic properties of the memristor, a dc current source would give rise to an infinite charge $q(q(t) \rightarrow \infty \text{ as } t \rightarrow \infty)$

and a dc voltage source would give rise to an infinite flux ($\psi(t) \rightarrow \infty$ as $t \rightarrow \infty$)

II.3- MECHANICAL ANALOGUE OF MEMRISTOR

What we considered so far is the memristor as an electrical device. But as in the case of other circuit elements the memristor also has analogues from other systems. [3]

Now let's consider the mechanical systems. In this case, what we have as basic variables are the velocity(e), displacement(q), force(f) and momentum(p). Again we can relate these variables to each other in 6 ways as in the case of electrical variables,

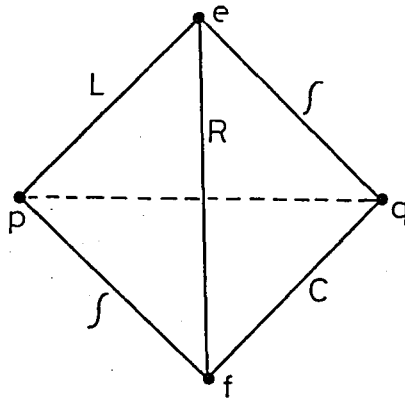


Figure II.3

explicitly two of these 6 relations are the definitions of displacement,

$$q(t) = q(0) + \int_0^t e(\tau) d\tau$$

and of momentum

$$p(t) = p(0) + \int_0^t f(\tau) d\tau$$

three of them are the constitutive relations of energy storage and dissipation elements.

$$F_C (f, q) = 0 \tag{II.31}$$

$$F_L (e, q) = 0 \tag{II.32}$$

$$F_R(e, f) = 0 \quad (II.33)$$

But, there is one missing constitutive relation relating p and q (which was drawn as hidden line by Paynter in 1961). This fourth constitutive relation can be defined as

$F_m(q, p) = 0$, and called as "memristor" i.e. memory resistor since it remembers both integrated flow(q) and integrated effort(p).

The constitutive relation for a 1-port memristor is a curve in the q - p plane. Depending on whether the memristor is displacement or momentum controlled the constitutive relation can be expressed as

$$p = G(q) \quad \text{or} \quad \text{as} \quad q = F(p) \quad (II.34)$$

differentiating with respect to time we obtain

$$\dot{p} = \frac{\partial G(q)}{\partial q} \cdot \frac{dq}{dt}, \quad f = M(q)e \quad (II.35)$$

$$\dot{q} = \frac{\partial F(p)}{\partial p} \cdot \frac{dp}{dt}, \quad e = W(p)f \quad (II.36)$$

$M(q)$: is called the incremental memristance.

$W(p)$: is called the incremental memductance.

We see that dynamically the memristor appears as either a displacement or momentum-modulated resistor. In the case of linear constitutive relation (i.e. $M = \text{constant}$, $W = \text{constant}$) the memristor appears as an ordinary resistor. So memristors have a meaning only for nonlinear systems.

To distinguish a memristor from a resistor, let's consider the tapered dashpot shown in the figure II.4. If we attempt to model the device on the e - f plane as a resistor we will not obtain a unique constitutive relation $F(e, f) = 0$, but rather some hysteretic behaviour,

since the incremental resistance depends on the instantaneous piston displacement. We may attempt to model the device as a modulated resistor, taking the state variable x as parameter in the constitutive relation. However x is not a defined state variable for any element in the system.



Figure II.4

What is required is the displacement of the dashpot. But modeling the system as a memristor eliminates the cumbersome modulation and permits us to characterize the device as a single curve in x - p plane.

Example:

Now let's study the mechanical system mentioned above in some detail. The mechanical system can be considered a crude model of an automobile suspension using a shock absorber whose characteristic depend on displacement. The schematic diagram of the mechanical suspension system is shown in figure II.5.

The mass could represent the mass of the car, the spring and dashpot its suspension system, and the velocity source the input due to undulations in the road.

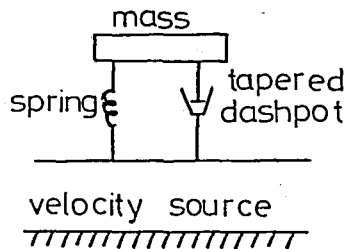


Figure II.5

The bond-graph, with the tapered dashpot as a memristor can be drawn as follows.

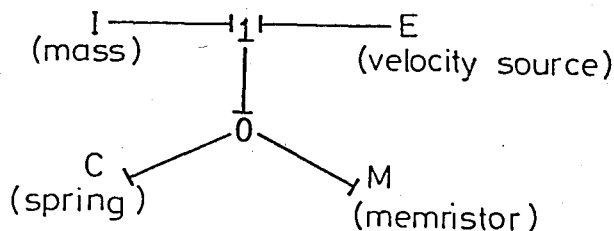


Figure II.6

Particularly for this system, it is also possible to represent the tapered dashpot as a modulated resistor since the displacement of the dashpot is the same as the displacement of the spring and proportional to the force in the spring. The bond-graph for this system is the following.

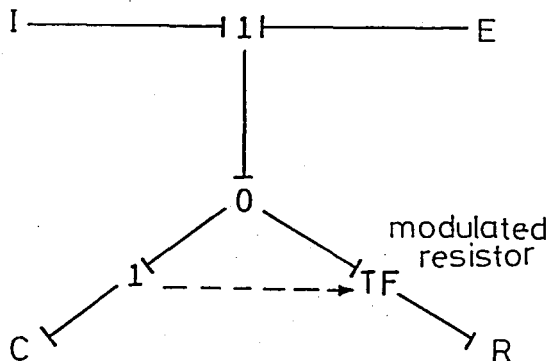


Figure II.7

But the bond graph with the memristor uses fewer elements and avoids the necessity of defining a different kind of bond (dashed bond for modulation).

Let's define the p-q relation for a dashpot as following and let's draw it in the p-q plane.

$$p = \text{sign}(q) \cdot (\text{Absolute}(q))^n \quad (\text{II.37})$$

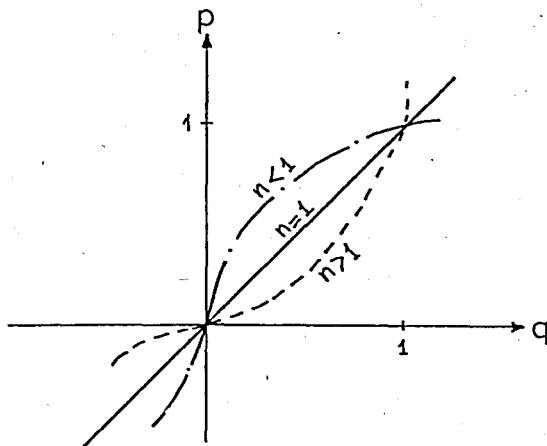


Figure II.8

The responses of the suspension system to a sinusoidal forcing velocity taking the tapered dashpot as a memristor that has the p-q relation as defined in the above equation II.37 are shown in the figure II.9 for different n's.

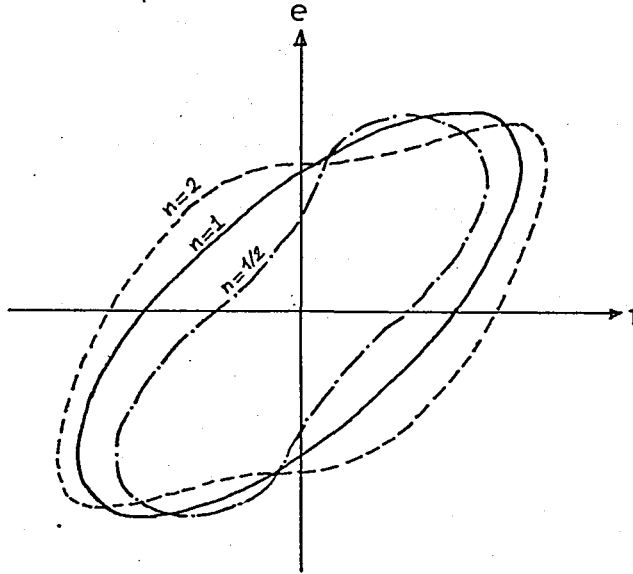


Figure II.9

It is said that these results are consistent with those obtained using the modulated resistor instead of memristor [3].

The case $n=1$ corresponds to an ordinary linear dashpot and its state-plane trajectory is an ellipse. The other two trajectories are non-elliptical, indicating that the nonlinear p-q relation causes frequencies other than the forcing frequency to appear in the output. The presence of these harmonics is typical of nonlinear systems. The slopes of the trajectories near the velocity axis (for spring force close to zero) shows the characteristics of the displacement modulated dashpot; for $n=2$ the dashpot is very soft around its center and the trajectory shows this property being nearly horizontal. On the other hand for $n = \frac{1}{2}$ the dashpot is very stiff near the center and its trajectory is very steep. (Theoretically for $n = \frac{1}{2}$ the slope is infinite at the origin. Use of finite-difference solution, however replaces the infinite slope with large but finite slope near the origin, which is a much more realistic situation.

C H A P T E R I I I
R E A L I Z A T I O N O F M E M R I S T O R S

I I I . 1 - R E A L I Z A B I L I T Y C O N D I T I O N S .

As stated before, a memristor in the form of a physical device without an internal power supply has not yet been discovered, but there are some active circuit realizations. In this section the realization of a memristor will be investigated.

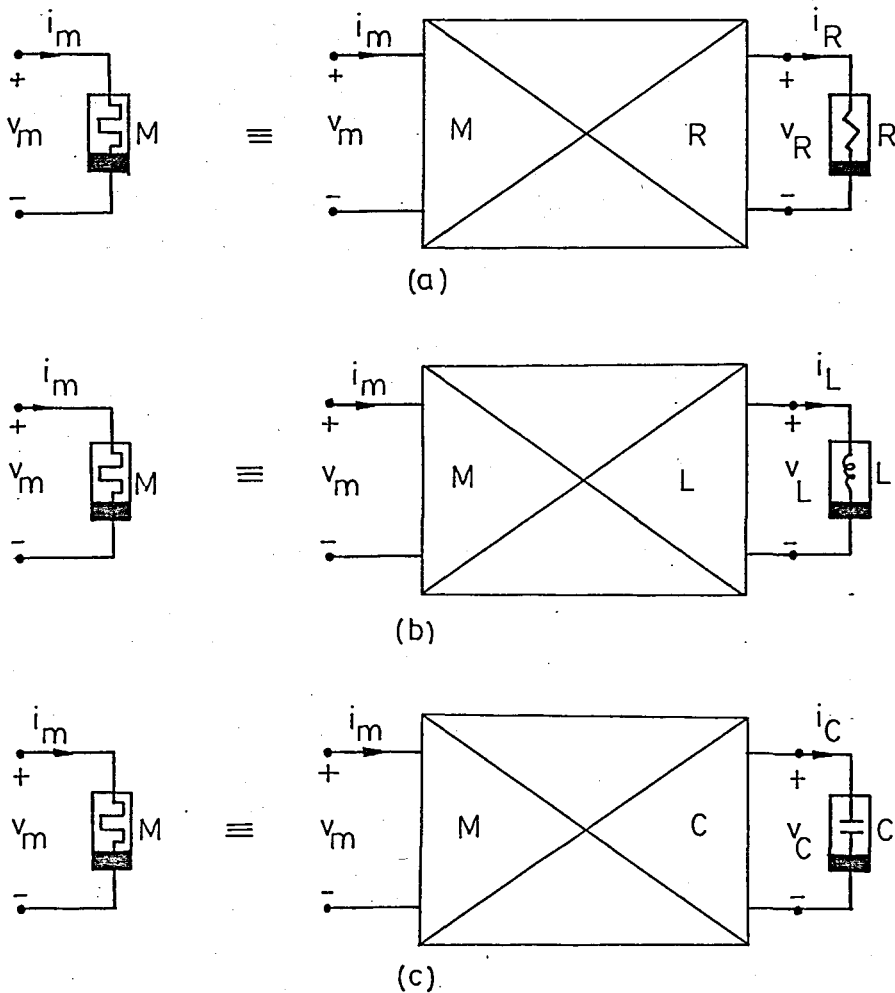


Figure III.1.

The passivity theorem II.1 shows that only memristors characterized by a monotonically increasing φ - q curve can exist in a device form without internal power supplies. But using a mutator a memristor with any prescribed φ - q curve can be realized by connecting an appropriate nonlinear resistor, inductor or capacitor across port-2 of an M-R, M-L or M-C mutator respectively as shown in figure III.1.

Now mutators will be defined and discussed in some detail.

III.2- MUTATORS

Mutator is a generic name for a family of linear algebraic 2-ports [4], [5]. A type 1 L-R mutator is characterized by the constitutive relation $\varphi_1 = v_2$ and $i_1 = -i_2$. If we terminate port-2 by a resistor having

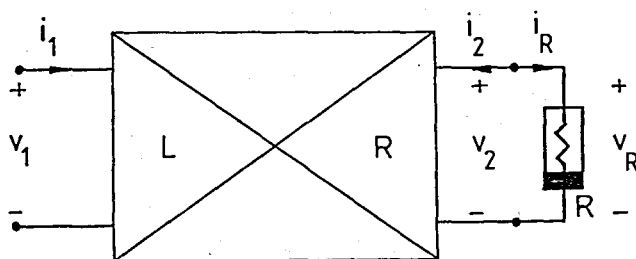


Figure III.2

a constitutive relation $i_R = g(v_R)$ then from figure III.2 and using the mutator constitutive relation we can write the following equations

$$v_2 = v_R, \quad i_2 = -i_R, \quad \varphi_1 = v_2, \quad i_1 = -i_2,$$

combining these equation

$$i_1 = -i_2 = i_R = g(v_R) = g(v_2) = g(\varphi_1)$$

we can obtain the equation

$$i_1 = g(\varphi_1)$$

In other words, the port-1 is equivalent to an inductor which is characterized by a constitutive relation identical to that of the

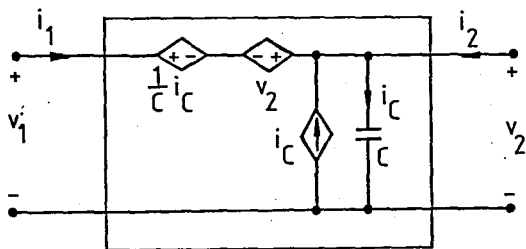
resistor connected to port-2. Conversely, if we terminate port-1 by an inductor having a constitutive relation $f(i_2, \psi_2)=0$ then what we observe from port-2 is a resistor having a constitutive relation $f(i_2, v_2)=0$.

This shows us that this 2-port transforms one type of element into another type element, and reveals the reason why the 2-port is called mutator.

A type-2 L-R mutator is characterized by the constitutive relation $\psi_1 = -i_2$ and $i_1 = v_2$. The same mutation property also holds in this case, except that the two variables in the resulting element are interchanged i.e. when we connect a resistor characterized by a constitutive relation $i_R = f(v_R)$ across port-2 of a type 1 L-R mutator we get an inductor having a constitutive relation $i_1 = f(\psi_1)$ but in the case of type 2 L-R mutator we get $\psi_1 = f(i_1)$.

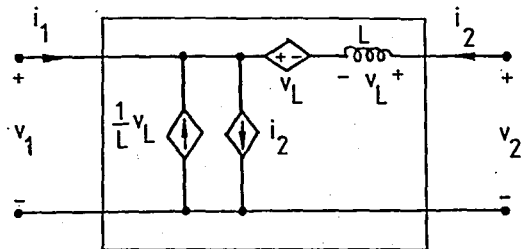
Similarly we can define other mutators namely L-C, C-R, M-R, M-C, M-L mutators.

We observe that by using different mutators, it is possible to synthesize any three of the four basic circuit elements R,L,C,M given the fourth element. Since mutators are linear 2-ports, they can be realized using only linear elements. For example a type 1 L-R mutator and type 1 C-R mutators can be synthesized by the circuits given in figure III.3.



Type 1 L-R mutator

(a)



Type 1 C-R mutator

(b)

Figure III.3

III.3- ACTIVE CIRCUIT REALIZATION

A memristor with a prescribed ψ - q curve can be realized using a M-R, M-C or M-L mutator. Characterization and realization of these mutators are given in table I.

Since it is easier to synthesize a nonlinear resistor with a prescribed v - i curve, only memristors realized with M-R mutators are studied. Practical active circuit realization of a type 1 M-R mutator is given in figure III.4. In order to verify that a memristor is indeed

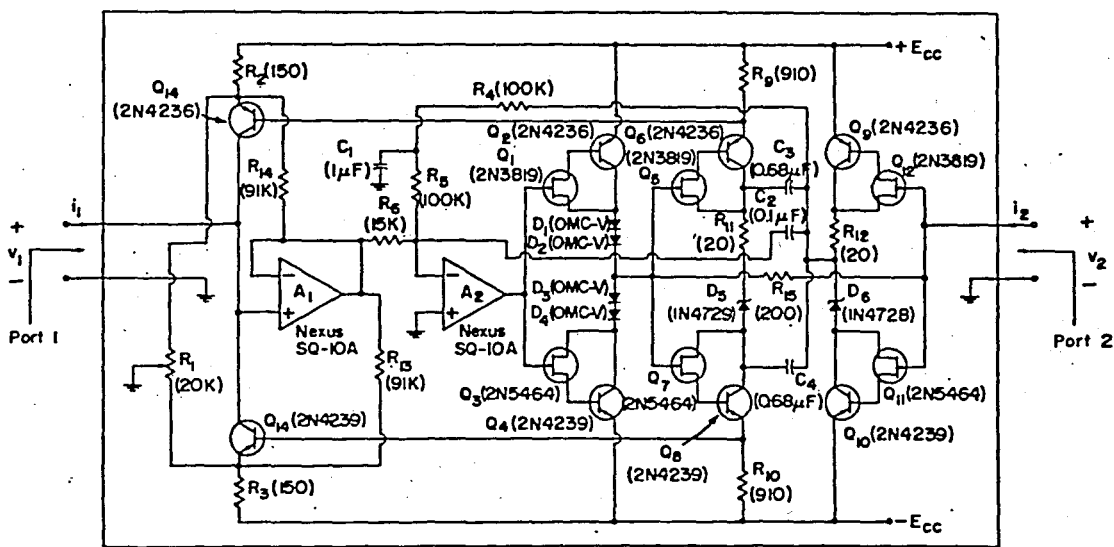


Figure III.4

realized across port 1 of an M-R mutator when a nonlinear resistor is connected across port-2 it will be necessary to use a ψ - q curve tracer. For more detail of the ψ - q curve tracer see [1]. Using this tracer the ψ - q curves of memristors realized by a type 1 M-R mutator and the corresponding V - I curves of nonlinear resistors are given in figure III.5.

TABLE I
CHARACTERIZATION AND REALIZATION OF M-R, M-L, AND M-C MUTATORS

| | TYPE | SYMBOL AND CHARACTERIZATION | TRANSMISSION MATRIX $\begin{bmatrix} V_1 \\ I_1 \end{bmatrix} = T(p) \begin{bmatrix} V_2 \\ -I_2 \end{bmatrix}$ | BASIC REALIZATIONS USING CONTROLLED SOURCES | |
|-------------|------|--|--|---|-------------------|
| M-R MUTATOR | 1 | $(q, \varphi) \leftrightarrow (i_R, v_R)$ $v_1 = \frac{dv_2}{dt}$ $i_1 = -\frac{di_2}{dt}$ | $T_{MR_1}(p) = \begin{bmatrix} p & 0 \\ 0 & p \end{bmatrix}$ | REALIZATION 1 | REALIZATION 2 |
| | 2 | $(q, \varphi) \leftrightarrow (v_R, i_R)$ $v_1 = -\frac{di_2}{dt}$ $i_1 = \frac{dv_2}{dt}$ | $T_{MR_2}(p) = \begin{bmatrix} 0 & p \\ p & 0 \end{bmatrix}$ | REALIZATION 1 | REALIZATION 2 |
| M-L MUTATOR | 1 | $(q, \varphi) \leftrightarrow (i_L, \varphi_L)$ $v_1 = v_2$ $i_1 = -\frac{di_2}{dt}$ | $T_{ML_1}(p) = \begin{bmatrix} 1 & 0 \\ 0 & p \end{bmatrix}$ (Identical to $T_{CR_1}(p)$ of a Type 1 C-R MUTATOR) | REALIZATION 1 | REALIZATION 2 |
| | 2 | $(q, \varphi) \leftrightarrow (\varphi_L, i_L)$ $v_1 = -\frac{di_2}{dt}$ $i_1 = v_2$ | $T_{ML_2}(p) = \begin{bmatrix} 0 & p \\ 1 & 0 \end{bmatrix}$ (Identical to $T_{LR_2}(p)$ of a Type 2 L-R MUTATOR) | REALIZATION 1 | REALIZATION 2 |
| M-C MUTATOR | 1 | $(q, \varphi) \leftrightarrow (q_C, v_C)$ $v_1 = \frac{dv_2}{dt}$ $i_1 = -i_2$ | $T_{MC_1}(p) = \begin{bmatrix} p & 0 \\ 0 & 1 \end{bmatrix}$ (Identical to $T_{LR_1}(p)$ of a Type 1 L-R MUTATOR) | REALIZATION 1 | REALIZATION 2 |
| | 2 | $(q, \varphi) \leftrightarrow (v_C, q_C)$ $v_1 = -i_2$ $i_1 = \frac{dv_2}{dt}$ | $T_{MC_2}(p) = \begin{bmatrix} 0 & 1 \\ p & 0 \end{bmatrix}$ (Identical to $T_{CR_2}(p)$ of a Type 2 C-R MUTATOR) | REALIZATION 1 | REALIZATION 2 |

$$q(t) = \int_{-\infty}^t i(z) dz$$

$$\psi(t) = \int_{-\infty}^t v(z) dz$$

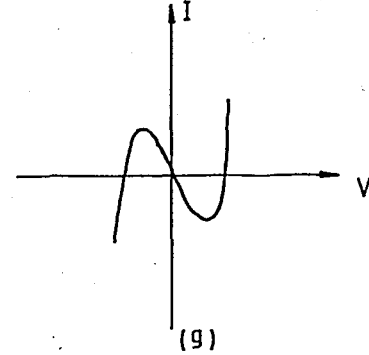
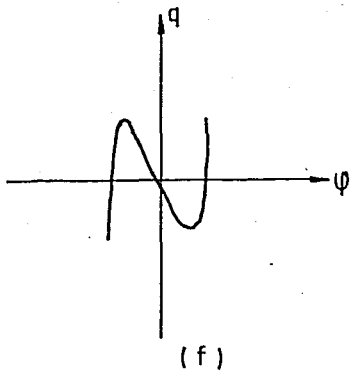
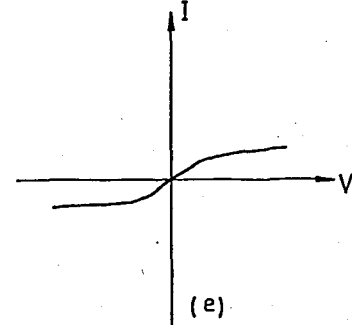
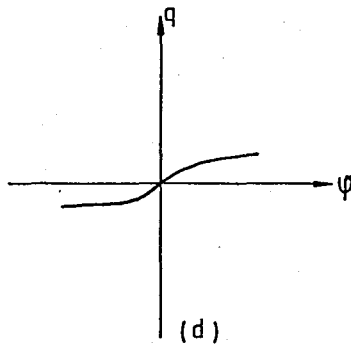
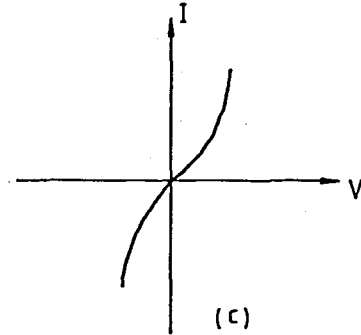
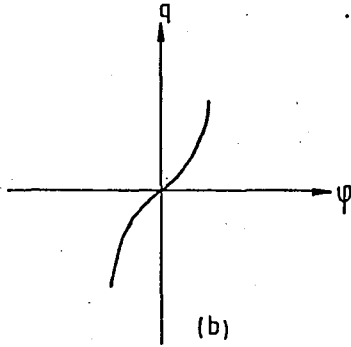
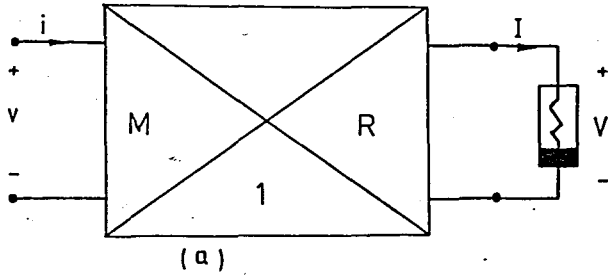


Figure III.5

Now consider the simple memristor-resistor circuit given in figure III.6.

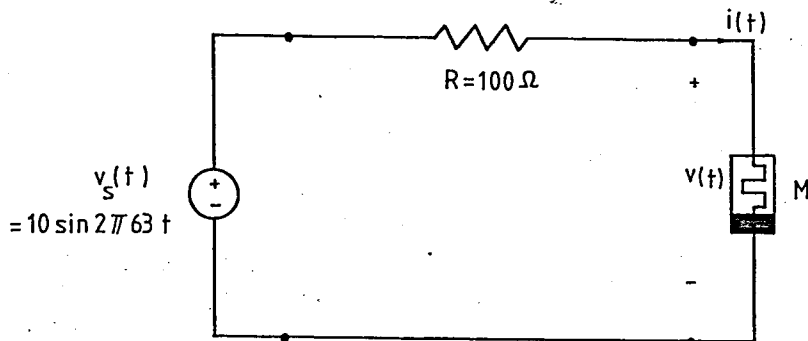
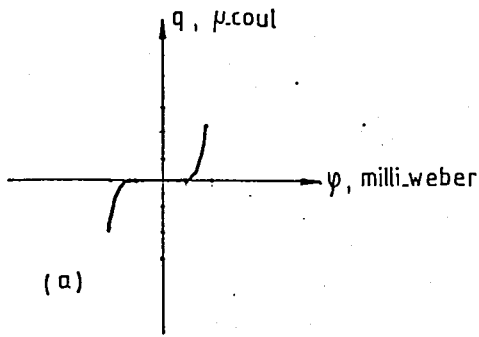


Figure III.6

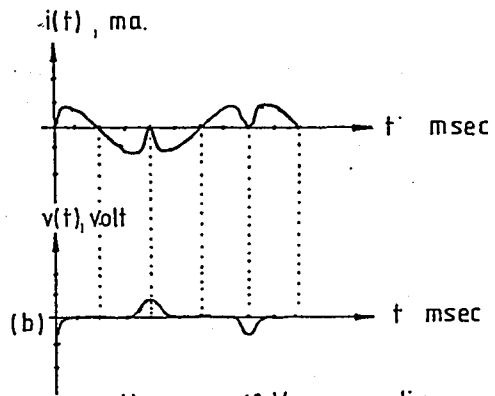
The oscilloscope tracing of the voltage $v(t)$ and the current $i(t)$ waveforms generated by this circuit and the corresponding ϕ - q curves are in Figure III.7.

In fact, it isn't so much surprising that the current and voltage waveforms are somewhat different although the ϕ - q curve is relatively smooth, because ϕ and q are the integrals of these quantities.

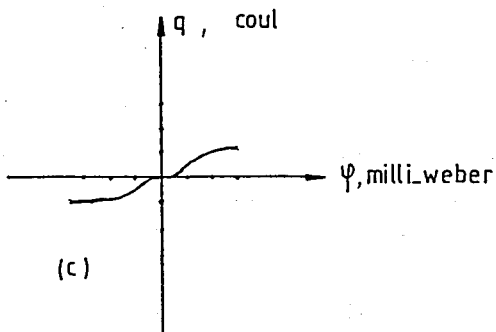
But, it is these unique signal-processing properties which are not shared by any other of the three circuit elements that have led to the belief that memristors will play an important role in nonlinear circuit theory, especially in the area of device modeling and unconventional signal-processing applications. Some examples of these will be given in the device modeling section.



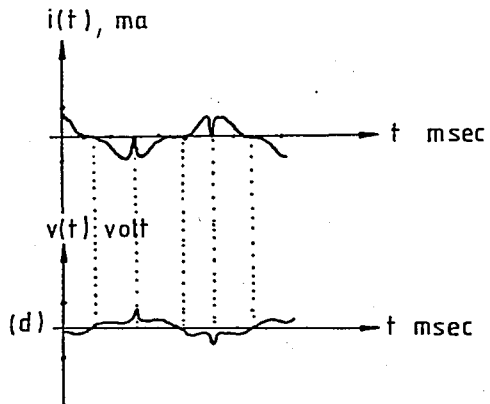
horizontal scale: 2.66 m.weber per div.
vertical scale: 5 μ .coul per div.



voltage s: 10 V. per div.
current s: 5 ma per div.
time s: 2 msec per div.



horizontal s: 2.66 mweber per div.
vertical s: 5 μ coul per div.



voltage s: 5 V. per div.
current s: 2 ma. per div.
time s: 5 msec per div.

Figure III.7

C H A P T E R IV
MEMRISTIVE SYSTEMS

IV.1- DEFINITION OF MEMRISTIVE SYSTEMS

The memristor that we have studied before is really a special case of a much more general class of dynamical systems called memristive systems [6]. The memristive systems are defined by the following set of equations.

$$\dot{\underline{x}} = f(\underline{x}, u, t) \tag{IV.1a}$$

$$y = g(\underline{x}, u, t)u \tag{IV.1b}$$

Where u and y are the input and output of the system and \underline{x} denotes the state of the system. The function $f: \mathbb{R}^n \times \mathbb{R} \times \mathbb{R} \rightarrow \mathbb{R}^n$ is a continuous n -dimensional vector function and for one-port $g: \mathbb{R}^n \times \mathbb{R} \times \mathbb{R} \rightarrow \mathbb{R}$ is a scalar continuous function. It is assumed that the state equation (IV.1a) has a unique solution for any initial state $\underline{x}_0 \in \mathbb{R}^n$. The output equation (IV.1b) is such that the output y is equal to the product between input u and the function g . This special structure of the readout map is what distinguishes a memristive system from an arbitrary dynamical system, namely the output y is zero whenever the input u is zero, regardless of the state \underline{x} . This property manifests itself in the form of a Lissajous figure which always passes through origin.

In terms of electrical variables an n 'th order current-controlled memristive one-port is represented by

$$\dot{\underline{x}} = f(\underline{x}, i, t) \tag{IV.2}$$

$$v = R(\underline{x}, i, t)i$$

and an n'th order voltage-controlled memristive one-port is represented by

$$\begin{aligned} \dot{\underline{x}} &= f(\underline{x}, v, t) \\ i &= G(\underline{x}, v, t)v \end{aligned} \quad (\text{IV.3})$$

where v and i denote the port voltage and current, respectively. The functions f , R , G are defined similar to f , g in equation (IV.1).

Now to motivate the significance of memristive systems, let's consider two examples below.

Example 1: Termistor.

A negative-temperature coefficient termistor is characterized by [7]

$$v = R_o(T_o) \exp \left[\beta \left(\frac{1}{T} - \frac{1}{T_o} \right) \right] i \triangleq R(T)i \quad (\text{IV.4})$$

where β is the material constant, T is the absolute body temperature of the termistor and T_o is the ambient temperature in Kelvin, and $R_o(T_o)$ is the cold temperature resistance at $T=T_o$.

The instantaneous temperature T , however, is a function of power dissipated in the termistor and is governed by the heat transfer equation,

$$p(t) = v(t) i(t) = k(T-T_o) + c \frac{dT}{dt} \quad (\text{IV.5})$$

where c is the heat capacitance and k is the dissipation constant of the termistor. Substituting (IV.4) into (IV.5) and rearranging the terms we get

$$\frac{dT}{dt} = - \frac{k}{c} (T-T_o) + \frac{R_o(T_o)}{c} \exp \left[\beta \left(\frac{1}{T} - \frac{1}{T_o} \right) \right] i^2 \triangleq f(T, i) \quad (\text{IV.6})$$

We see from (IV.4) and (IV.6) that a termistor in fact is not

a memoryless, temperature-dependent linear resistor, but rather a first-order time-invariant current-controlled memristive one-port.

Example 2: Discharge Tubes.

The behavior of a discharge tube is described by the following equations [8]

$$\dot{n} = \alpha i v - \beta n \tag{IV.7a}$$

$$v = \frac{F}{n} i \triangleq R(n)i \tag{IV.7b}$$

where α, β, F are constants depending on the dimensions of the tube and the gas filling the tube; n denotes the electron density inside the tube. Substituting (IV.7b) into (IV.7a) we get

$$\dot{n} = \alpha \frac{F}{n} i^2 - \beta n \triangleq f(n, i) \tag{IV.7c}$$

Again we see from (IV.7b) and (IV.7c) that the discharge tube should be modeled as a first-order time-invariant current-controlled memristive one-port.

Thus some systems classified as a certain class of dynamical systems should really be considered as memristive systems.

Now let's see the generic properties of memristive systems which distinguish them from other systems. We will only consider time-invariant current-controlled memristive one-ports.

IV.2- GENERIC PROPERTIES OF MEMRISTIVE ONE-PORTS.

Property 1. Passivity:

A generalized n -port memristor with the state representation $\dot{\underline{x}} = \underline{u}$, $\underline{y} = \underline{R}(\underline{x})\underline{u}$ is passive if, and only if $\underline{R}(\underline{x})$ is positive semidefinite at each point $\underline{x} \in \Sigma$ [12].

Proof:

Sufficiency: If $\underline{R}(\underline{x})$ is positive semidefinite, then for any input-output pair $\{\underline{u}(\cdot), \underline{y}(\cdot)\}$ and any time $t \geq 0$ the power input $\langle \underline{u}(t), \underline{y}(t) \rangle = \underline{u}^T(t) [\underline{R}(\underline{x}(t))] \underline{u}(t) \geq 0$

Hence n -port is passive.

Necessity part will be proved by contradiction. Suppose n -port is passive, but $\underline{R}(\underline{x})$ is not positive semidefinite everywhere. In other words, there exists $\underline{x}^* \in \Sigma$, $\underline{u}^* \in U$ such that $\underline{u}^{*T} [\underline{R}(\underline{x}^*)] \underline{u}^* = -a < 0$.

Since the entries of $R(\underline{x})$ are continuous functions, there exists an ϵ such that $\|\underline{x} - \underline{x}^*\| \leq \epsilon$ which implies $\underline{u}^{*T} [R(\underline{x})] \underline{u}^* < -a/2 < 0$. Let $\hat{\underline{u}}(\cdot)$ be given by $\hat{\underline{u}}(t) = (\epsilon / \|\underline{u}^*\|) \underline{u}^* \cos t$, for all $t \geq 0$, let $\hat{\underline{x}}(\cdot)$ be the trajectory resulting from the input $\hat{\underline{u}}(\cdot)$ with initial state \underline{x}^* and let $\hat{\underline{y}}(\cdot)$ be the corresponding output. Then for all $t \geq 0$

$$\|\hat{\underline{x}}(t) - \underline{x}^*\| = \left\| \int_0^t (\epsilon / \|\underline{u}^*\|) \underline{u}^* \cos t' dt' \right\| = \epsilon |\sin t| \leq \epsilon$$

so

$$\underline{u}^{*T} R[\hat{\underline{x}}(t)] \underline{u}^* < -a/2, \text{ for all } t \geq 0$$

Furthermore

$$\begin{aligned} - \int_0^T \langle \hat{\underline{u}}(t), \hat{\underline{y}}(t) \rangle dt &= - \int_0^T \left(\frac{\epsilon}{\|\underline{u}^*\|} \right)^2 (\underline{u}^{*T} R[\hat{\underline{x}}(t)] \underline{u}^*) \cos^2 t dt \\ &\geq \left(\frac{\epsilon}{\|\underline{u}^*\|} \right)^2 \left(\frac{a}{2} \right) \int_0^T \cos^2 t dt \end{aligned}$$

Then the available energy at the state \underline{x}^*

$$E_A(\underline{x}^*) \triangleq \sup_{\substack{\underline{x} \rightarrow \underline{x}^* \\ T \geq 0}} \left\{ - \int_0^T \langle \hat{\underline{u}}(t), \hat{\underline{y}}(t) \rangle dt \right\} = +\infty$$

Since, $E_A(\underline{x}^*) = +\infty$ we can extract infinite amount energy from the system which contradicts our assumption that n-port was passive. The proof of the passivity theorem for the current-controlled memristive one-ports defined by the equations $\dot{\underline{x}} = f(\underline{x}, i)$, $v = R(\underline{x}, i)i$ can be found in the reference [6].

Property 2. No Energy Discharge Property:

If the readout map of a current-controlled memristive one-port is such that $R(\underline{x}, i) \geq 0$, then the instantaneous power entering the one-port is always nonnegative.

Proof: It is given that $R(\underline{x}, i) \geq 0$ for any admissible input signal.

$$p(t) = v(t) \cdot i(t) = R(\underline{x}(t), i(t)) i^2(t)$$

Therefore, the instantaneous power entering the one-port is always nonnegative.

We see that energy discharge from a memristive one-port satisfying the above constraint is never possible.

Property 3. DC Characteristics :

A time-invariant current-controlled memristive one-port under dc operation is equivalent to a time-invariant current-controlled nonlinear resistor if $f(\underline{x}, I) = 0$ has a unique solution $\underline{x} = X(I)$ such that for each value of I the equilibrium point $\underline{x} = X(I)$ is globally asymptotically stable.

Proof: Substituting $\underline{x} = X(I)$ into the output equation in (IV.2) we obtain $V = R[X(I), I] I \triangleq \hat{V}(I)$. Since $X(I)$ is globally asymptotically stable, each value of dc input current I gives a stable, hence measurable dc voltage V . And the function $\hat{V}(I)$ can be regarded as the V - I curve of a time-invariant nonlinear resistor.

In practical analysis this property is still valid under low frequency periodic operation so long as the period of the excitation source is much larger than the settling time of the associated transient response.

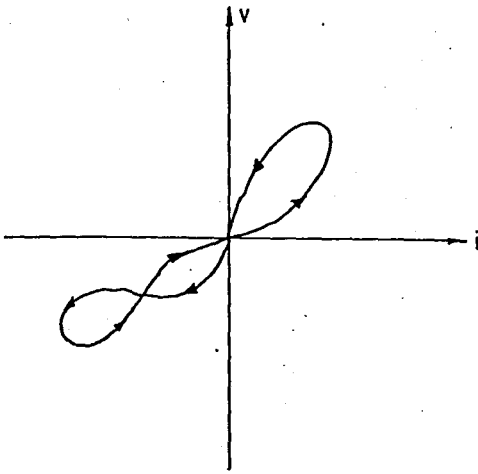
It is because of this behaviour that so many memristive devices are improperly identified as nonlinear resistors.

Property 4. Double-Valued Lissajous Figure Property:

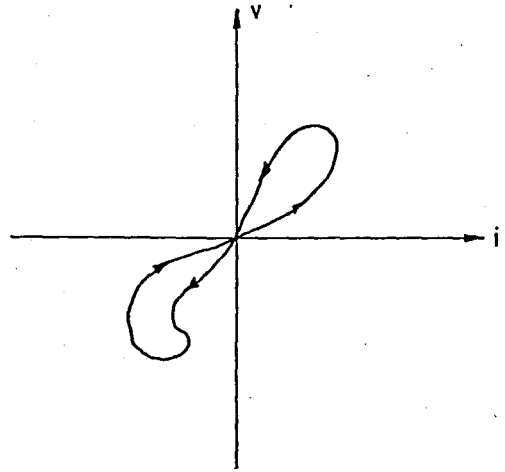
A current-controlled memristive one-port under periodic operation with $i(t) = I \cos \omega t$ always gives rise to a v - i Lissajous figure whose voltage is at most a double-valued function of i .

Proof: In the time-invariant version of the representation IV-2 the state equation has a unique solution $\underline{x}(t)$ for all $t \geq t_0$, given any t_0 , any $\underline{x}(t_0)$ and any piecewise $i(\cdot)$, moreover $\underline{x}(t)$ is continuous by the fundamental theorem of the differential equations. It is also given that the function $R(\cdot)$ is continuous, then the voltage $v(t) = R[\underline{x}(t), i(t)] i(t)$

for $i(t) = I \cos \omega t$ is also continuous. Hence for any value of the current $i \in [-I, I]$ there correspond at most two distinct values of $v(t)$.



A possible Lissajous Figure



An impossible Lissajous Figure

Figure IV.1

Property 5. Symmetric Lissajous Figure Property:

First let's define half-wave symmetric and quarter-wave symmetric waveforms.

A periodic waveform $x(t)$ of period T is said to be half-wave symmetric if $x(t + k\frac{T}{2}) = x(-t + k\frac{T}{2})$ for $k=1, 2$ for all $t \in [0, T/2]$ and it is said to be quarter-wave symmetric if $x(t + k\frac{T}{4}) = x(-t + k\frac{T}{4})$ for $k=1, 3$ for all $t \in [0, T/4]$.

Now let's state the property.

If the readout map of a time-invariant current-controlled memristive one-port is such that $R(\underline{x}, i) = R(\underline{x}, -i)$, then the $v-i$ Lissajous figure corresponding to the input current $i(t) = I \cos \omega t$ is open (i.e. not a closed loop) whenever the state $\underline{x}(t)$ is periodic of the same period as that of the input $i(t)$ and is half-wave symmetric. Moreover it is odd symmetric with respect to the origin whenever the state $\underline{x}(t)$ is periodic of the same period as that of $i(t)$ and is quarter-wave symmetric.

Proof: If both $x(t)$ and $i(t)$ are half-wave symmetric, then it follows from the output equation $v = R(x, i) i$ that

$$\begin{aligned} v(t + \frac{T}{2}) &= R[x(t + \frac{T}{2}), i(t + \frac{T}{2})] i(t + \frac{T}{2}) \\ &= R[x(-t + \frac{T}{2}), i(-t + \frac{T}{2})] i(-t + \frac{T}{2}) \\ &= v(-t + \frac{T}{2}) \text{ for all } t \in [0, \frac{T}{2}] \end{aligned}$$

where T is the period of both $x(t)$ and $i(t)$. Hence the $v-i$ curve doesn't form a closed loop. If $x(t)$ is quarter-wave symmetric, then since $i(t + \frac{T}{4}) = -i(-t + \frac{T}{4})$ for all $t \in [0, \frac{T}{4}]$ when $i(t) = I \cos \omega t$ we get

$$\begin{aligned} v(t + \frac{T}{4}) &= R[x(t + \frac{T}{4}), i(t + \frac{T}{4})] i(t + \frac{T}{4}) \\ &= -R[x(-t + \frac{T}{4})] i(-t + \frac{T}{4}) \\ &= -v(-t + \frac{T}{4}) \text{ for all } t \in [0, \frac{T}{4}] \end{aligned}$$

Hence $v-i$ curve is odd symmetric with respect to the origin.

Property 6. Limiting Linear Characteristics:

If a time-invariant current-controlled memristive one-port described by

$$\dot{x} = f(x, i)$$

$$v = R(x) i$$

is bounded-input bounded-state stable, then under periodic operation

it degenerates into a linear time-invariant resistor as the excitation frequency increases toward infinity.

Proof: It is sufficient to show that the state vector $\underline{x}(t) \rightarrow \underline{x}_0$ as the excitation frequency $\omega \rightarrow \infty$ where \underline{x}_0 is a constant vector in \mathbb{R}^n .

From bounded-input bounded-state stability and the continuity of the function f , for any bounded-input $i(t)$, $f(\underline{x}, i)$ can be written as

$$f(\underline{x}, i) = \underline{\alpha}_0 + \sum_{\substack{k=-\infty \\ k \neq 0}}^{k=\infty} \exp(jk\omega t) \underline{\alpha}_k \quad (\text{IV.8})$$

$\underline{\alpha}_0, \underline{\alpha}_k \in \mathbb{C}^n$ (\mathbb{C}^n is the space of n -tuples of complex numbers).

Note that the vectors $\underline{\alpha}_0$ and $\underline{\alpha}_k$ are bounded because of bounded-input bounded-state stability.

From $\dot{\underline{x}} = f(\underline{x}, i)$ and (IV.8) we obtain

$$\begin{aligned} \underline{x}(t) &= \underline{x}(t_0) + \int_{t_0}^t f[\underline{x}(z), i(z)] dz \\ &= \underline{x}(t_0) + \int_{t_0}^t \left[\underline{\alpha}_0 + \sum_{\substack{k=-\infty \\ k \neq 0}}^{k=\infty} \exp(jk\omega z) \underline{\alpha}_k \right] dz \\ &= \underline{x}(t_0) + \underline{\alpha}_0(t-t_0) + \sum_{\substack{k=-\infty \\ k \neq 0}}^{k=\infty} \left[\frac{-\exp(jk\omega t_0) + \exp(jk\omega t)}{jk\omega} \underline{\alpha}_k \right] \end{aligned}$$

Since $\underline{x}(t)$ is bounded and periodic by assumption, $\underline{\alpha}_0 = 0$ and as $\omega \rightarrow \infty$ $\underline{x}(t) \rightarrow \underline{x}(t_0)$.

Property 7. Small-Signal AC Characteristics.

If a time-invariant current-controlled memristive one-port is globally asymptotically stable for all dc input currents I , then its small-signal equivalent circuit about the dc operating point is as shown in the figure IV.2.

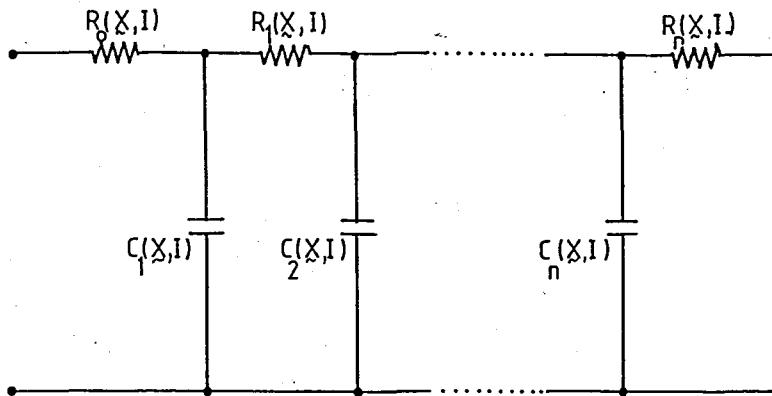


Figure IV.2

Proof: Let the input current $i(t)$ be such that $i(t) = I + \delta i(t)$ where $\sup_{t \in R} |\delta i(t)| \ll |I|$ and let the time-invariant current-controlled memristive one-port be characterized by

$$\begin{aligned} \dot{\underline{x}} &= f(\underline{x}, i) \\ v &= R(\underline{x}, i)i \triangleq h(\underline{x}, i) \end{aligned} \tag{IV.9}$$

If we linearize (IV.9) about (\underline{x}, I) where \underline{x} is the solution of $f(\underline{x}, I) = 0$, we will get

$$\delta \dot{\underline{x}} = \frac{\partial f(\underline{x}, I)}{\partial \underline{x}} \delta \underline{x} + \frac{\partial f(\underline{x}, I)}{\partial i} \delta i = A(\underline{x}, I) \delta \underline{x} + b(\underline{x}, I) \delta i \tag{IV.10}$$

$$\delta v = \frac{\partial h(\underline{x}, I)}{\partial \underline{x}} \delta \underline{x} + \frac{\partial h(\underline{x}, I)}{\partial i} \delta i = c(\underline{x}, I) \delta \underline{x} + d(\underline{x}, I) \delta i \tag{IV.11}$$

where

$$A(\underline{x}, I) \triangleq \begin{bmatrix} \frac{\partial f_1(\underline{x}, I)}{\partial x_1} & \frac{\partial f_1(\underline{x}, I)}{\partial x_2} & \dots & \frac{\partial f_1(\underline{x}, I)}{\partial x_n} \\ \vdots & \vdots & & \vdots \\ \frac{\partial f_n(\underline{x}, I)}{\partial x_1} & \frac{\partial f_n(\underline{x}, I)}{\partial x_2} & \dots & \frac{\partial f_n(\underline{x}, I)}{\partial x_n} \end{bmatrix}$$

$$b(\underline{x}, I) \triangleq \begin{bmatrix} \frac{\partial f_1(\underline{x}, I)}{\partial i} \\ \frac{\partial f_2(\underline{x}, I)}{\partial i} \\ \vdots \\ \frac{\partial f_n(\underline{x}, I)}{\partial i} \end{bmatrix} \quad c(\underline{x}, I) \triangleq \left[\frac{\partial h(\underline{x}, I)}{\partial x_1} \quad \frac{\partial h(\underline{x}, I)}{\partial x_2} \quad \dots \quad \frac{\partial h(\underline{x}, I)}{\partial x_n} \right]$$

$$d(\underline{x}, I) \triangleq \frac{\partial h(\underline{x}, I)}{\partial i}$$

Taking Laplace transform of both sides of (IV.10) and IV.11) with $\delta \underline{x}(0) = 0$ we obtain

$$s \Delta \underline{X}(s) = A(\underline{x}, I) \Delta \underline{X}(s) + b(\underline{x}, I) \Delta I(s) \tag{IV.12}$$

$$\Delta V(s) = C(\underline{x}, I) \Delta \underline{X}(s) + d(\underline{x}, I) \Delta I(s) \tag{IV.13}$$

solving (IV.12) for $\Delta \underline{X}(s)$ we get

$$\Delta \underline{X}(s) = [sU - A(\underline{x}, I)]^{-1} b(\underline{x}, I) \Delta I(s) \text{ and substituting this into (IV.13)}$$

$$\Delta V(s) = \left\{ c(\underline{x}, I) [sU - A(\underline{x}, I)]^{-1} b(\underline{x}, I) + d(\underline{x}, I) \right\} \Delta I(s) \tag{IV.14}$$

is obtained.

It follows from this equation that the small-signal impedance about the operating point (\underline{x}, I) for a time-invariant current-controlled memristive one-port is given by

$$Z_Q(s) = \frac{\Delta V(s)}{\Delta I(s)} = d(\underline{x}, I) + \frac{\beta_1 s^{n-1} + \beta_2 s^{n-2} + \dots + \beta_{n-1} s + \beta_n}{s^n + \alpha_1 s^{n-1} + \dots + \alpha_{n-1} s + \alpha_n} \tag{IV.15}$$

where α_i, β_k are dependent on (\underline{x}, I)

$Z_Q(s)$ can be written in the form of continued fraction expansion as

$$Z_Q(s) = d(\underline{x}, I) + \frac{1}{SC_1 + \frac{1}{R_1 + \frac{1}{SC_n + \frac{1}{R_n}}}}$$

(IV.16)

And the equivalent-circuit follows from the equation (IV.16).

For the case of time-invariant current-controlled memristive one-port described by

$$\dot{\underline{x}} = f(\underline{x}, i)$$

$$v = R(\underline{x})i$$

the associated small-signal equivalent circuit is as shown in the figure.(IV.3) Where I appearing in the element values is the operating current. The small signal equivalent circuit can easily be obtained by the procedure that we have applied above.

More explicitly, $A(\underline{X}, I)$ and $b(\underline{X}, I)$ are the same as before. $c(\underline{X}, I)$ and $d(\underline{X}, I)$ can be written as:

$$c(\underline{X}, I) = \left[\frac{\partial R(\underline{X})}{\partial x_1} I, \frac{\partial R(\underline{X})}{\partial x_2} I, \dots, \frac{\partial R(\underline{X})}{\partial x_n} I \right] = I \left[\frac{\partial R(\underline{X})}{\partial x_1}, \frac{\partial R(\underline{X})}{\partial x_2}, \dots, \frac{\partial R(\underline{X})}{\partial x_n} \right]$$

and $d(\underline{X}, I) = \frac{\partial h(\underline{X}, I)}{\partial i} = R(\underline{X}) = R_o(\underline{X})$. Then the small signal impedance is given by

$$Z_Q(s) = R_o(\underline{X}) + I \frac{\gamma_1 s^{n-1} + \gamma_2 s^{n-2} + \dots + \gamma_n}{s^n + k_1 s^{n-1} + \dots + k_n}$$

. And the small signal

equivalent circuit shown in Figure IV.3 follows from the continued fraction expansion of $Z_Q(s)$. Where γ_i and k_i depends on (\underline{X}, I)

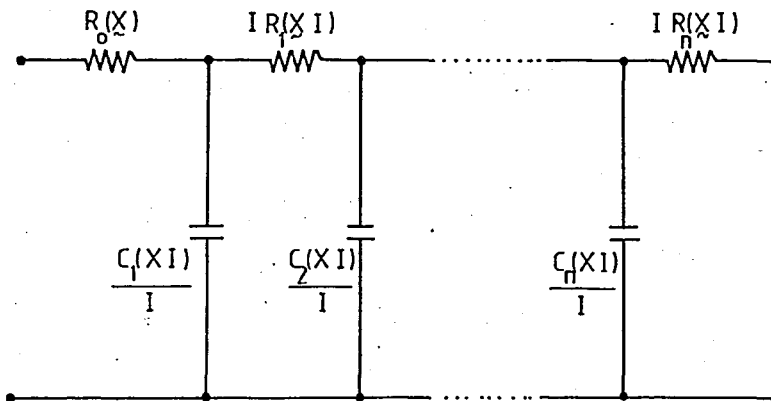


Figure IV.3

When the biasing current $I=0$ the small-signal input impedance $Z_Q(s)$ reduces to the linear resistor $R_o(X)$.

As the frequency of the small signal $\delta i(t)$ approaches zero the small-signal impedance of the above figure degenerates into

$Z_Q(s) = R_o(\underline{x}) + I \sum_{i=1}^n R_i(\underline{x}, I)$ and this corresponds to the slope of the dc V-I curve at $I=I_Q$. And as the frequency of small signal $\delta i(t)$ approaches to infinity the impedance goes to

$$Z_Q(s) = R_o(\underline{x})$$

We see from the above consideration that the small signal impedance depends on the biasing point. And this small signal impedance can either be capacitive or inductive depending again on the value of biasing.

Property 8. Local Passivity Criteria:

A first-order time-invariant current-controlled memristive one-port described by

$$\dot{x} = f(x, i)$$

$$v = R(x) i$$

is locally passive with respect to an operating point $I=I_Q$ if and only if.

$$i) \quad \frac{\partial f(x, I)}{\partial x} \leq 0$$

$$ii) \quad R(x) \geq 0 \quad \text{and} \quad \left\{ \begin{array}{l} R(x) \geq \frac{\frac{\partial f(x, I)}{\partial i} \frac{\partial R(x)}{\partial x} I}{\frac{f(x, I)}{x}} \quad \text{when} \quad \frac{\partial f(x, I)}{\partial x} \neq 0 \\ \frac{\partial f(x, I)}{\partial i} \frac{\partial R(x)}{\partial x} I \geq 0 \quad \text{when} \quad \frac{\partial f(x, I)}{\partial x} = 0 \end{array} \right.$$

Proof: The small-signal impedance of a first-order time-invariant current-controlled memristive one-port described above is

$$Z_Q(s) = R(X) + \frac{\frac{\partial f(X,I)}{\partial i} \frac{\partial R(X)}{\partial x} I}{s - \frac{\partial f(X,I)}{\partial x}}$$

Then, in order for $Z_Q(s)$ to be the impedance of a passive one-port it is necessary and sufficient that $Z_Q(s)$ be positive real.

And the above conditions are equivalent to the positive realness of $Z_Q(s)$.

Remarks On The Generic Properties [6].

The properties derived above can be used not only to identify those memristive devices and systems which have so far been identified incorrectly, but also to suggest some different applications. For example by using two thermistors one having a positive temperature coefficient and the other a negative temperature coefficient and biasing them in their locally active regions we can design an ultra-low frequency oscillator [9]. It is also interesting that Hodgkin-Huxley circuit model of the nerve axon membrane is locally active and hence is capable of firing nerve impulses [10].

We see that many physical and biological systems should be modeled as memristive one-ports. To identify such devices and systems we look for the following properties of the one-port Π under investigation.

- 1- The dc characteristic curve of Π passes through the origin.
- 2- The $v-i$ Lissajous figures corresponding to any periodic excitation having a zero mean always pass through the origin.
- 3- The one-port Π behaves as a linear resistor as the excitation frequency ω increases toward infinity.

- 4- Its small-signal impedance can be resistive, inductive or capacitive depending on the operating point.
- 5- The order of the small-signal impedance is invariant with respect to the dc biasing.

IV.3- A CANONICAL MODEL FOR MEMRISTIVE ONE-PORTS

Our objective in this section is to present a canonical model which will correctly mimic the steady-state response of memristive one-ports to the following class of input signals.

- 1- DC or slowly varying waveforms.
- 2- Sinusoidal signals of arbitrary amplitudes and frequencies.
- 3- Sinusoidal signals of arbitrary amplitudes and frequencies superimposed on top of a dc bias.

Let's denote these signals by

$$\mathcal{U} \triangleq \left\{ u(t) \triangleq A_0 + A \cos \omega t \mid (t, \omega) \in \mathbb{R} \times [1, \infty) \right\} \quad (\text{IV.17})$$

where $(A_0, A) \in \mathbb{R} \times \mathbb{R}_+$, $\mathbb{R}_+ \triangleq [0, \infty)$.

Although the lower bound of the frequency range seems to be restricted in the above expression, in fact it is not a strong restriction because we can always normalize any given set of frequencies so that the lowest frequency becomes unity.

Our main assumption in the following derivation is that the system response $y(t)$ tends to a unique steady state for each input $u(t)$ such that the function $\rho(t)(y(t) = \rho(t)u(t))$ tends to a periodic waveform of the same period as that of the input $u(t)$ in the steady state.

Observe that each input signal $u(t) \in \mathcal{U}$ is uniquely specified by three numbers, namely; A_0, A, ω . Hence for each combination of $\{A_0, A, \omega\}$ there corresponds a unique $\rho(t)$. In other words $\rho(t)$ is actually a function of A_0, A and ω . We may denote it by $\rho(t, A_0, A, \omega)$. Let $\rho_s(t)$ to be the steady-state component of $\rho(t)$. Since the function $\rho_s(t)$ is periodic of the same period as that of the input $u(t)$, by assumption, it admits the following Fourier series representation:

$$\rho_s(t) = a_0(A_0, A, w) + \sum_{k=1}^N \left\{ a_k(A_0, A, w) \cos kwt + b_k(A_0, A, w) \sin kwt \right\} \quad (\text{IV.18})$$

where N is an arbitrary number which is determined by $\rho_s(t)$. The Fourier coefficients in (IV.18) are determined as follows

$$a_0(A_0, A, w) = \frac{w}{2\pi} \int_0^{2\pi/w} \rho_s(\tau, A_0, A, w) d\tau \quad (\text{IV.19})$$

$$a_k(A_0, A, w) = \frac{w}{\pi} \int_0^{2\pi/w} \rho_s(\tau, A_0, A, w) \cos k\tau d\tau \quad (\text{IV.20})$$

$$b_k(A_0, A, w) = \frac{w}{\pi} \int_0^{2\pi/w} \rho_s(\tau, A_0, A, w) \sin k\tau d\tau \quad (\text{IV.21})$$

These coefficients are assumed to be continuous functions of A_0 and A in the mean-square sense and to be square-integrable functions of w ; namely

1) for each $\varepsilon > 0$ and for each $(\hat{A}_0, \hat{A}) \in \mathbb{R} \times \mathbb{R}^+$ there exists a neighborhood N_ε of (\hat{A}_0, \hat{A}) such that

$$\| a_0(A_0, A, w) - a_0(\hat{A}_0, \hat{A}, w) \|_{L^2} < \varepsilon \quad (\text{IV.22})$$

$$\| a_k(A_0, A, w) - a_k(\hat{A}_0, \hat{A}, w) \|_{L^2} < \varepsilon \quad (\text{IV.23})$$

and

$$\| b_k(A_0, A, w) - b_k(\hat{A}_0, \hat{A}, w) \|_{L^2} < \varepsilon \quad (\text{IV.24})$$

for all $(A_0, A) \in N_\varepsilon$ where L^2 denotes the space of square-integrable functions.

2) $a_0(A_0, A, \cdot)$, $a_k(A_0, A, \cdot)$ and $b_k(A_0, A, \cdot)$ are square-integrable functions of w .

Before proceeding further let's introduce two families of complete orthonormal functions in $L^2_{[1/k, \infty)}$

These functions will allow a unique decomposition of the Fourier

coefficients into the product between a frequency-dependent component and a frequency-independent component which depends only on A_0 and A .

The two families of complete orthonormal functions are defined by

$$\mathcal{P}_k \triangleq \left\{ a_{k\ell}(w) \triangleq k^{1/2} \sum_{m=1}^{\ell} \frac{\alpha_{\ell m}}{(kw)^{2m}} \mid w \in \left[\frac{1}{k}, \infty \right), \ell \in \mathbb{N} \right\} \quad (\text{IV.25})$$

$$\mathcal{B}_k \triangleq \left\{ b_{k\ell}(w) \triangleq k^{1/2} \sum_{m=1}^{\ell} \frac{\beta_{\ell m}}{(kw)^{2m}} \mid w \in \left[\frac{1}{k}, \infty \right), \ell \in \mathbb{N} \right\} \quad (\text{IV.26})$$

where \mathbb{N} denotes the set of natural numbers $\alpha_{\ell m}$ and $\beta_{\ell m}$ are constants defined by

$$\alpha_{\ell m} \triangleq (4\ell-1)^{1/2} \frac{\prod_{n=1}^{\ell-1} [2(m+n)-1]}{\prod_{\substack{n=1 \\ n \neq m}}^{\ell} 2(m-n)} \quad m \leq \ell \quad (\text{IV.27})$$

$$\beta_{\ell m} \triangleq (4\ell+1)^{1/2} \frac{\prod_{n=1}^{\ell-1} [2(m+n)+1]}{\prod_{\substack{n=1 \\ n \neq m}}^{\ell} 2(m-n)} \quad m \leq \ell \quad (\text{IV.28})$$

The families \mathcal{P}_k and \mathcal{B}_k will be used to construct the readout map of our state-space model. To model the steady-state response of

memristive one-ports subject to the input signals $u(t) \in \mathcal{U}$ the following is proposed.

State equation:

$$\dot{x}_1 = -a(t)x_1 + b(t)u$$

$$\dot{x}_2 = -x_1 + u$$

$$\dot{x}_3 = p(u - x_1 - x_3)$$

(IV.29a)

$$\dot{x}_4 = p(-x_2 - x_4)$$

where

$x_0 \triangleq [x_1(0), x_2(0), x_3(0), x_4(0)]^T = 0$ and $p(\cdot)$ is a monotonically increasing function whose graph is similar to the diode characteristic curve and

$$a(t) = \frac{1 - e^{-Kt}}{t + (1/K)e^{-Kt}}, \quad b(t) = \frac{1}{t + (1/K)e^{-Kt}} \quad K \gg 1$$

Output equation:

$$y = g(x_1, x_2, x_3, x_4, u)u \quad (\text{IV.29b})$$

The nonlinear map $g(\cdot)$ in the output equation (IV.29b) is defined by

$$g(x_1, x_2, x_3, x_4, u) \triangleq \sum_{\ell=1}^M \psi_{\ell}(x_1, x_3) a_{\ell} \left(\left(1 + \frac{\pi}{2}\right) \frac{x_3}{x_4} \right) + \sum_{k=1}^N \left\{ \left[\sum_{\ell=1}^M \delta_{k\ell}(x_1, x_3) a_{k\ell} \left(\left(1 + \frac{\pi}{2}\right) \frac{x_3}{x_4} \right) \right] T_k \left(\frac{u - x_1}{x_3} \right) + \left[\sum_{\ell=1}^M \delta_{k\ell}(x_1, x_3) \cdot b_{k\ell} \left(\left(1 + \frac{\pi}{2}\right) \frac{x_3}{x_4} \right) \right] \left(\left(1 + \frac{\pi}{2}\right) \frac{x_2}{x_4} + \frac{\pi}{2} \right) U \left(\frac{u - x_1}{x_3} \right) \right\} \quad (\text{IV.30})$$

Where M is an integer, and $\psi_{0\ell}(\cdot)$, $\gamma_{k\ell}(\cdot)$ and $\delta_{k\ell}(\cdot)$ are scalar nonlinear functions of x_1, x_3 which are identified via the following Fourier coefficient expansions.

$$\psi_{0\ell}(A_0, A) = \int_1^{\infty} a_0(A_0, A, w) a_{1\ell}(w) dw \quad (\text{IV.31})$$

$$\gamma_{k\ell}(A_0, A) = \int_{1/k}^{\infty} a_k(A_0, A, w) a_{k\ell}(w) dw \quad (\text{IV.32})$$

$$\delta_{k\ell}(A_0, A) = \int_{1/k}^{\infty} b_k(A_0, A, w) b_{k\ell}(w) dw \quad (\text{IV.33})$$

The functions $a_0(\cdot)$, $a_k(\cdot)$ and $b_k(\cdot)$ in these equations are themselves Fourier coefficients of $\beta_s(t)$ defined in (IV.18) while $a_{k\ell}(\cdot)$ and $b_{k\ell}(\cdot)$ are basis functions defined in (IV.25) and (IV.26). In (IV.30) N is a fixed integer defined in (IV.18) and $T_k(\cdot)$, $U_k(\cdot)$ are Chebyshev polynomial functions of the first and second kind. Namely:

$$T_k(z) \triangleq \frac{k}{2} \sum_{j=0}^{[k/2]} (-1)^j \frac{(k-j-1)!}{j! (k-2j)!} (2z)^{k-2j} \quad (\text{IV.34})$$

$$U_k(z) \triangleq \sum_{j=0}^{[k/2]} (-1)^j \frac{(k-j)!}{j! (k-2j)!} (2z)^{k-2j} \quad (\text{IV.35})$$

where $[k/2]$ denotes largest integer less than or equal to $k/2$.

We observe that in spite of seemingly complicated algebraic structure of the preceding canonical model the only model parameter and model functions that need to be identified are the integer M , nonlinear functions $\psi_{0\ell}(\cdot)$, $\gamma_{k\ell}(\cdot)$, $\delta_{k\ell}(\cdot)$ and the nonlinear function $p(\cdot)$. As we said before the function $p(\cdot)$ may be any strictly monotonically increasing Lipschitz continuous function whose graph is

similar to the diode curve. However for simplicity it can be chosen as a piecewise linear function defined by

$$p(e) \triangleq \alpha e + (1/\alpha - \alpha)r(e) \quad (IV.36)$$

where $\alpha \in (0,1)$ and $r(\cdot)$ is a unit ramp function i.e.

$$r(e) \triangleq \begin{cases} e & \text{for } e \geq 0 \\ 0 & \text{for } e < 0 \end{cases} \quad (IV.37)$$

Hence only the parameter α has to be determined to uniquely specify the function $p(\cdot)$.

Now we will present an algorithm that will determine the model parameters α , M and the nonlinear functions. Before stating the algorithm let's first define the following stopping rule. Given any set of input signal $\mathcal{U}_D = \{u_{ijk}(t) \triangleq A_{oi} + A_j \cos w_k t\}$ where the subscripts i, j, k range from 1 to N_{Ao}, N_A, N_w respectively, the performance index of the model with respect to these input signals is defined to be

$$\eta = \sum_{i=1}^{N_{Ao}} \sum_{j=1}^{N_A} \sum_{k=1}^{N_w} \frac{w_k}{2\pi} \int_0^{2\pi/w_k} |\rho_s(z, u_{ijk}) - \hat{\rho}_s(z, u_{ijk})|^2 dz \quad (IV.38)$$

where $\rho_s(t, u_{ijk})$ denotes the steady-state component of $\rho(t)$ in the original system and $\hat{\rho}_s(t, u_{ijk})$ denotes the steady-state component of $\hat{\rho}(t)$ in the model subject to the input $u_{ijk}(t) \in \mathcal{U}_D$. Another error index to be used is

$$\epsilon_M \triangleq \sum_{i=1}^{N_{Ao}} \sum_{j=1}^{N_A} \sum_{k=1}^{N_w} \left| a_o(A_{oi}, A_j, w_k) - \sum_{\ell=1}^M \psi_{o\ell}(A_{oi}, A_j) a_{\ell o}(w_k) \right|^2$$

$$+ \sum_{n=1}^N \left\{ \left| a_n(A_{oi}, A_j, w_k) - \sum_{\ell=1}^M \psi_{n\ell}(A_{oi}, A_j) a_{\ell n}(w_k) \right|^2 \right.$$

$$+ \left| b_n(A_{oi}, A_j, w_k) - \sum_{l=1}^M \delta_{nl}(A_{oi}, A_j) b_{nl}(w_k) \right|^2 \quad (IV.39)$$

where $a_o(\cdot)$, $a_n(\cdot)$ and $b_n(\cdot)$ are the Fourier coefficients of $\beta_s(t, u_{ijk})$ defined in (IV.18)-(IV.21), $a_n(\cdot)$, $b_n(\cdot)$ are defined in (IV.25) (IV.26)

The error index ϵ_M is used to ensure that the model parameter M and the nonlinear model functions $\psi_{of}(\cdot)$, $\gamma_{nl}(\cdot)$ and $\delta_{nl}(\cdot)$ are determined properly so that the Fourier coefficients $a_o(\cdot)$, $a_n(\cdot)$ and $b_n(\cdot)$ can be approximated closely for the given components A_{oi}, A_j and w_k .

To initiate the algorithm we need to prescribe an upper bound $\eta_{max} \in (0,1)$ for the performance index η . We also need to assume an initial guess on the iterative parameter $\alpha \in (0,1)$

The algorithm is as follows:

Step 0: Select an $\alpha \in (0,1)$ and $\eta_{max} \in (0,1)$ set $l=1$

Step 1: Compute $\psi_{of}(A_{oi}, A_j)$, $\gamma_{nl}(A_{oi}, A_j)$ and $\delta_{nl}(A_{oi}, A_j)$

from (IV.31)-(IV.33) for $n=1,2,\dots,N$ for each i,j ranging from 1 to N_{A_o} and N_A respectively.

Step 2: Set $M=l$ and compute ϵ_M using (IV.39)

Step 3: If $\epsilon_M > \eta_{max}/3$ set $l=l+1$ and go to step 1.

Step 4: Compute the performance index η using (IV.38)

Step 5: If $\eta > \eta_{max}$, set $\alpha = \alpha/2$ and go to step 4.

Otherwise stop.

The convergence of the iterative process is guaranteed by the following theorem.

Theorem: If the Fourier series representation of $a_o(A_o, A, \cdot)$ relative to the basis functions in \mathcal{P}_i , $a_k(A_o, A, \cdot)$ relative to the basis functions in \mathcal{P}_k and $b_k(A_o, A, \cdot)$ relative to the basis functions in \mathcal{B}_k converge uniformly over the set of testing signal components $\{(A_{oi}, A_j)\}$ for i,j ranging from 1 to N_{A_o} and N_A respectively

and for $k=1,2,\dots,N$ then for each $\eta_{\max} > 0$ the preceding algorithm terminates in a finite number of iterations.

The proof will not be given here.

The model is canonical in the sense that given any memristive one-port satisfying the technical assumptions described earlier, we can construct a dynamical system model having the same structure given in (IV.29). The state equation (IV.29a) is fixed (independent of the device or system being modeled) except for the parameter α defining the nonlinear function $p(\cdot)$ which has to be chosen properly so that the time constant of the model is much smaller than the period of the input signals. To illustrate the implementation and the validity of the preceding algorithm an hypothetical memristive system and its associated model is presented.

Example: Let's consider a fifth-order memristive one-port characterized by

$$\dot{x}_1 = -2x_1 + 2x_2 i$$

$$\dot{x}_2 = -x_2 + i$$

$$\dot{x}_3 = -4x_3 + 2x_4 i^2$$

$$\dot{x}_4 = -2x_4 + i^2$$

$$\dot{x}_5 = 1 - x_5$$

$$v = (x_1 + x_2^2 + x_3 + x_4^2 + x_5) i \triangleq R(x_1, x_2, x_3, x_4, x_5) i.$$

The steady-state component $R(\underline{x}(t))$ of the zero-state solution $\underline{x}(t)$ due to the input current $i(t) = A_0 + A \cos \omega t$ has been found analytically and is given by

$$\begin{aligned} \beta_s(t) &\triangleq R(\underline{x}(t)) \\ &= a_0(A_0, A, \omega) + \sum_{n=1}^4 \left\{ a_n(A_0, A, \omega) \cos n\omega t \right. \\ &\quad \left. + b_n(A_0, A, \omega) \sin n\omega t \right\} \end{aligned}$$

where

$$a_0(A_0, A, w) = 1 + 2A_0^2 + \frac{1}{2} A_0^4 + \frac{1}{2} A_0^2 A^2 + \frac{1}{8} A^4 + \frac{A^2}{w^2+1}$$

$$+ 4\left(\frac{A_0 A w}{w^2+4}\right)^2 + 16\left(\frac{A_0 A}{w^2+4}\right)^2 + \frac{A^4}{16(w^2+1)}$$

$$a_1(A_0, A, w) = 4 \frac{A_0 A}{w^2+1} + 4(A_0^2 + A^2) \frac{A_0 A}{w^2+4} + \frac{A_0 A^3(w^2+2)}{(w^2+1)(w^2+4)}$$

$$a_2(A_0, A, w) = \frac{A^2(1-w^2)}{(w^2+1)^2} + \left(\frac{A_0^2}{2} + \frac{A^2}{4}\right) \frac{A^2}{w^2+1} + \frac{2A_0^2 A^2(4-w^2)}{(w^2+4)^2}$$

$$a_3(A_0, A, w) = \frac{A_0 A^3(2-w^2)}{(w^2+1)(w^2+4)}$$

$$a_4(A_0, A, w) = \frac{A^4(1-w^2)}{16(w^2+1)^2}$$

$$b_1(A_0, A, w) = \frac{4A_0 A w}{w^2+1} + (4A_0^2 + 2A^2) \frac{A_0 A w}{w^2+4} + \frac{A_0 A^3 w}{(w^2+1)(w^2+4)}$$

$$b_2(A_0, A, w) = \frac{4A^2 w}{w^2+1} + \left(A_0^2 + \frac{A^2}{2}\right) \frac{w}{w^2+1} + \frac{16A_0^2 A^2 w}{(w^2+4)^2}$$

$$b_3(A_o, A, w) = \frac{3A_o A^3 w}{(w^2+1)(w^2+4)}$$

$$b_4(A_o, A, w) = \frac{A^4 w}{4(w^2+1)^2}$$

The model parameters and model functions were identified from the above data and from the system response to the input testing signals

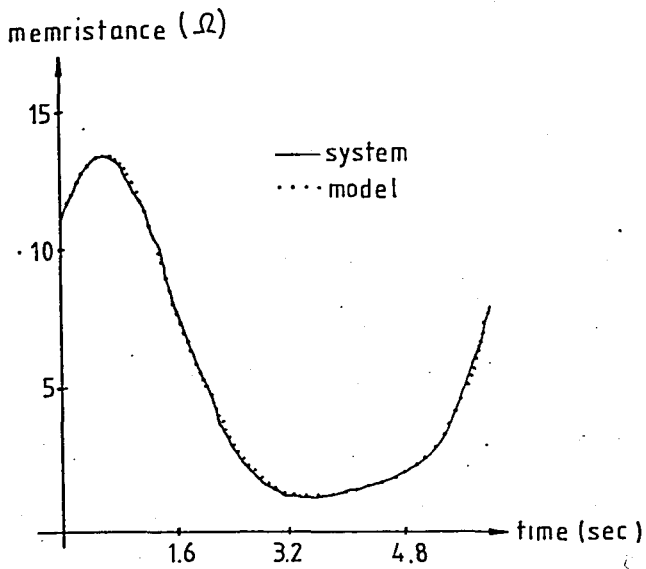
$$U_D = \left\{ \begin{array}{l} i(t) = A_{oi} + A_j \cos w_k t \\ A_{oi}, A_j \in (1, 2, 3, 4, 5) \\ w_k \in (1, 2, 3, 10^4) \end{array} \right\}$$

The model parameters determined by the algorithm subject to $\eta_{\max} = 0,5$ is found to be

$$M = 3 \quad \alpha = \frac{1}{15\pi}$$

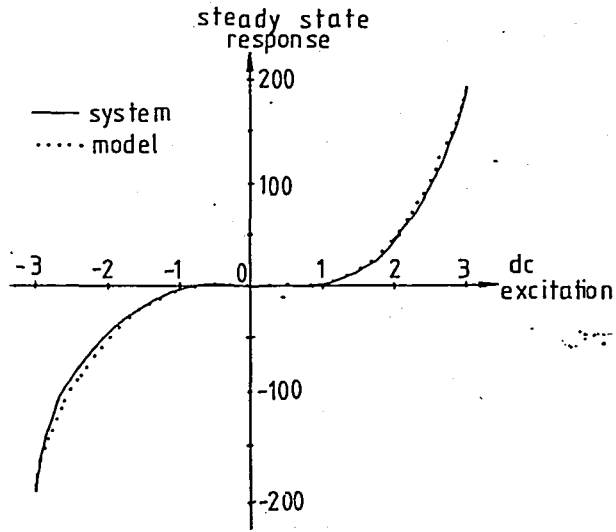
and the nonlinear model functions $\psi_{ol}(\cdot)$, $\gamma_{nl}(\cdot)$ and $\delta_{nl}(\cdot)$ are also identified using the algorithm and the nonlinear map $g(\cdot)$ is constructed using the above results.

Then to verify that the model can indeed simulate the original system for the above class of input signals, the results obtained for the steady-state response $\hat{f}_s(t)$ given by the model and $f_s(t)$ exact steady-state response of the system are compared. These are given in the figures. IV.4, IV.5, IV.6.



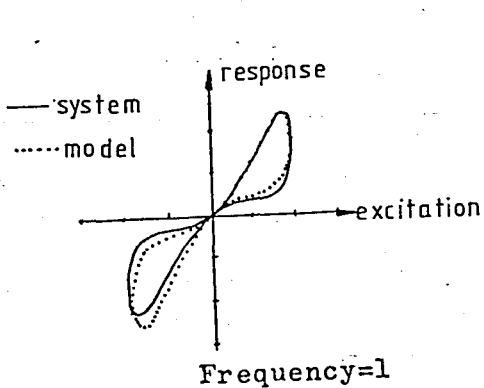
The Steady-state model and system response, for $i(t) = A_0 + A \cos \omega t$ where $(A_0, A, \omega) = (1, 1, 1)$

Figure IV.4

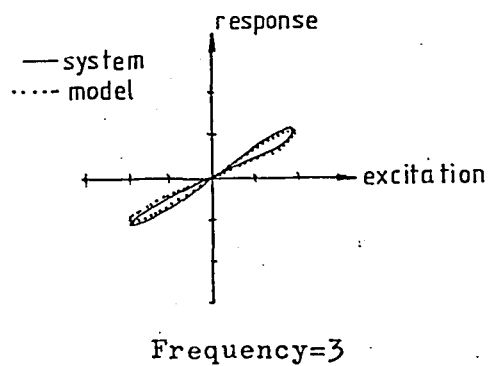


The dc characteristics of the system and the model.

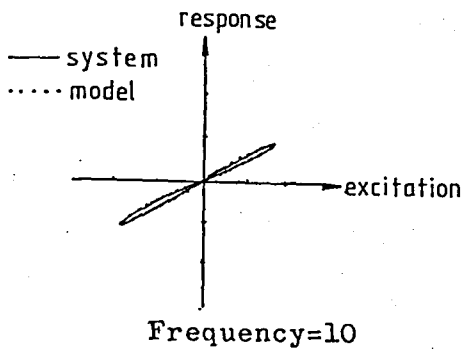
Figure IV.5



a)



b)



Frequency dependance of Lissajous figures for the system and the model.

c)

Figure IV.6

We see from the above figures that the waveforms of the model and those of the original system are very similar and we also see that Lissajous figures of both the model and the system shrink and tend to a straight line passing through the origin. The model is also tested under the triangular input signal which is not a member of the above mentioned class of signals but the results are again close to each other.

In this section we have considered an interesting class of nonlinear systems called memristive systems. One of the most important feature of these kind of systems is the zero-crossing property. In other words the output is zero whenever the input is zero and this corresponds to a Lissajous figure which always passes through the origin. And among the various properties of the memristive systems the frequency response of Lissajous figure is interesting. As the frequency increases toward infinity the Lissajous figure shrink and tends to a straight line passing through the origin. The physical interpretation of this phenomenon is that the system has a certain inertia and can not respond as rapidly to the fast variation in the excitation waveform and therefore must settle to some equilibrium state. This implies that the hysteretic effect of the memristive system decreases

as the frequency increases and eventually degenerates into a pure resistive system. Another property is the behaviour of the system either as inductive or capacitive depending on the bias point.

The model presented above is useful for simulating dynamic behaviour of the system properly, once it is identified as a memristive system [6].

C H A P T E R V

DEVICE MODELING USING MEMRISTORS AND EXAMPLES

In this chapter, the applications of memristor to device modeling will be discussed and examples will be given. But first let's consider the nonlinear device modeling problem in general.

Device modeling is more of an art than science. Although no general theory of device modeling is presently available, most existing circuit models of devices have been derived mainly by two basic approaches: a) the physical approach, b) black-box approach.

The physical approach consists of four basic steps: 1) device physics analysis, 2) physical equation formulation, 2) equation simplification and solution, 4) nonlinear network synthesis.

The black-box approach also consists of four basic steps. 1) experimental observations 2) mathematical modeling, 3) model validation, 4) nonlinear network synthesis. In either approach a mathematical description which approximates the behavior of a device is first derived. This crucial step is where most of the art is involved.

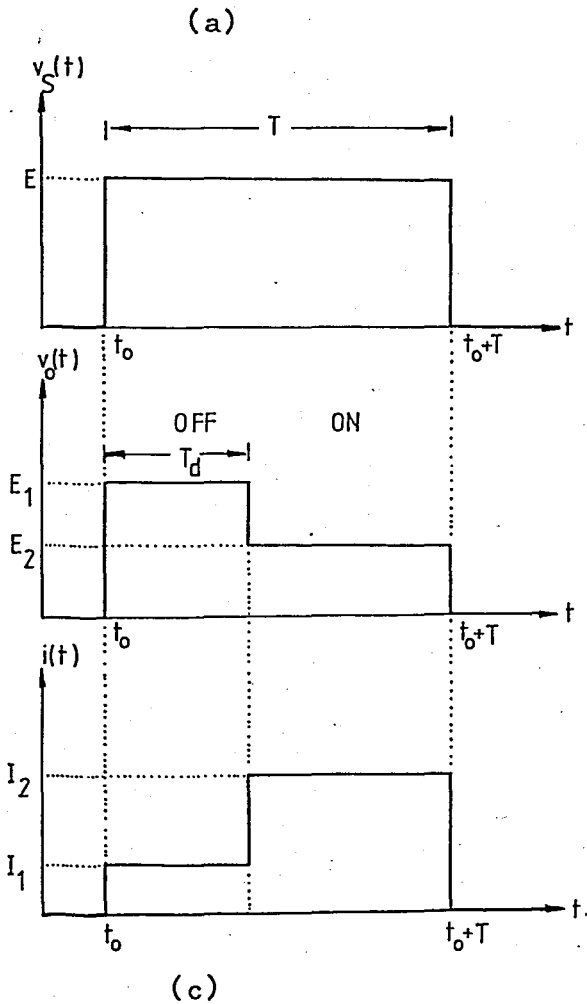
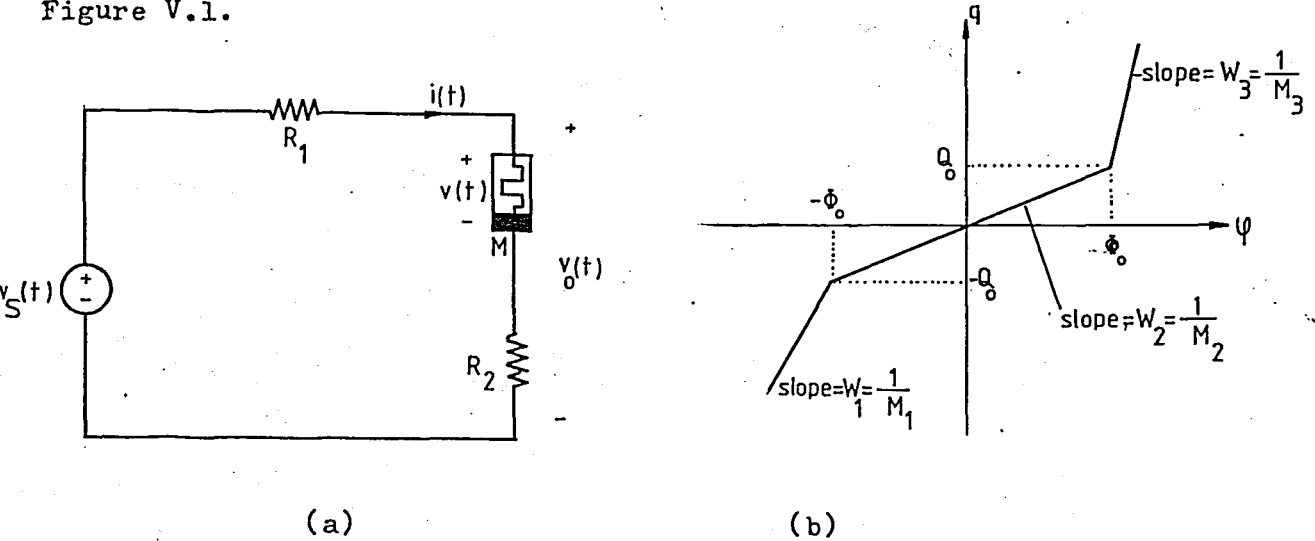
Once the mathematical description has been obtained, systematic methods from nonlinear network synthesis can be applied to arrive to a suitable circuit model made of some prescribed set of nonlinear circuit elements[20].

Now we will give the examples of some systems or devices modeled by making use of the memristor concept.

1- An Amorphous Ovonic Threshold Switch Model

An amorphous ovonic threshold switch is a two-terminal device which uses amorphous-glass rather than the more common crystalline

semiconductor material used in most solid-state devices. To show that the memristor provides a reasonable model for some types of amorphous devices, let's consider the memristor circuit shown in the Figure V.1.



where

$$E_1 = [(M_2 + R_2) / (M_2 + R_1 + R_2)] E$$

$$E_2 = [(M_3 + R_2) / (M_3 + R_1 + R_2)] E$$

$$I_1 = E / (M_2 + R_1 + R_2)$$

$$I_2 = E / (M_3 + R_1 + R_2)$$

$$T_d = [\phi_0 + (R_1 + R_2) Q_0] / E$$

Figure V.1

Then

$$(R_1 + R_2 + M(q)) \frac{dq}{dt} = V_s(t) \quad q \neq \pm Q_0 \quad (V.1)$$

Integrating both sides with respect to time from t_0 to t

$$\int_{t_0}^t (R_1 + R_2 + M(q)) \frac{dq}{dz} \cdot dz = \int_{t_0}^t V_s(z) dz$$

and

$$(R_1 + R_2) [q(t) - q(t_0)] + \varphi(q(t)) = \int_{t_0}^t V_s(z) dz + \varphi(q(t_0)) \quad (V.2)$$

are obtained.

Defining

$$h(q) \triangleq (R_1 + R_2) (q - q_0) + \varphi(q) \quad (V.3)$$

and observing that $h(q)$ is a strictly monotonically increasing function of q , $h^{-1}(\cdot)$ always exists and

$$q(t) = h^{-1} \left(\int_{t_0}^t V_s(\tau) d\tau + \varphi(q(t_0)) \right) \quad (V.4)$$

Then the output voltage is given by

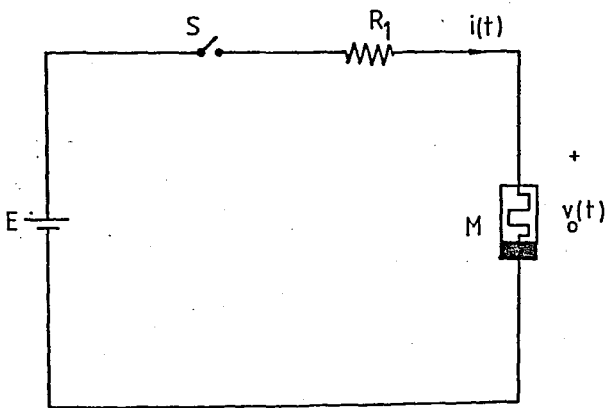
$$V_o(t) = V_s(t) - R_1 \left(\frac{dq(t)}{dt} \right) \quad (V.5)$$

Let $V_s(t)$ be a square-wave pulse as shown in Figure V.1c with $q(t_0) = 0$; then the waveforms $V_o(t)$ and $i(t)$ for the memristor $q-\varphi$ curve shown in Figure V-1b can be drawn using equations (V.1)-(V.5). These waveforms are shown in Figure V.1c. The expression for the time delay T_d shows that for a given memristor, T_d increases with decreasing E . The comparison of the results obtained from the above analysis with

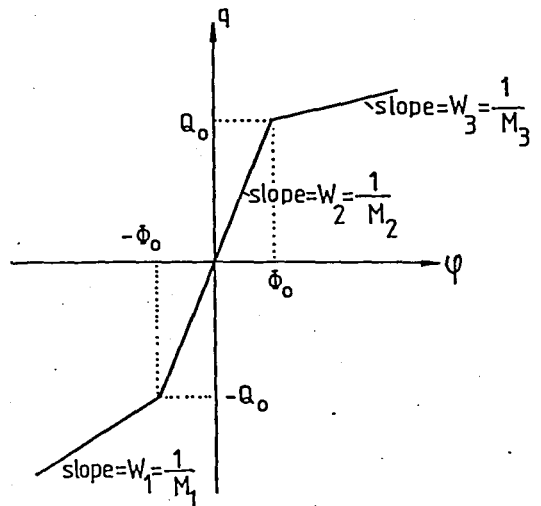
those obtained for an amorphous threshold switch reveals an interesting resemblance [13]. Thus the memristor seems to simulate well not only the shape of the waveforms but also the variation of T_d with E .

2- Modeling An Electrolytic E-Cell.

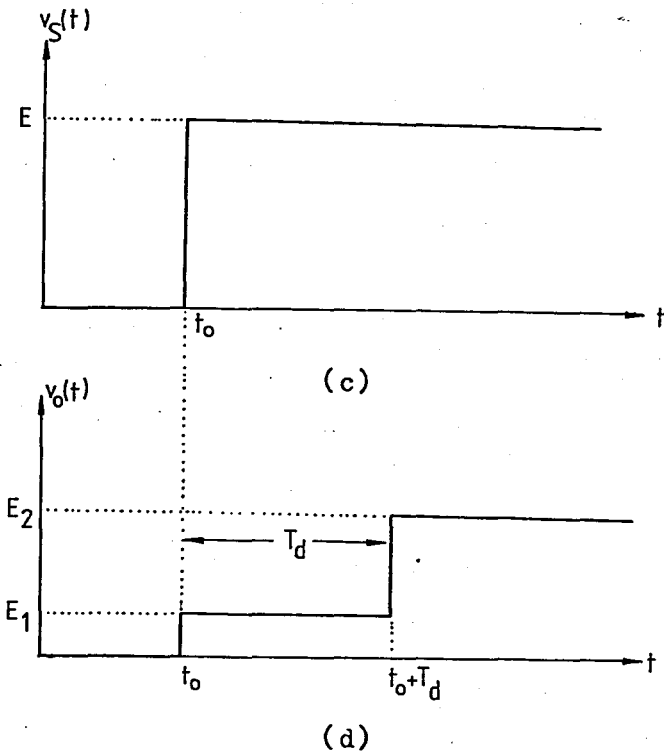
An E-cell (also known as Coul Cell) is an electrochemical two-terminal device capable of producing time delays ranging from seconds to months. An E-cell is a small electrolytic plating tank consisting of three basic components namely an anode, a cathode and an electrolyte. The anode, usually made of gold, is immersed in the electrolyte solution which in turn is housed within a silver tank can that also serve as the cathode. The time delay is controlled by the initial quantity of silver that has been previously plated from the cathode onto anode and the operating current. During the specified timing interval silver ions will be transferred from anode to the cathode, and E-cell behaves like a linear resistor with a low resistance. The end of timing interval corresponds to the time in which all of the silver has been plated off the anode, then the E-cell behaves like a linear resistor with a high resistance. We will now show that this behaviour of the device can be precisely modeled by a memristor with a ψ - q curve as shown in Figure V.2b. Let's consider the Figure V.2a,



(a)



(b)



$$E_1 = \left(\frac{M_2}{M_2 + R_1} \right) E$$

$$E_2 = \left(\frac{M_3}{M_3 + R_1} \right) E$$

$$T_d = \frac{\Phi_o + Q_o R_1}{E}$$

Figure V.2

where the E-cell has been replaced by a memristor. The output waveform is almost identical to the corresponding waveform measured from an E-cell timing circuit. The only discrepancy between this waveform and that actually measured with an E-cell timing circuit is that in practice, the rise time is not zero. It always takes a nonzero but small time interval for an E-cell to switch completely from a low resistance to high resistance. The step jump in the Figure V.2d is due to the piecewise-linear shape of the assumed Ψ - q curve. Hence even the finite switching time can be accurately modeled by replacing the Ψ - q curve with a curve having a continuous derivative that essentially approximates the piecewise-linear curve.

3- A Model For p-n Junction Diodes.

Consider the one-dimensional p-n junction diode shown in figure V.3a with an n-type region width W_n and junction area A .

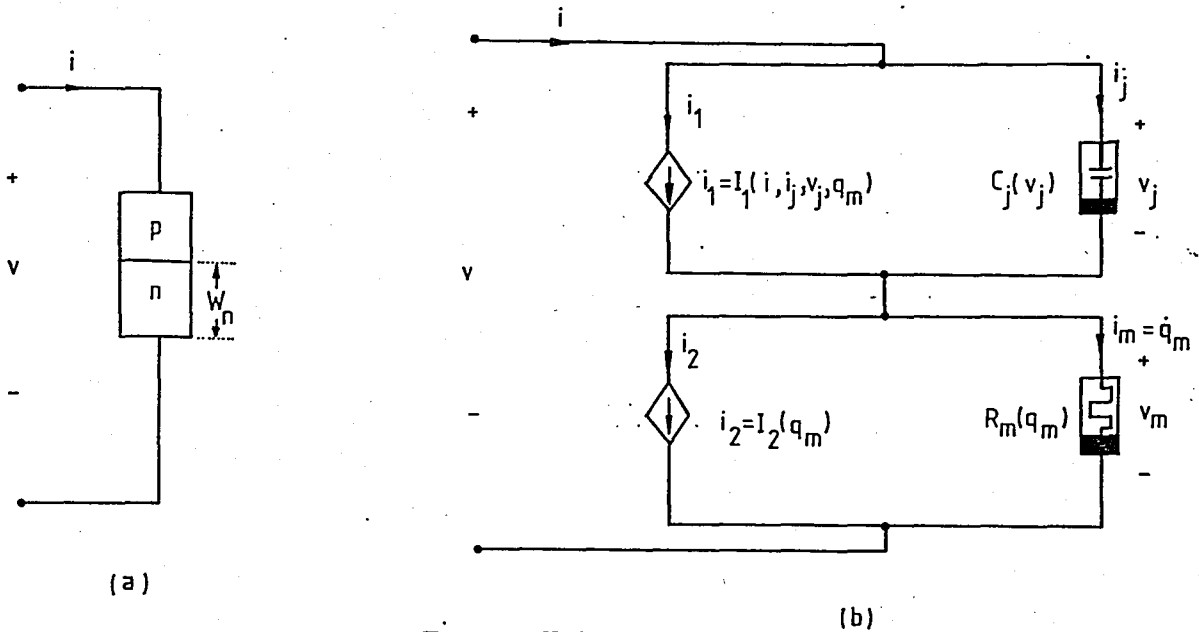


Figure V.3

Assume that the p-type region is much more heavily doped than the n-type region. Hence, the hole current at the junction is approximately equal to the total diode current. It is known from diode physics that there exists a thin transition layer at the junction and that the resistance in the neutral region depends on the carriers available there.

Observe that as carriers flow through the diode, they either flow into the transition layer and change the amount of charge stored there, or leak through the layer into the neutral regions (actually these two mechanisms occur simultaneously) where they are recombined or stored. In the latter case, the carrier concentration in the neutral regions may change, thereby inducing a corresponding change in

conductance. These basic diode operating mechanisms are incorporated in the model shown in Figure V.3b, where C_j is used to represent the effect of the transition layer, i_1 is used to simulate the leakage of carriers through the layer, R_m is used to simulate the conductance of the neutral regions, and i_2 is used to represent the recombination of carriers. The characterizing functions for these four elements are derived from basic physical principles [14].

The nonlinear junction capacitance $C_j(v_j)$:

For simplicity we choose the standard expression for $C_j(v_j)$ derived from the depletion approximation for a one-dimensional diode. This expression is given as follows [15]

$$C_j(v_j) = \frac{A [2\epsilon q N_D]^{1/2}}{2} (\psi_o - v_j)^{-1/2} \quad (V.6)$$

where

ψ_o = Built-in voltage

ϵ = Dielectric permittivity of the semiconductor

q = Charge of electron

N_D = Donor concentration in the n-type region.

A = Junction area of the diode.

The memristor $R_m(q_m)$:

The memristor is a two-terminal circuit element defined by $v_m = R_m(q_m) i_m$, where $R_m(q_m)$ is a linear resistance whose value depends on the charge q_m passing through its terminals.

$$R_m(q_m) = \frac{1}{A} \int_0^{W_m} \frac{dx}{\nabla(x, q_m)} \quad (V.7)$$

where $\nabla(x, q_m)$ is the conductivity of the semiconductor. Therefore a memristor can be considered as a charge-controlled linear resistor.

Now let's derive the expression for the conductivity $\nabla(x, q_m)$. If N_A is the acceptors concentration in the p-type region, the resistance of the diode is mainly contributed by the n-type region (base region), since $N_A \gg N_D$. The conductivity $\nabla(x)$ of the base region under low injection condition is

$$\nabla(x) = q(\mu_n n_{no} + \mu_p p_n(x)) \quad (V.8)$$

where $p_n(x)$ is the hole concentration at x (x is measured from the junction into the base region). The expression for $p_n(x)$ is found from the solution of the steady-state diffusion equation under appropriate boundary conditions.

$$\frac{\partial^2 p_n'(x)}{\partial x^2} - \frac{p_n'(x)}{L_p^2} = 0 \quad (V.9)$$

where $p_n'(x) = p_n(x) - p_{no}$ is the excess hole concentration at x_1 and L_p is the hole diffusion length.

The solution of (V.9) is given by the expression

$$p_n'(x) = p_n'(0) \left[\cosh\left(\frac{x}{L_p}\right) - \coth\left(\frac{W}{L_p}\right) \sinh\left(\frac{x}{L_p}\right) \right] \quad (V.10)$$

where

$$p_n'(0) = p_{no} \left[\exp\left(\frac{V_j}{V_T}\right) - 1 \right] \quad (V.11)$$

The stored excess minority charge q_p' is given by

$$q_p' = \int_0^{W_n} A_q p_n'(x) dx = A_q p_n'(0) L_p \left[\frac{\cosh(W_n/L_p) - 1}{\sinh(W_n/L_p)} \right] = q_m \quad (V.12)$$

Solving this equation for $p_n'(0)$ and substituting it into (V.10), we obtain $p_n'(x)$ in terms of q_m . Then again substituting the expression for $p_n(x)$ into (V.8) (where we also used $p_n(x) = p_n'(x) + p_{no}$)

$$v(x, q_m) = q_n \mu_n n_{no} + q_p \mu_p \left\{ p_{no} + \frac{q_m}{A_q L_p} \left(\frac{\sinh(W_n/L_p)}{\cosh(W_n/L_p) - 1} \right) \left[\cosh\left(\frac{x}{L_p}\right) - \coth\left(\frac{W_n}{L_p}\right) \sinh\left(\frac{x}{L_p}\right) \right] \right\} \quad (V.13)$$

is obtained; in (V.13)

μ_n = electron mobility

μ_p = hole mobility

n_{no} = equilibrium electron concentration in n-type region

p_{no} = equilibrium hole concentration in n-type region.

W_n = width of the n-type region (base-width)

$L_p = \sqrt{D_p \tau_p}$ = hole diffusion length.

D_p = hole diffusion constant

τ_p = hole recombination life time

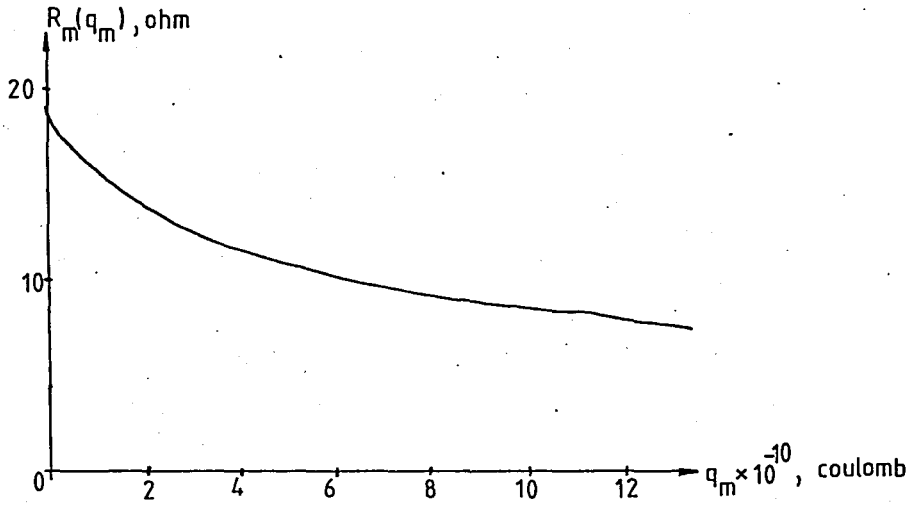


Figure V.4

A typical relationship for memristor $R_m(q_m)$ as a function of charge q_m is shown in Figure V.4.

The controlled current source $i_2 = I_2(q_m)$:

From equation (V.12)

$$q_m = Aq p_n'(0) L_p \left[\frac{\cosh(W_n/L_p) - 1}{\sinh(W_n/L_p)} \right]$$

$$= \left[\frac{Aq D_p p_n'(0)}{L_p} \coth\left(\frac{W_n}{L_p}\right) \left\{ \left[1 - \operatorname{sech}\left(\frac{W_n}{L_p}\right) \right] z_p \right\} \right] \quad (V.14)$$

where the identity $L_p^2 = D_p z_p$ was used.

On the other hand the diode current is given by

$$i = -AqD_p \left. \frac{\partial p_n'(x)}{\partial x} \right|_{x=0} \quad (V.15)$$

From (V.14) and (V.15)

$$i = \frac{AqD_p p_n'(0)}{L_p} \coth \left(\frac{W_n}{L_p} \right) \quad (V.16)$$

or

$$i = \frac{q_m}{\tau} \quad \text{where } \tau = \tau_p \left[1 - \operatorname{sech} \left(\frac{W_n}{L_p} \right) \right] \quad (V.17)$$

and τ is called the effective hole life time.

The controlled current source $i_1 = I_1(i, i_j, v_j, q_m)$:

The source i_1 can be described by

$$I_1(i, i_j, v_j, q_m) = I_{1f} U(i) + I_{1r} U(-i) \quad (V.18)$$

where $U(\cdot)$ is the unit step function and

$$I_{1f} \triangleq I_s \left[\exp\left(\frac{v_j}{v_T}\right) - 1 \right] + \frac{C_d(v_j)}{C_j(v_j)} i_j \quad (V.19)$$

where I_s is the diode saturation current and $v_T = \frac{kT}{q}$ is the thermal voltage

$$C_d(v_j) \triangleq \frac{I_s \tau}{v_T} \exp\left(\frac{v_j}{v_T}\right) \quad \text{is the diode} \quad (V.20)$$

diffusion capacitance and $C_j(v_j)$ is as defined in (V.6)

I_{1r} is defined by

$$I_{1r} \triangleq i - C_j(v_j) \max(\gamma_a, \gamma_b) \quad (V.21)$$

where

$$\gamma_a = \frac{i}{C_j(v_j) \left\{ 1 + \alpha \left[\frac{|q_m| + I_s \tau}{(|i| + I_s)} \right] U(-v_j) \right\}} \quad (V.22)$$

$$\gamma_b \triangleq -\max(\gamma_c, \gamma_d) \quad (V.23)$$

$$\gamma_c = \frac{I_s \left[\exp\left(\frac{v_j}{v_T}\right) - 1 \right] - i}{C_d(v_j) + C_j(v_j)} \quad (V.24)$$

$$\gamma_d \triangleq \frac{\left\{ \frac{V_T \sinh(W_n/L_p)}{AqL_p [\cosh(W_n/L_p) - 1]} \right\}^{q_m}}{p_{no} \left\{ 1 + \exp\left(\frac{v_j}{[1 - 0,5v_j U(-v_j)] v_T}\right) \right\} \left\{ 0,25 \tau \left[\frac{|q_m| + I_s \tau}{(|i| + I_s) \tau} \right]^\beta \right\}} \quad (V.25)$$

All the parameters in the above equations are the physical parameters except α and β . α and β are the empirical parameters whose values have to be chosen to obtain accurate predictions for the storage time t_s and fall time t_f .

In the definition of the controlled current source i_1 , we didn't give the explicit derivation of the quantities appearing in the expression of i_1 , but only the results are given [14]. In fact, our main purpose is to emphasize the use of memristor in the modeling of the device.

The model is tested using the following circuits and the computer simulated results are also given.

a) Reverse Transient:

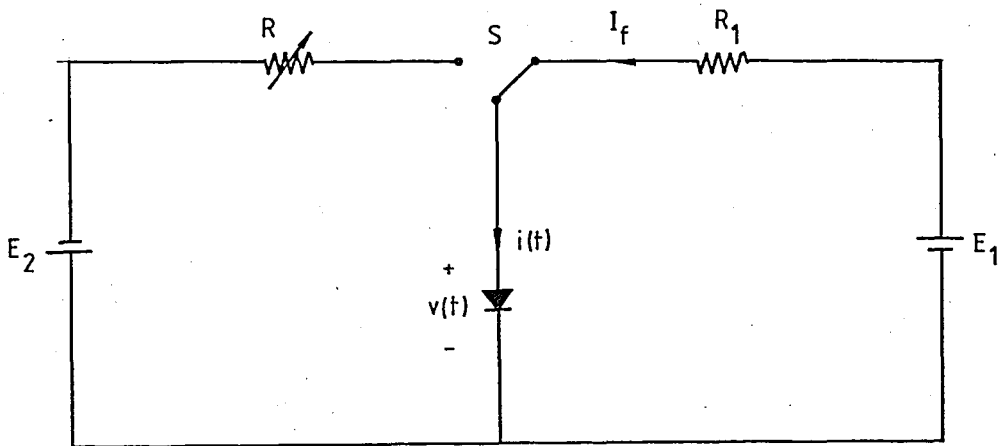


Figure V.5

It is assumed that switch S is thrown from right to left at $t=t_0=0$ and that before $t=0$ the diode is at steady state with current $i=I_f=10\text{mA}$. E_2 is taken to be 10V . α is chosen to be unity and β to be 1.5 . For this case, the computer simulated results are shown in Figure V.6.

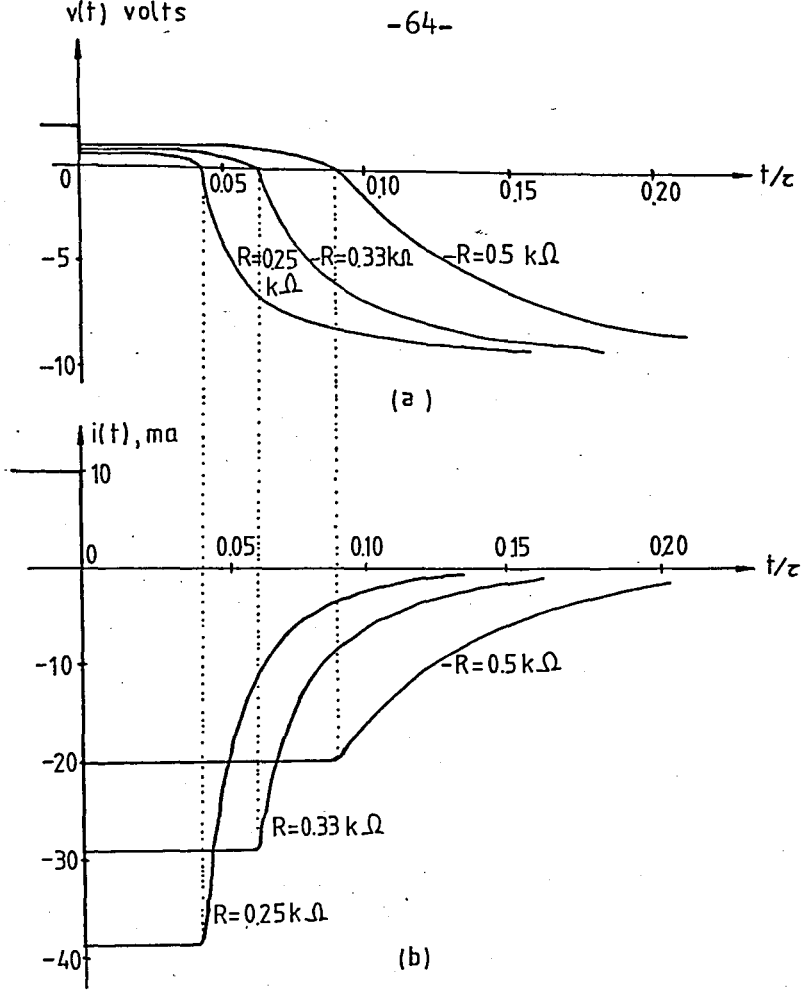


Figure V.6

b) Forward Transient:

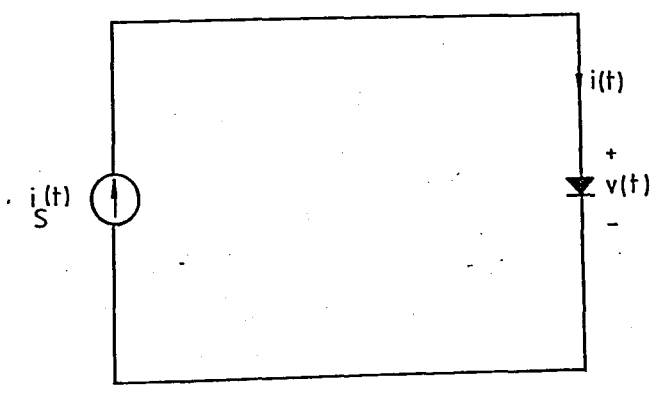


Figure V.7

Different current steps are applied and the computed voltage transient waveforms are shown in Figure V.8

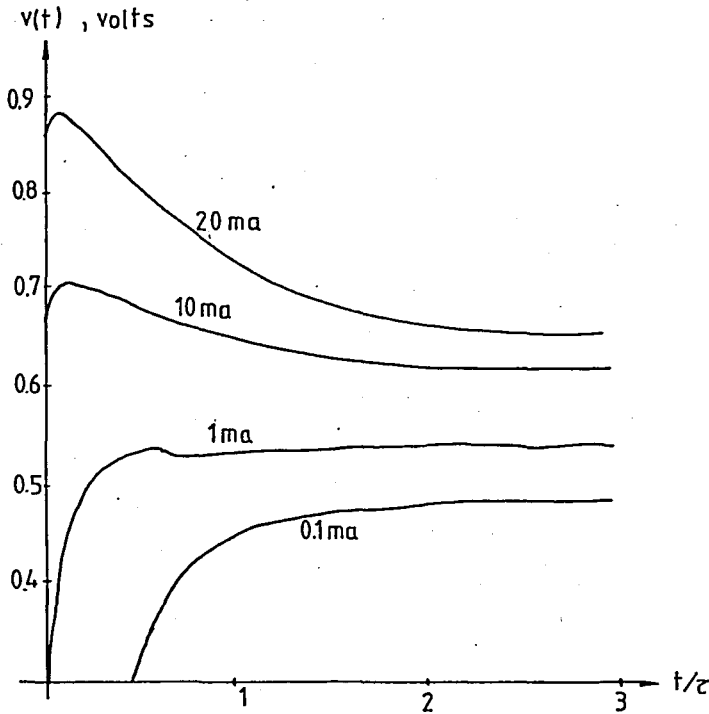


Figure V.8

These computed waveforms are very similar to those obtained from real observations [16]-[18].

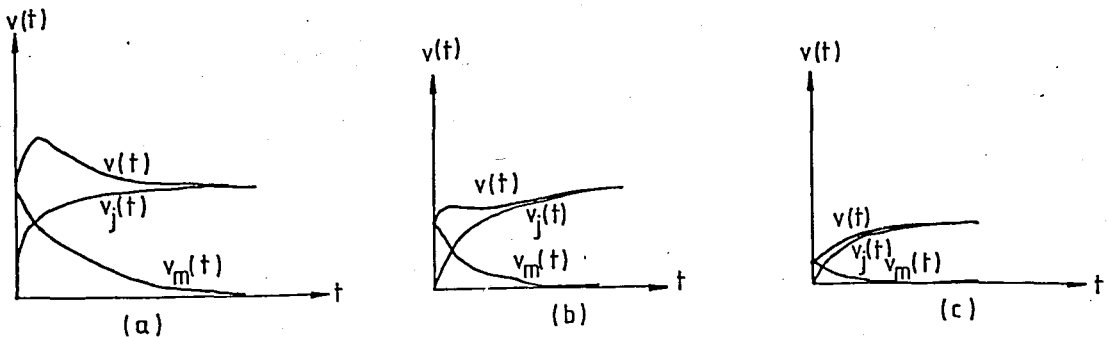


Figure V.9

The qualitative forward transient waveforms of voltages $v(t)$, $v_j(t)$ and $v_m(t)$ across the memristive diode model, the junction capacitor C_j and the memristor R_m respectively are shown in Figure V.9 for a) high input current, b) intermediate input current and c) low input current.

c) Rectifying Circuits:

The circuits shown in Figures V.10a and V.11a are also simulated in the computer and the calculated waveforms are plotted in Figures V.10b and V.11b.

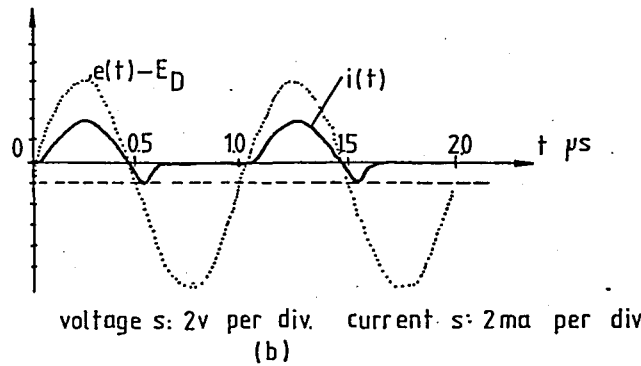
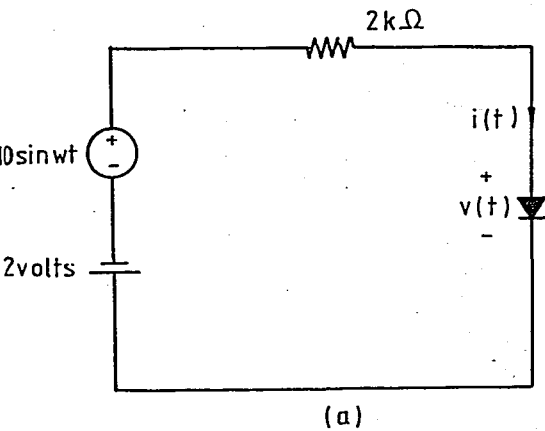


Figure V.10

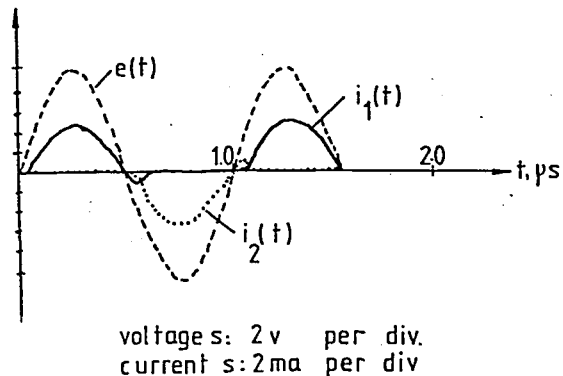
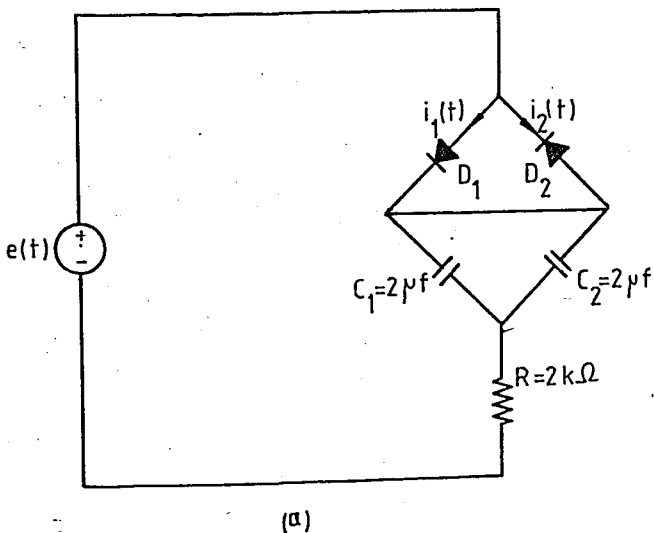


Figure V.11

Again the computed results agree remarkably well with real observations [19].

d) Small Signal Impedance of The Model:

Assuming that the junction diode is under forward bias ($i > 0$), the memristive diode model reduces to the model shown in Figure V.12

$$r_j = \left(\frac{dI_j}{dV_j} \right)^{-1} = \left[\frac{d}{dV_j} \left\{ I_s \left[\exp \left(\frac{V_j}{V_T} \right) - 1 \right] \right\} \right]^{-1}$$

$$C_d = \frac{z I_s}{V_T} \exp \left(\frac{V_j}{V_T} \right)$$

$$i_2(q_m) = \frac{q_m}{z}$$

$$R_m(q_m) = \frac{1}{A} \int_0^{W_n} \frac{dx}{v(x, q_m)}$$

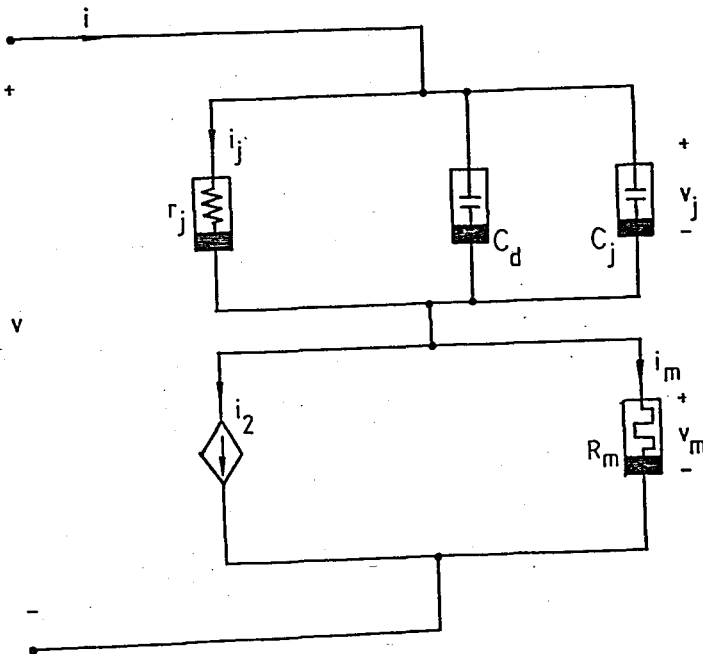


Figure V.12

Since $C_d \gg C_j$ under forward bias, C_j can be neglected, and a dc current source I_{in} upon which a small signal $i_{in}(t)$ is superimposed as shown in the Figure V.13 is applied to the diode.

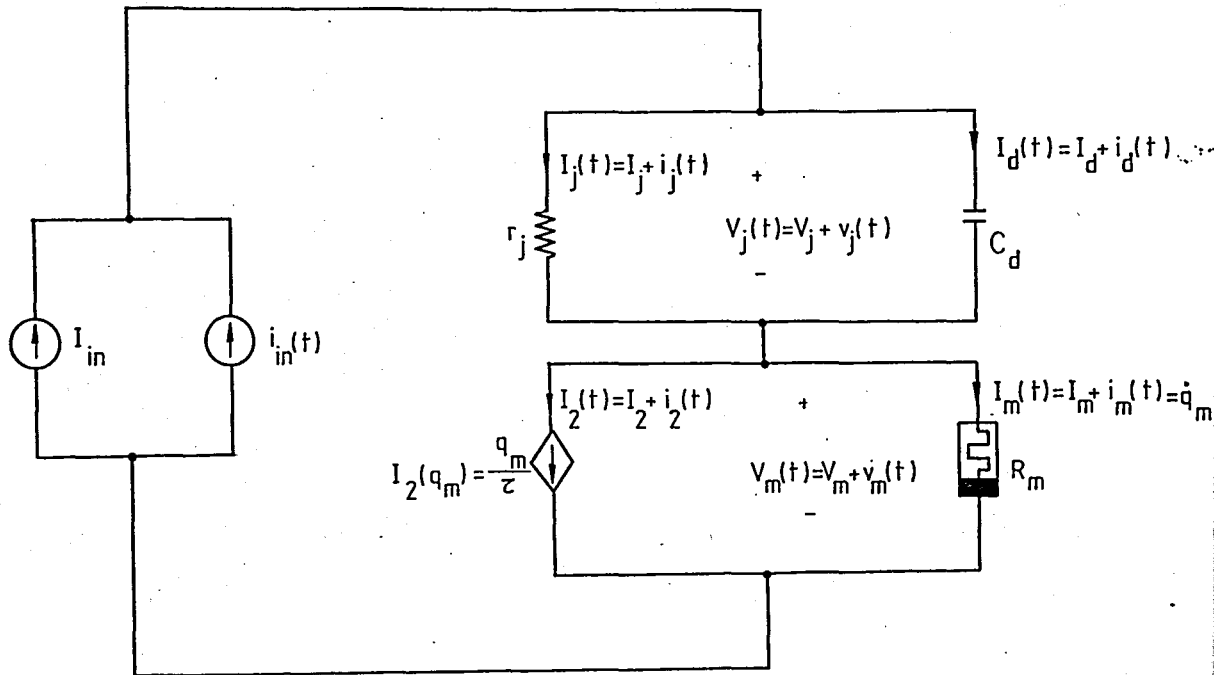


Figure V.13

The impedance Z_1 of the parallel connection of r_j with C_d as shown in Figure V.13 is given by:

$$Z_1 = \frac{1}{1/r_j + j\omega C_d} = \frac{r_j}{1 + j\omega r_j C_d} \quad (V.26)$$

Where the incremental resistance r_j and capacitance C_d are given by:

$$r_j = \left(\frac{dI_j}{dV_j} \right)^{-1} = \left[\frac{d}{dV_j} \left\{ I_s \left[\exp\left(\frac{V_j}{V_T}\right) - 1 \right] \right\} \right]^{-1} = \left[\frac{I_s}{V_T} \exp\left(\frac{V_j}{V_T}\right) \right]^{-1} = \left[\frac{I_s + I_j}{V_T} \right]^{-1} \quad (V.27)$$

and

$$C_d = \frac{I_s \tau}{V_T} \exp\left(\frac{V_j}{V_T}\right) = \frac{\tau(I_s + I_j)}{V_T} \quad (V.28)$$

about the dc operating point. Substituting equations (V.27) and (V.28) into (V.26) we obtain

$$Z_1 = \frac{V_T(1-jw\tau)}{(I_s + I_j)(1+w^2\tau^2)} \quad (V.29)$$

Now let's calculate the impedance Z_2 of the parallel connection of the controlled current source $I_2(q_m)$ with the memristor $R_m(q_m)$.

From the Kirchoff's current law we can write

$I_{in} + i_{in}(t) = \dot{q}_m(t) + \frac{q_m(t)}{\tau}$. If we solve this equation under the initial condition $q_m(0)=0$, we obtain

$$q_m(t) = \tau [1 - \exp(-\frac{t}{\tau})] I_{in} + \int_0^t [\exp(-\frac{1}{\tau}(t-t'))] i_{in}(t') dt' \quad \text{for } t \geq 0 \quad (V.30)$$

The first term in the expression of $q_m(t)$ goes to τI_{in} as t goes to infinity. Since $I_2(q_m) = \frac{q_m}{\tau}$, then at the steady state the dc component of the current passing through the controlled source $I_2(q_m) = I_2(t)$ will be equal to the I_{in} , i.e. it is equal to the dc component of the input current source and the dc component of the current passing through the memristor is equal to zero at steady state. Then at the steady state

$$i_{in}(t) = i_2(t) + i_m(t) \quad (V.31)$$

And, by the definition of $I_2(q_m)$ we can write

$$I_2(t) = \frac{\int_0^t I_m(t') dt'}{\tau} \quad \text{or in differential form} \quad \tau \frac{dI_2(t)}{dt} = I_m(t).$$

At steady state this equation gives

$$\tau \frac{di_2(t)}{dt} = i_m(t) \quad (V.32)$$

combining equations (V.31) and (V.32) we obtain $i_{in}(t) = i_2(t) + \tau \frac{di_2(t)}{dt}$ and taking the Laplace transformation of both sides with $i_2(0) = 0$ we can write

$$i_{in}(s) = i_2(s) + \tau s i_2(s) \quad \text{which gives}$$

$$\frac{i_2(s)}{i_{in}(s)} = \frac{1}{1 + \tau s} \quad (V.33)$$

On the other hand

$Z_2 \triangleq \frac{v_m(s)}{i_{in}(s)}$ but $v_m(s) = R_m i_m(s)$. From (V.32) we can write $\tau s i_2(s) = i_m(s)$. Then

$$Z_2 = \frac{v_m(s)}{i_{in}(s)} = \frac{R_m i_m(s)}{i_{in}(s)} = \frac{\tau R_m s i_2(s)}{i_{in}(s)} \quad (V.34)$$

Substituting equation (V.33) into (V.34) we obtain

$$Z_2 = \frac{\tau R_m s}{1 + \tau s} \quad (V.35)$$

In $j\omega$ -domain $Z_2 = \frac{j\omega \tau R_m}{1 + j\omega \tau} = \frac{R_m (j\omega \tau + \omega^2 \tau^2)}{1 + \omega^2 \tau^2}$

Finally, the total impedance can be obtained as

$$Z = Z_1 + Z_2 = \frac{V_T + (I_j + I_s) \omega^2 \tau^2 R_m}{(I_s + I_j)(1 + \omega^2 \tau^2)} + \frac{j\omega \left[\tau R_m - \frac{\tau V_T}{I_s + I_j} \right]}{1 + \omega^2 \tau^2} \quad (V.36)$$

If we consider this expression we see that when I_j is small so that $R_m < \frac{V_T}{I_s + I_j}$ then the reactive component of Z is negative and the impedance is capacitive. Similarly if I_j is large so that $R_m > \frac{V_T}{I_s + I_j}$ then the impedance is inductive.

We again observe that this property of the model well coincides with the real physical behaviour of the device.

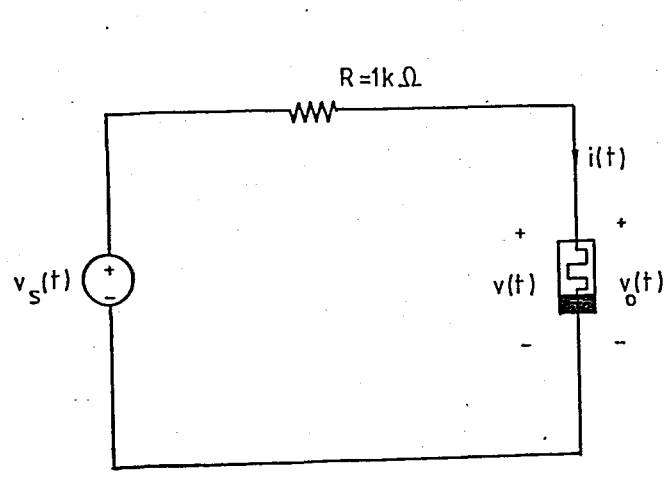
Another conclusion is that if the applied current is pure d.c. having no a.c signal superimposed on it then at steady state, the model

reduces to a nonlinear resistor obeying the diode junction law.

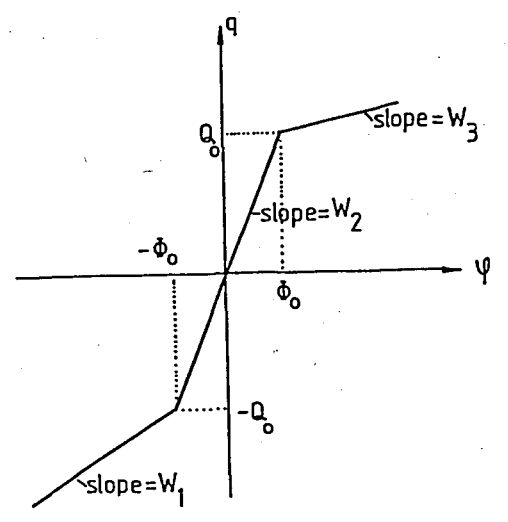
4- Use of The Memristor in Signal Processing.

Memristors can also be used to process many types of signals and generate various types of waveforms. Here we will present a typical application that uses a memristor to generate a staircase waveform.

Let's consider the design of a four step staircase waveform generator. If we drive the circuit in Figure V.14a symmetrical square-wave voltage source then the output voltage is a four step staircase waveform, provided that the memristor ψ - q curve is as shown in Figure V.14b.



(a)



(b)

Figure V.14

The input and output waveforms are as shown in Figure V.15

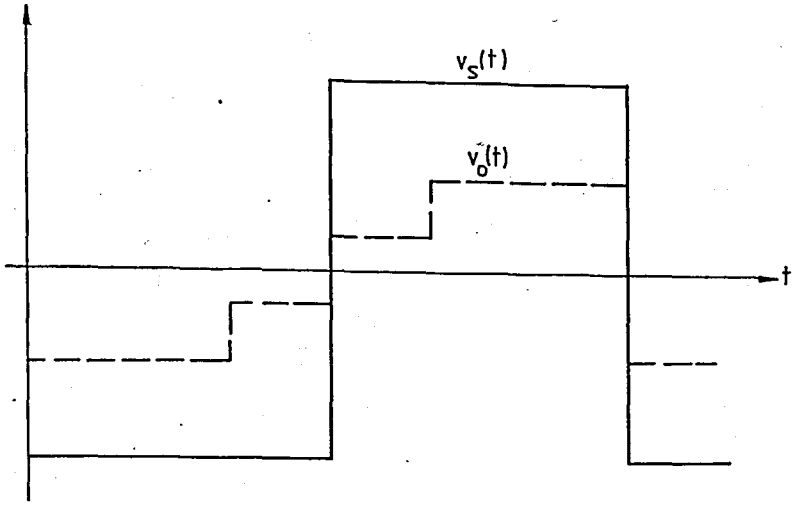
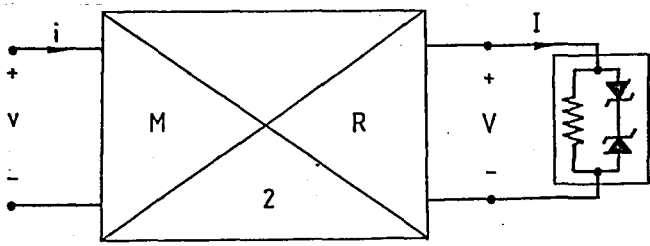
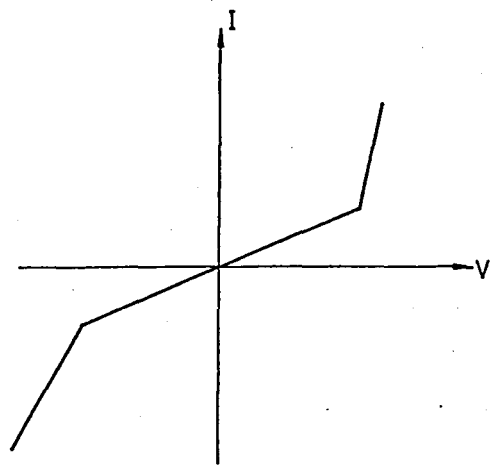


Figure V.15

The memristor with the ψ - q curve given in Figure V.14b can be synthesized by the methods presented in the realization section. The memristor for the above circuit can be synthesized by connecting a nonlinear resistor across port-2 of a type-2 M-R mutators, and the nonlinear resistor can be realized by two back-to-back zener diodes in parallel with a linear resistor. This realization is shown in the Figure V.16.



(a)



(b)

Figure V.16

In this chapter we have studied the device modeling problem using memristors by giving examples and we have also given an example on the application of memristor to signal processing. These examples show that the memristor is a new and powerful tool in the device modeling. Indeed a new model of bipolar junction transistors that I will give just below somehow justifies this idea.

CHAPTER VI

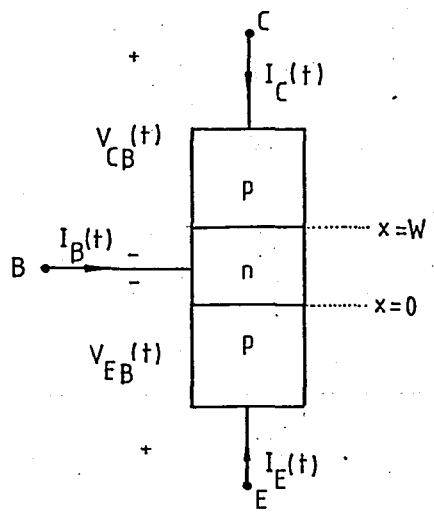
A MODEL OF THE BIPOLAR JUNCTION TRANSISTOR USING MEMRISTORS

In this chapter, a new model of the bipolar junction transistor using memristors will be given; this model will also illustrate the use of memristors in device modeling.

First, some preliminary studies of the device physics will be presented, then the new model will be given and justified.

VI.1- PRELIMINARY STUDIES.

Let us consider a one-dimensional p-n-p transistor with uniform equilibrium hole density concentration p_n in the base region. Further



let's assume that the hole diffusion current is large in comparison with the hole drift current in the base region (low-injection level case). In that case the hole density concentration p in the base region satisfies hole diffusion equation which may be written as follows [21].

Figure VI-1.

$$\frac{\partial p}{\partial t} = - \frac{(p-p_n)}{\tau_p} + D_p \frac{\partial^2 p}{\partial x^2} \tag{VI.1}$$

Where τ_p is the hole lifetime, D_p is the hole diffusion constant and

$L_p^2 = D_p \tau_p$ is the hole diffusion length in the base region.

The hole density concentrations at $x=0$ and at $x=W$ are as follows

$$p(x,t) \Big|_{x=0} = p(0,t) = p_n \exp \left[\frac{eV_{EB}(t)}{kT} \right] \quad (\text{VI.2})$$

$$p(x,t) \Big|_{x=W} = p(W,t) = p_n \exp \left[\frac{eV_{CB}(t)}{kT} \right] \quad (\text{VI.3})$$

where e is the charge of electron, k is the Boltzmann's constant, T is absolute temperature in Kelvin, $V_T = \frac{kT}{e}$ is the thermal voltage and W is the width of the base region.

We also have the followings as the emitter and the collector currents.

$$I_E(t) = - eD_p A \frac{\partial p(x,t)}{\partial x} \Big|_{x=0} \quad (\text{VI.4})$$

$$I_C(t) = eD_p A \frac{\partial p(x,t)}{\partial x} \Big|_{x=W} \quad (\text{VI.5})$$

where A is the cross sectional area of the base region, $I_E(t)$ flows into the emitter and $I_C(t)$ into the collector.

Case 1:

Now let's apply a voltage $V_{EB}(t) = V_{EB} + v_{eb} e^{j\omega t}$ to the base-emitter junction and $V_{CB}(t)$ is such that the base-collector junction is reverse biased i.e $p(W,t)=0$ then for $p(0,t)$ we have

$$p(0,t) = p_n \exp \left[\frac{V_{EB}(t)}{V_T} \right] = p_n \exp \left[\frac{V_{EB}}{V_T} + \frac{v_{eb}}{V_T} e^{j\omega t} \right]$$

$$= p_n \exp \left(\frac{V_{EB}}{V_T} \right) \cdot \exp \left[\frac{v_{eb}}{V_T} e^{j\omega t} \right]$$

If v_{eb} is taken to be small compared to V_T then we have

$$p(0,t) = p_n \exp \left(\frac{V_{EB}}{V_T} \right) \cdot \left(1 + \frac{v_{eb}}{V_T} e^{j\omega t} \right)$$

$$= p_n \exp \left(\frac{V_{EB}}{V_T} \right) + p_n \frac{v_{eb}}{V_T} \exp \left(\frac{V_{EB}}{V_T} \right) \cdot e^{j\omega t} \quad (VI.6)$$

where $\exp x = 1+x$ was used for small x .

Under these boundary conditions the solution of the equation (VI.1) can be written as follows [21]

$$p(x,t) = p_n \left[\exp \left(\frac{V_{EB}}{V_T} \right) - 1 \right] \frac{\sinh \left(\frac{W-x}{L_p} \right)}{\sinh \frac{W}{L_p}} + p_n \frac{v_{eb}}{V_T} \exp \left(\frac{V_{EB}}{V_T} \right) \frac{\sinh \left(\frac{W-x}{L_{p1}} \right)}{\sinh \frac{W}{L_{p1}}} e^{j\omega t}$$

$$- p_n \frac{\sinh \frac{x}{L_p}}{\sinh \frac{W}{L_p}} + p_n \quad (VI.7)$$

where $L_p = (D_p \tau_p)^{1/2}$ and $L_{pl} = \left(\frac{D_p \tau_p}{1+j\omega \tau_p} \right)^{1/2}$

Indeed, as $p(x,t)$ satisfies both initial conditions and the differential equation then it is the solution.

Now, let's find the currents $I_E(t)$ and $I_C(t)$. From (VI.4)

$$I_E(t) = -eD_p A \left\{ \left(\frac{-1}{L_p} \right) p_n \left[\exp \left(\frac{V_{EB}}{V_T} \right) - 1 \right] \frac{\cosh \left(\frac{W-x}{L_p} \right)}{\sinh \frac{W}{L_p}} + \left(\frac{-1}{L_{pl}} \right) \exp \left(\frac{V_{EB}}{V_T} \right) p_n \frac{v_{eb}}{V_T} \right.$$

$$\left. \frac{\cosh \left(\frac{W,x}{L_{pl}} \right)}{\sinh \frac{W}{L_{pl}}} e^{j\omega t} - \frac{p_n \cosh \frac{x}{L_p}}{L_p \sinh \frac{W}{L_p}} \right\} \Big|_{x=0}$$

$$I_E(t) = \frac{eD_p A p_n \left[\exp \left(\frac{V_{EB}}{V_T} \right) - 1 \right]}{L_p \tanh \frac{W}{L_p}} + \frac{eD_p A p_n (v_{eb}/V_T) \exp \left(\frac{V_{EB}}{V_T} \right)}{L_{pl} \tanh \frac{W}{L_{pl}}} e^{j\omega t}$$

$$+ \frac{eD_p A p_n}{L_p \sinh \frac{W}{L_p}} \tag{VI.8}$$

and from (VI.5)

$$I_C(t) = - \frac{eD_p A p_n \left[\exp \left(\frac{V_{EB}}{V_T} \right) - 1 \right]}{L_p \sinh \frac{W}{L_p}} - \frac{eD_p A p_n (v_{eb}/V_T) \exp \left(\frac{V_{EB}}{V_T} \right)}{L_{pl} \sinh \frac{W}{L_{pl}}} e^{j\omega t}$$

$$= \frac{eD_p A_p n}{L_p \tanh \frac{W}{L_p}} \quad (VI.9)$$

From Kirchhoff's current law

$$-I_B(t) = \frac{eD_p A_p n \exp\left(\frac{V_{EB}}{V_T}\right) - 1}{L_p \sinh \frac{W}{L_p}} \left(\cosh \frac{W}{L_p} - 1\right) + \frac{eD_p A_p n (v_{eb}/V_T) \exp\left(\frac{V_{EB}}{V_T}\right)}{L_{pl} \sinh \frac{W}{L_{pl}}} \left(\cosh \frac{W}{L_{pl}} - 1\right)$$

$$e^{j\omega t} - \frac{eD_p A_p n}{L_p \sinh \frac{W}{L_p}} \left(\cosh \frac{W}{L_p} - 1\right) \quad (VI.10)$$

These are the steady state and periodical components of currents which are obtained from the semiconductor theory in the case, the voltage $V_{EB}(t) = V_{EB} + v_{eb} e^{j\omega t}$ is applied to the base-emitter junction, the base-collector junction is reverse biased and $v_{eb} \ll V_T$.

Case 2:

Now let

$$V_{EB}(t) = V_{EB} + v_{eb} e^{j\omega t}$$

$$V_{CB}(t) = V_{CB} + v_{cb} e^{j2\omega t} e^{j\phi}$$

and again assume that $v_{eb} \ll V_T$ and $v_{cb} \ll V_T$

Then

$$\begin{aligned}
 p(0,t) &= p_n \exp\left[\frac{V_{EB}(t)}{V_T}\right] \\
 &= p_n \exp\left[\frac{V_{EB}}{V_T} + \frac{v_{eb}}{V_T} e^{j\omega t}\right] = p_n \exp\left(-\frac{V_{EB}}{V_T}\right) \exp\left(\frac{v_{eb}}{V_T} e^{j\omega t}\right) \\
 &= p_n \exp\left(\frac{V_{EB}}{V_T}\right) \cdot \left(1 + \frac{v_{eb}}{V_T} e^{j\omega t}\right) \tag{VI.11}
 \end{aligned}$$

Similarly

$$p(W,t) = p_n \exp\left(\frac{V_{CB}}{V_T}\right) \left(1 + \frac{v_{cb}}{V_T} e^{j\omega t}\right) \tag{VI.12}$$

And the solution of the time-dependent diffusion equation (VI.1) subject to these conditions is

$$\begin{aligned}
 p(x,t) &= p_n \left[\exp\left(\frac{V_{EB}}{V_T}\right) - 1 \right] \frac{\sinh\left(\frac{W-x}{L_p}\right)}{\sinh\frac{W}{L_p}} + p_n \left[\exp\left(\frac{V_{CB}}{V_T}\right) - 1 \right] \frac{\sinh\frac{x}{L_p}}{\sinh\frac{W}{L_p}} \\
 &+ p_n \exp\left(\frac{V_{EB}}{V_T}\right) \cdot \left(\frac{v_{eb}}{V_T}\right) \frac{\sinh\left(\frac{W-x}{L_{p1}}\right)}{\sinh\frac{W}{L_{p1}}} e^{j\omega t}
 \end{aligned}$$

$$+ p_n \exp\left(-\frac{V_{CB}}{V_T}\right) (v_{cb}/V_T) \frac{\sinh \frac{x}{L_{p2}}}{\sinh \frac{W}{L_{p2}}} e^{j2\omega t} \cdot e^{j\phi} + p_n \quad (\text{VI.13})$$

where $L_p = (D_p \tau_p)^{1/2}$, $L_{p1} = \left(\frac{D_p \tau_p}{1+j\omega\tau_p}\right)^{1/2}$, $L_{p2} = \left(\frac{D_p \tau_p}{1+j2\omega\tau_p}\right)^{1/2}$

The emitter current from (VI.4)

$$I_E(t) = \frac{e D_p A p_n \left[\exp\left(\frac{V_{EB}}{V_T}\right) - 1\right]}{L_p \tanh \frac{W}{L_p}} - \frac{e D_p A p_n \left[\exp\left(\frac{V_{CB}}{V_T}\right) - 1\right]}{L_p \sinh \frac{W}{L_p}} \quad (\text{VI.14})$$

$$+ \frac{e D_p A p_n \exp\left(-\frac{V_{EB}}{V_T}\right) (v_{eb}/V_T)}{L_{p1} \tanh \frac{W}{L_{p1}}} e^{j\omega t} - \frac{e D_p A p_n \exp\left(-\frac{V_{CB}}{V_T}\right) (v_{cb}/V_T)}{L_{p2} \sinh \frac{W}{L_{p2}}} e^{j2\omega t} e^{j\phi}$$

and the collector current form (VI.15)

$$I_C(t) = \frac{e D_p A p_n \left[\exp\left(\frac{V_{EB}}{V_T}\right) - 1\right]}{L_p \sinh \frac{W}{L_p}} + \frac{e D_p A p_n \left[\exp\left(\frac{V_{CB}}{V_T}\right) - 1\right]}{L_p \tanh \frac{W}{L_p}} \quad (\text{VI.15})$$

$$- \frac{e D_p A p_n \exp\left(\frac{V_{EB}}{V_T}\right) (v_{eb}/V_T)}{L_{p1} \sinh \frac{W}{L_{p1}}} e^{j\omega t} + \frac{e D_p A p_n \exp\left(-\frac{V_{CB}}{V_T}\right) (v_{cb}/V_T)}{L_{p2} \tanh \frac{W}{L_{p2}}} e^{j2\omega t} e^{j\phi}$$

Case 3:

Now the following more general case will be considered.

$$V_{EB}(t) = V_{EB} + v_{e1} e^{j\omega_1 t} + v_{e2} e^{j\omega_2 t}$$

$$V_{CB}(t) = V_{CB} + v_{c1} e^{j\omega_3 t} + v_{c2} e^{j\omega_4 t}$$

Where the conditions $v_{e1} \ll V_T$, $v_{e2} \ll V_T$, $v_{c1} \ll V_T$ and $v_{c2} \ll V_T$ don't hold.

Then

$$p(0,t) = p_n \exp \left[\frac{V_{EB}(t)}{V_T} \right]$$

$$= p_n \exp \left[\frac{V_{EB}}{V_T} + \frac{v_{e1}}{V_T} e^{j\omega_1 t} + \frac{v_{e2}}{V_T} e^{j\omega_2 t} \right]$$

$$= p_n \exp \left(\frac{V_{EB}}{V_T} \right) \exp \left[\frac{v_{e1}}{V_T} e^{j\omega_1 t} \right] \exp \left[\frac{v_{e2}}{V_T} e^{j\omega_2 t} \right]$$

$$= p_n \exp \left(\frac{V_{EB}}{V_T} \right) \left\{ 1 + \frac{v_{e1}}{V_T} e^{j\omega_1 t} + \frac{1}{2!} \left(\frac{v_{e1}}{V_T} \right)^2 e^{j2\omega_1 t} + \dots \right\} \left\{ 1 + \frac{v_{e2}}{V_T} e^{j\omega_2 t} + \frac{1}{2!} \left(\frac{v_{e2}}{V_T} \right)^2 e^{j2\omega_2 t} + \dots \right\}$$

$$= p_n \exp\left(-\frac{V_{EB}}{V_T}\right) \cdot \left\{ \sum_{k_1=0}^{n_1} \sum_{k_2=0}^{n_2} \frac{1}{k_1! k_2!} \left(\frac{v_{e1}}{V_T}\right)^{k_1} \left(\frac{v_{e2}}{V_T}\right)^{k_2} e^{j(k_1 w_1 + k_2 w_2)t} \right\} \quad (\text{VI.16})$$

and similarly

$$p(W,t) = p_n \exp\left(-\frac{V_{CB}}{V_T}\right) \left\{ \sum_{r_1=0}^{m_1} \sum_{r_2=0}^{m_2} \frac{1}{r_1! r_2!} \left(\frac{v_{c1}}{V_T}\right)^{r_1} \left(\frac{v_{c2}}{V_T}\right)^{r_2} e^{j(r_1 w_3 + r_2 w_4)t} \right\} \quad (\text{VI.17})$$

are obtained, where n_1, n_2, m_1, m_2 must in fact be infinite and w_1, w_2, w_3, w_4 are not restricted but positive.

Then the steady-state, periodic solution of the equation (VI.1) subject to the above conditions

$$p(x,t) = p_n \exp\left(-\frac{V_{EB}}{V_T}\right) \left\{ \sum_{k_1=0}^{n_1} \sum_{k_2=0}^{n_2} \frac{1}{k_1! k_2!} \left(\frac{v_{e1}}{V_T}\right)^{k_1} \left(\frac{v_{e2}}{V_T}\right)^{k_2}$$

$$\frac{\sinh\left[\frac{W-x}{L_p} [1 + j(k_1 w_1 + k_2 w_2) \tau_p]^{1/2}\right]}{\sinh\left[\frac{W}{L_p} [1 + j(k_1 w_1 + k_2 w_2) \tau_p]^{1/2}\right]} \cdot e^{j(k_1 w_1 + k_2 w_2)t} \right\}$$

$$+ p_n \exp\left(-\frac{V_{CB}}{V_T}\right) \left\{ \sum_{r_1=0}^{m_1} \sum_{r_2=0}^{m_2} \frac{1}{r_1! r_2!} \left(\frac{v_{c1}}{V_T}\right)^{r_1} \left(\frac{v_{c2}}{V_T}\right)^{r_2}$$

$$\frac{\sinh \frac{x}{L_p} [1+j(r_1 w_3+r_2 w_4) \frac{z}{p}]^{1/2}}{\sinh \frac{W}{L_p} [1+j(r_1 w_3+r_2 w_4) \frac{z}{p}]^{1/2}} \cdot e^{j(r_1 w_3+r_2 w_4)t}$$

$$-p_n \frac{\sinh \frac{W-x}{L_p}}{\sinh \frac{W}{L_p}} \quad -p_n \frac{\sinh \frac{x}{L_p}}{\sinh \frac{W}{L_p}} + p_n \quad (VI.18)$$

is obtained. Then the emitter current

$$I_E(t) = e D_p A p_n \exp\left(\frac{V_{EB}}{V_T}\right) \left\{ \sum_{k_1=0}^{n_1} \sum_{k_2=0}^{n_2} \frac{1}{k_1! k_2!} \left(\frac{v_{e1}}{V_T}\right)^{k_1} \left(\frac{v_{e2}}{V_T}\right)^{k_2} \right.$$

$$\left. \frac{[1+j(k_1 w_1+k_2 w_2) \frac{z}{p}]^{1/2}}{L_p \tanh \frac{W}{L_p} [1+j(k_1 w_1+k_2 w_2) \frac{z}{p}]^{1/2}} \cdot e^{j(k_1 w_1+k_2 w_2)t} \right\}$$

$$-e D_p A p_n \exp\left(\frac{V_{CB}}{V_T}\right) \left\{ \sum_{r_1=0}^{m_1} \sum_{r_2=0}^{m_2} \frac{1}{r_1! r_2!} \left(\frac{v_{c1}}{V_T}\right)^{r_1} \left(\frac{v_{c2}}{V_T}\right)^{r_2} \right.$$

$$\left. \frac{[1+j(r_1 w_3+r_2 w_4) \frac{z}{p}]^{1/2}}{L_p \sinh \frac{W}{L_p} [1+j(r_1 w_3+r_2 w_4) \frac{z}{p}]^{1/2}} \cdot e^{j(r_1 w_3+r_2 w_4)t} \right\}$$

$$- \frac{eD_p A p_n}{L_p \tanh \frac{W}{L_p}} + \frac{eD_p A p_n}{L_p \sinh \frac{W}{L_p}} \quad (VI.19)$$

and similarly the collector current

$$I_C(t) = -eD_p A p_n \exp\left(\frac{V_{EB}}{V_T}\right) \left\{ \sum_{k_1=0}^{n_1} \sum_{k_2=0}^{n_2} \frac{1}{k_1! k_2!} \left(\frac{v_{e1}}{V_T}\right)^{k_1} \left(\frac{v_{e2}}{V_T}\right)^{k_2}$$

$$\frac{[1+j(k_1 w_1 + k_2 w_2) \frac{z}{L_p}]^{1/2}}{L_p \sinh[1+j(k_1 w_1 + k_2 w_2) \frac{z}{L_p}]^{1/2}} e^{j(k_1 w_1 + k_2 w_2)t} \right\}$$

$$+ eD_p A p_n \exp\left(\frac{V_{CB}}{V_T}\right) \left\{ \sum_{r_1=0}^{m_1} \sum_{r_2=0}^{m_2} \frac{1}{r_1! r_2!} \left(\frac{v_{c1}}{V_T}\right)^{r_1} \left(\frac{v_{c2}}{V_T}\right)^{r_2}$$

$$\frac{[1+j(r_1 w_3 + r_2 w_4) \frac{z}{L_p}]^{1/2}}{L_p \tanh \frac{W}{L_p} [1+j(r_1 w_3 + r_2 w_4) \frac{z}{L_p}]^{1/2}} e^{j(r_1 w_3 + r_2 w_4)t} \right\}$$

$$+ \frac{eD_p A p_n}{L_p \sinh \frac{W}{L_p}} - \frac{eD_p A p_n}{L_p \tanh \frac{W}{L_p}} \quad (VI.20)$$

What is done so far is finding the theoretic, steady-state, periodic currents for different applied voltages.

Now the model for a p-n-p transistor will be given. The inspiration for this choice of the model is explained in the section VI-2.

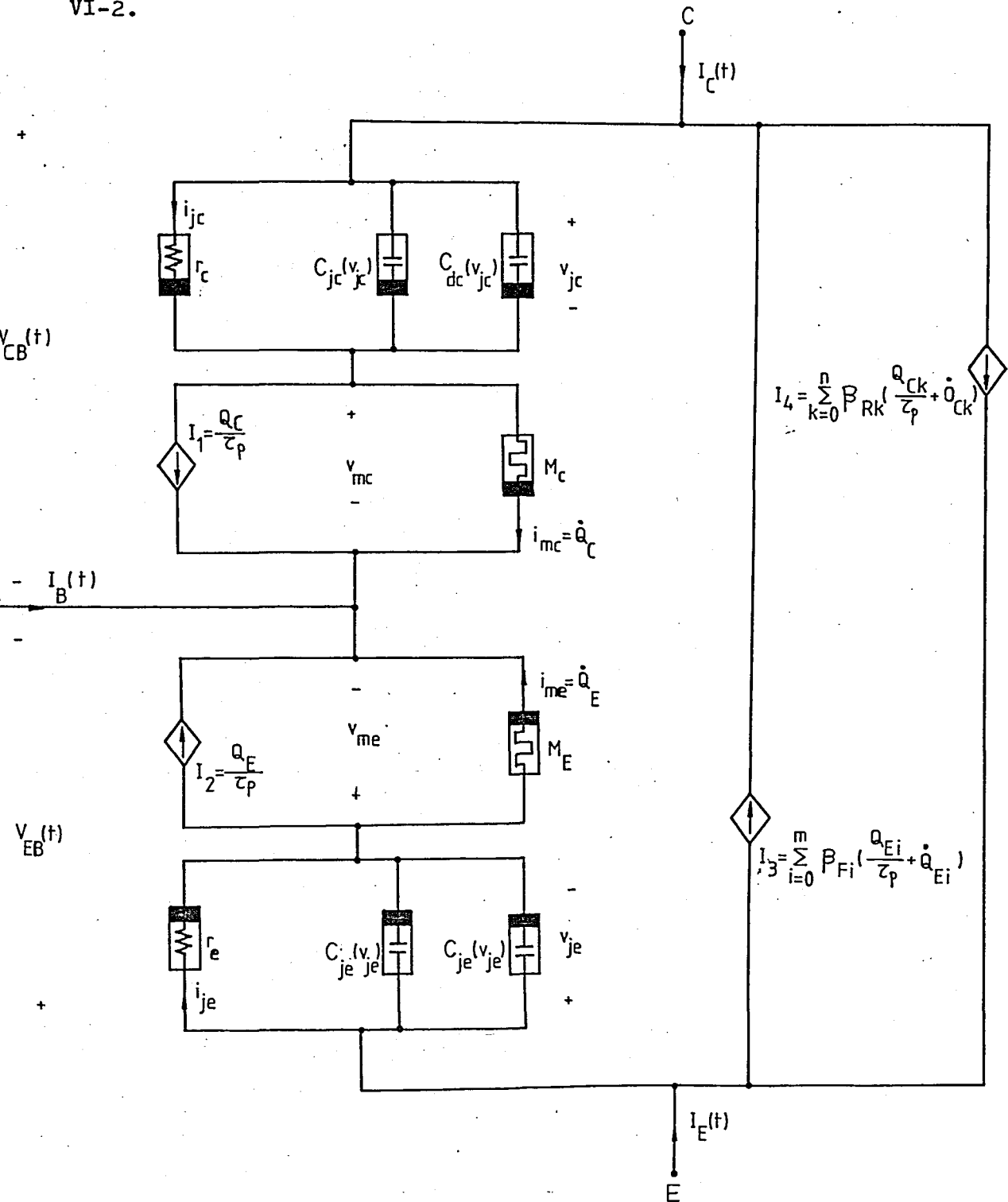


Figure VI.1

VI.2- CONSTRUCTION OF THE MODEL.

While constructing the model in Figure VI.1 a) the memristive circuit model for p-n junction diodes given by Leon O. Chua and Chong-Wei Tseng[14], b) the charge controlled transistor model given by Randal W. Jensen[22], c) the Ebers-Moll model of the transistor[23] have been a source of inspiration and motivation.

By considering the first two models and thinking that there exist two p-n junctions in a transistor, base-emitter and base-collector parts have been constructed based on the Ebers-Moll model. In the definition of the dependent current sources placed between collector and emitter the second and the third models and the previous theoretic study have been used.

In the model, the memristors M_C and M_E are used to simulate the conductivity modulation phenomena; C_{je} , C_{jc} represent the junction capacitances of base-emitter and base-collector junctions respectively; C_{de} , C_{dc} represent the diffusion capacitances of the emitter and collector regions; the dependent current sources I_1 and I_2 represent the recombination of the carriers.

Now the parameters and the quantities used in the model will be defined.

$Q_T(t)$ is the total excess hole charge stored in the base region.

$$Q_T(t) = eA \int_0^W p'(x,t) dx \quad (VI.21)$$

$Q_E(t)$ is the total excess hole charge stored in the base when $V_{CB}(t)=0$ and $Q_C(t)$ is the total excess hole charge stored in the base when $V_{EB}(t)=0$. When both voltages are different from zero, total excess hole charge stored in the base is

$$Q_T(t) = Q_E(t) + Q_C(t) \quad (VI.22)$$

As seen from the previous study in section VI.1, $p(x,t)$ contains some frequency components.

Thus, the same frequency components will come into the expression for $Q_T(t)$, i.e

$$Q_T(t) = \sum_{i=0}^m Q_{Ei}(t) + \sum_{k=0}^n Q_{CK}(t)$$

or

$$Q_E(t) = \sum_{i=0}^m Q_{Ei}(t) \text{ and } Q_C(t) = \sum_{k=0}^n Q_{CK}(t) \quad (\text{VI.23})$$

The β 's appearing in the expression of the dependent current sources I_3 and I_4 are defined as follows,

$$\beta_{Fi} = \frac{1}{\cosh \frac{w_i}{L_p} [1 + jw_i \tau_p]^{1/2} - 1} \quad (\text{VI.24})$$

where w_i is the frequency of $Q_{Ei}(t)$ and

$$\beta_{Rk} = \frac{1}{\cosh \frac{w_k}{L_p} [1 + jw_k \tau_p]^{1/2} - 1} \quad (\text{VI.25})$$

w_k is the frequency of $Q_{CK}(t)$.

The memristor M_E and M_C may be defined as follows. The conductivity of the base region is

$$\sigma(x) = e \left[\mu_n n_{no} + \mu_p p(x) \right] \quad (\text{VI.26})$$

$$M_E = \frac{1}{A} \int_0^W \frac{dx}{\left[\frac{V(x)}{V_{CB=0}} \right]} = \frac{1}{A} \int_0^W \frac{dx}{e^{[\mu_n n_{no} + \mu_p p(x)]} \left[\frac{V(x)}{V_{CB=0}} \right]} \quad (\text{VI.27})$$

$$M_C = \frac{1}{A} \int_0^W \frac{dx}{\left[\frac{V(x)}{V_{EB=0}} \right]} = \frac{1}{A} \int_0^W \frac{dx}{e^{[\mu_n n_{no} + \mu_p p(x)]} \left[\frac{V(x)}{V_{EB=0}} \right]} \quad (\text{VI.28})$$

The other circuit elements are defined as follows [23],[21]

$$C_{je}(v_{je}) = C_{jeo} \left(1 - \frac{v_{je}}{\phi_E}\right)^{-1/2} \quad (\text{VI.29})$$

$$C_{jc}(v_{jc}) = C_{jco} \left(1 - \frac{v_{jc}}{\phi_C}\right)^{-1/2} \quad (\text{VI.30})$$

$$C_{de}(v_{je}) = k_1 \frac{\tau_F I_{s1}}{V_T} \exp\left(\frac{v_{je}}{V_T}\right) \quad (\text{VI.31})$$

$$C_{dc}(v_{jc}) = k_2 \frac{\tau_R I_{s2}}{V_T} \exp\left(\frac{v_{jc}}{V_T}\right) \quad (\text{VI.32})$$

$$r_e : i_{je} = I_{s1} \left[\exp\left(\frac{v_{je}}{V_T}\right) - 1 \right] \quad (\text{VI.33})$$

$$r_c : i_{jc} = I_{s2} \left[\exp\left(\frac{v_{jc}}{V_T}\right) - 1 \right] \quad (\text{VI.34})$$

VI.3- JUSTIFICATION OF THE MODEL.

As a first confirmation of the model it will be shown that the base current given by the model is the same as the one obtained theoretically.

The base current given by the model is

$$I_B(t) = - \frac{Q_c}{\tau_p} - \dot{Q}_c - \frac{Q_E}{\tau_p} - \dot{Q}_E \quad (\text{VI.35})$$

Since $Q_E + Q_C = Q_T$

$$I_B(t) = - \frac{Q_T}{\tau_p} - \dot{Q}_T \quad (\text{VI.36})$$

is obtained.

Now let's consider the diffusion equation (VI.1). The excess hole concentration is $p'(x,t) \triangleq p(x,t) - p_n$ and using this definition, equation (VI.1) becomes

$$\frac{\partial p'(x,t)}{\partial t} = - \frac{p'(x,t)}{\tau_p} + D_p \frac{\partial^2 p'(x,t)}{\partial x^2} \quad (\text{VI.37})$$

Multiplying both sides with the constant eA and integrating from 0 to W with respect to x

$$eA \int_0^W \frac{\partial p'(x,t)}{\partial t} dx = -eA \int_0^W \frac{p'(x,t)}{\tau_p} dx + eA \int_0^W D_p \frac{\partial^2 p'(x,t)}{\partial x^2} dx$$

$$\frac{\partial}{\partial t} \int eAp'(x,t)dx = -\frac{1}{\tau_p} \int eAp'(x,t)dx + eAD_p \left. \frac{\partial p'(x,t)}{\partial x} \right|_0^W \quad (\text{VI.38})$$

results; but the term $\int_0^W eAp'(x,t)dx$ is the total excess stored hole charge $Q_T(t)$ in the base region and hence

$$\frac{\partial}{\partial t} Q_T(t) = -\frac{1}{\tau_p} Q_T(t) + eAD_p \left. \frac{\partial p'(x,t)}{\partial x} \right|_{x=W} - eAD_p \left. \frac{\partial p'(x,t)}{\partial x} \right|_{x=0} \quad (\text{VI.39})$$

On the other hand, as $eAD_p \left. \frac{\partial p'(x,t)}{\partial x} \right|_{x=W} = I_C(t)$ and $-eAD_p \left. \frac{\partial p'(x,t)}{\partial x} \right|_{x=0} =$

$I_E(t)$ it follows from equation (VI.39) that

$$\frac{\partial}{\partial t} Q_T(t) + \frac{1}{\tau_p} Q_T(t) = I_C(t) + I_E(t) \quad (\text{VI.40})$$

Since $I_B(t) + I_C(t) + I_E(t) = 0$ by KCL, then

$$I_b(t) = -\frac{\partial}{\partial t} Q_T(t) - \frac{1}{\tau_p} Q_T(t) = -\dot{Q}_T(t) - \frac{1}{\tau_p} Q_T(t) \quad (\text{VI.41})$$

which is as given by the model.

Now the expressions of collector and emitter currents given by the model for different applied voltages will be written.

Let's consider case 1 studied in section VI.1. For this case $p(x,t)$ is given by the equation (VI.7) as

$$p(x,t) = p_n \left[\exp\left(\frac{V_{EB}}{V_T}\right) - 1 \right] \frac{\sinh\left(\frac{W-x}{L_p}\right)}{\sinh\left(\frac{W}{L_p}\right)} + p_n \frac{v_{eb}}{V_T} \exp\left(\frac{V_{EB}}{V_T}\right)$$

$$\frac{\sinh\left(\frac{W-x}{L_{pl}}\right)}{\sinh\left(\frac{W}{L_{pl}}\right)} e^{j\omega t} - p_n \frac{\sinh\left(\frac{x}{L_p}\right)}{\sinh\left(\frac{W}{L_p}\right)} + p_n$$

Then from equation (VI.21) the total excess stored hole charge will be found as follows

$$Q_T(t) = eA \int_0^W p(x,t) dx$$

$$Q_T(t) = \frac{eA p_n \left[\exp\left(\frac{V_{EB}}{V_T}\right) - 1 \right] L_p \left(\cosh\left(\frac{W}{L_p}\right) - 1 \right)}{\sinh\left(\frac{W}{L_p}\right)}$$

$$+ \frac{eA (v_{eb}/V_T) p_n \exp\left(\frac{V_{EB}}{V_T}\right) L_{pl} \left(\cosh\left(\frac{W}{L_{pl}}\right) - 1 \right)}{\sinh\left(\frac{W}{L_{pl}}\right)} e^{j\omega t}$$

$$-\frac{eA p_n L_p (\cosh \frac{W}{L_p} - 1)}{\sinh \frac{W}{L_p}} \quad (\text{VI.42})$$

Then

$$Q_{CO} = -\frac{eA p_n L_p (\cosh \frac{W}{L_p} - 1)}{\sinh \frac{W}{L_p}} \quad (\text{VI.43})$$

$$Q_{EO} = \frac{eA p_n [\exp(\frac{V_{EB}}{V_T}) - 1] L_p (\cosh \frac{W}{L_p} - 1)}{\sinh \frac{W}{L_p}} \quad (\text{VI.44})$$

$$Q_{E1} = \frac{eA (v_{eb}/V_T) p_n \exp(\frac{V_{EB}}{V_T}) L_{p1} (\cosh \frac{W}{L_{p1}} - 1)}{\sinh \frac{W}{L_{p1}}} e^{j\omega t} \quad (\text{VI.45})$$

where $L_{p1} = \frac{L_p}{(1+j\omega \tau_p)^{1/2}}$. On the other hand, the emitter current can

be obtained from the model as

$$I_E = \frac{Q_E}{p} + \dot{Q}_E + \beta_{FO} \left(\frac{Q_{EO}}{\tau_p} + \dot{Q}_{EO} \right) + \beta_{F1} \left(\frac{Q_{E1}}{\tau_p} + \dot{Q}_{E1} \right) - \beta_{RO} \left(\frac{Q_{CO}}{\tau_p} + \dot{Q}_{CO} \right)$$

(VI.46)

where

$$\beta_{FO} = \beta_{RO} = \frac{1}{\cosh \frac{W}{L_p} - 1} \quad \text{and} \quad \beta_{F1} = \frac{1}{\cosh \frac{W}{L_p} (1+jw\tau_p)^{1/2} - 1}$$

Arranging the terms of equation (VI.46) we find

$$I_E = (1+\beta_{FO}) \frac{Q_{EO}}{\tau_p} + (1+\beta_{F1}) \left(\frac{1}{p} + jw \right) Q_{E1} - \beta_{RO} \frac{Q_{CO}}{\tau_p} \quad (\text{VI.47})$$

And calculating the parameters $(\beta_{FO}+1)$ and $(\beta_{F1}+1)$

$$\beta_{FO}+1 = \frac{1}{\cosh \frac{W}{L_p} - 1} + 1 = \frac{\cosh \frac{W}{L_p}}{\cosh \frac{W}{L_p} - 1}$$

$$\beta_{F1}+1 = \frac{1}{\cosh \frac{W}{L_p} (1+jw\tau_p)^{1/2} - 1} + 1 = \frac{\cosh \frac{W}{L_p} (1+jw\tau_p)^{1/2}}{\cosh \frac{W}{L_p} (1+jw\tau_p)^{1/2} - 1}$$

are obtained. Substitution of these parameter into equation (VI.47) yield

$$I_E = \frac{eA_p n \left[\exp\left(\frac{V_{EB}}{V_T}\right) - 1 \right] L_p \cosh \frac{W}{L_p}}{\tau_p \sinh \frac{W}{L_p}} \quad (\text{VI.48})$$

$$+ \frac{eA_p n_{eb} (v_{eb}/V_T) \exp\left(\frac{V_{EB}}{V_T}\right) (1+jw\tau_p) L_{pl} \cosh \frac{W}{L_{pl}}}{\tau_p \sinh \frac{W}{L_{pl}}} e^{jwt} + \frac{eA_p n_p L_p}{\tau_p \sinh \frac{W}{L_p}}$$

Using now $L_p^2 = D_p \tau_p$ and $L_{pl}^2 = \frac{D_p \tau_p}{1+jw\tau_p}$ the final expression for I_E is obtained as

$$I_E = \frac{eAD_p n_p \left[\exp\left(\frac{V_{EB}}{V_T}\right) - 1 \right]}{L_p \tanh \frac{W}{L_p}} + \frac{eAD_p n_p (v_{eb}/V_T) \exp\left(\frac{V_{EB}}{V_T}\right)}{L_{pl} \tanh \frac{W}{L_{pl}}} e^{jwt} + \frac{eAD_p n_p}{L_p \sinh \frac{W}{L_p}}$$

(VI.49)

which agrees with expression (VI.8) for I_E as developed from the diffusion equation (VI.1).

Similarly, the collector current I_C calculated from the model agrees with equation (VI.9) as shown below. The collector current from the model can be written as

$$I_c = \frac{Q_c}{\tau_p} + \dot{Q}_c + \beta_{RO} \left(\frac{Q_{co}}{\tau_p} + \dot{Q}_{co} \right) - \beta_{FO} \left(\frac{Q_{EO}}{\tau_p} + \dot{Q}_{EO} \right) - \beta_{FL} \left(\frac{Q_{E1}}{\tau_p} + \dot{Q}_{E1} \right)$$

$$= (1 + \beta_{RO}) \frac{Q_{co}}{\tau_p} - \beta_{FO} \frac{Q_{EO}}{\tau_p} - \beta_{FL} \frac{(1+jw\tau_p)}{\tau_p} Q_{E1} \quad (VI.50)$$

Substituting the expressions of β_{RO} , β_{FO} , β_{FL} and Q_{CO} , Q_{EO} , Q_{EL} into (VI.50) yield

$$I_c = - \frac{eA p_n L_p \cosh \frac{W}{L_p}}{z_p \sinh \frac{W}{L_p}} - \frac{eA p_n [\exp(\frac{V_{EB}}{V_T}) - 1] L_p}{z_p \sinh \frac{W}{L_p}}$$

$$- \frac{(1+j\omega_p) eA p_n (v_{eb}/V_T) \exp(\frac{V_{EB}}{V_T}) L_{pl}}{z_p \sinh \frac{W}{L_{pl}}} e^{j\omega t} \tag{VI.51}$$

and using $L_p^2 = D_p z_p$ and $L_{pl}^2 = \frac{D_p z_p}{1+j\omega z_p}$

$$I_c = - \frac{eA p_n D_p}{L_p \tanh \frac{W}{L_p}} - \frac{eA p_n D_p [\exp(\frac{V_{EB}}{V_T}) - 1]}{L_p \sinh \frac{W}{L_p}}$$

$$- \frac{eA D_p p_n (v_{eb}/V_T) \exp(\frac{V_{EB}}{V_T})}{L_{pl} \sinh \frac{W}{L_{pl}}} e^{j\omega t} \tag{VI.52}$$

is obtained.

For case 2, $p(x,t)$ is given in equation (VI.13). Then, the total excess hole stored charge in the base region becomes

$$Q_T = eA \int_0^W p'(x, t) dx$$

$$Q_T = \frac{eA p_n \left[\exp\left(\frac{V_{EB}}{V_T}\right) - 1 \right] L_p \left(\cosh \frac{W}{L_p} - 1 \right)}{\sinh \frac{W}{L_p}} + \frac{eA p_n \left[\exp\left(\frac{V_{CB}}{V_T}\right) - 1 \right] L_p \left(\cosh \frac{W}{L_p} - 1 \right)}{\sinh \frac{W}{L_p}}$$

$$+ \frac{eA p_n \exp\left(\frac{V_{EB}}{V_T}\right) (v_{eb}/V_T) L_{p1} \left(\cosh \frac{W}{L_{p1}} - 1 \right)}{\sinh \frac{W}{L_{p1}}} e^{j\omega t} \quad (VI.53)$$

$$+ \frac{eA p_n \exp\left(\frac{V_{CB}}{V_T}\right) (v_{cb}/V_T) L_{p2} \left(\cosh \frac{W}{L_{p2}} - 1 \right)}{\sinh \frac{W}{L_{p2}}} e^{j2\omega t} \cdot e^{j\phi}$$

The components of Q_T are as follows.

$$Q_{EO} = \frac{eA p_n \left[\exp\left(\frac{V_{EB}}{V_T}\right) - 1 \right] L_p \left(\cosh \frac{W}{L_p} - 1 \right)}{\sinh \frac{W}{L_p}} \quad (VI.54)$$

$$Q_{E1} = \frac{eA p_n \exp\left(\frac{V_{EB}}{V_T}\right) (v_{eb}/V_T) L_{p1} \left(\cosh \frac{W}{L_{p1}} - 1 \right)}{\sinh \frac{W}{L_{p1}}} e^{j\omega t} \quad (VI.55)$$

$$Q_{CO} = \frac{eA p_n \left[\exp\left(\frac{V_{CB}}{V_T}\right) - 1 \right] L_p \left(\cosh \frac{W}{L_p} - 1 \right)}{\sinh \frac{W}{L_p}} \quad (\text{VI.56})$$

$$Q_{C1} = \frac{eA p_n \exp\left(\frac{V_{CB}}{V_T}\right) (v_{cb}/V_T) L_{p2} \left(\cosh \frac{W}{L_{p2}} - 1 \right) e^{j2\omega t} e^{j\phi}}{\sinh \frac{W}{L_{p2}}} \quad (\text{VI.57})$$

Now let's find the currents.

$$I_E = \frac{Q_E}{\tau_p} + \dot{Q}_E + \beta_{FO} \left(\frac{Q_{EO}}{\tau_p} + \dot{Q}_{EO} \right) + \beta_{F1} \left(\frac{Q_{E1}}{\tau_p} + \dot{Q}_{E1} \right)$$

$$- \beta_{RO} \left(\frac{Q_{CO}}{\tau_p} + \dot{Q}_{CO} \right) - \beta_{R1} \left(\frac{Q_{C1}}{\tau_p} + \dot{Q}_{C1} \right)$$

$$= (1 + \beta_{FO}) \frac{Q_{EO}}{\tau_p} + (1 + j\omega\tau_p)(1 + \beta_{F1}) \frac{Q_{E1}}{\tau_p} - \beta_{RO} \frac{Q_{CO}}{\tau_p} - (1 + j2\omega\tau_p)\beta_{R1} \frac{Q_{C1}}{\tau_p}$$

(VI.58)

Substituting the equations (VI.24), (VI.25), (VI.54)-(VI.57) into the equation (VI.58) and making necessary algebraic manipulations we get

$$\begin{aligned}
 I_E = & \frac{eAD_p p_n \left[\exp\left(\frac{V_{EB}}{V_T}\right) - 1 \right] \cosh \frac{W}{L_p}}{L_p \sinh \frac{W}{L_p}} - \frac{eAD_p p_n \left[\exp\left(\frac{V_{CB}}{V_T}\right) - 1 \right]}{L_p \sinh \frac{W}{L_p}} \\
 & + \frac{eAD_p p_n \exp\left(\frac{V_{EB}}{V_T}\right) (v_{eb}/V_T) \cosh \frac{W}{L_{p1}}}{L_{p1} \sinh \frac{W}{L_{p1}}} e^{j\omega t} \\
 & - \frac{eAD_p p_n \exp\left(\frac{V_{CB}}{V_T}\right) (v_{cb}/V_T)}{L_{p2} \sinh \frac{W}{L_{p2}}} e^{j2\omega t} e^{j\phi}
 \end{aligned} \tag{VI.59}$$

Where $L_p^2 = D_p z_p^2$, $L_{p1}^2 = \frac{D_p z_p^2}{(1+j\omega z_p)}$, $L_{p2}^2 = \frac{D_p z_p^2}{(1+j2\omega z_p)}$

Similarly,

$$\begin{aligned}
 I_C = & \frac{Q_C}{z_p} + \dot{Q}_C + \beta_{RO} \left(\frac{Q_{CO}}{z_p} + \dot{Q}_{CO} \right) + \beta_{R1} \left(\frac{Q_{C1}}{z_p} + \dot{Q}_{C1} \right) \\
 & - \beta_{FO} \left(\frac{Q_{EO}}{z_p} + \dot{Q}_{EO} \right) - \beta_{F1} \left(\frac{Q_{E1}}{z_p} + \dot{Q}_{E1} \right)
 \end{aligned}$$

$$= (1 + \beta_{RO}) \frac{Q_{CO}}{z_p} + (1 + 2jwz_p)(1 + \beta_{R1}) \frac{Q_{E1}}{z_p} - \beta_{FO} \frac{Q_{EO}}{z_p} - (1 + jwz_p) \beta_{F1} \frac{Q_{E1}}{z_p}$$

(VI.60)

and going through the same algebra as for I_E we get the following expression for I_c .

$$I_c = \frac{eAD_{p_n} [\exp(\frac{V_{CB}}{V_T}) - 1] \cosh \frac{W}{L_p}}{L_p \sinh \frac{W}{L_p}} - \frac{eAD_{p_n} [\exp(\frac{V_{EB}}{V_T}) - 1]}{L_p \sinh \frac{W}{L_p}}$$

$$+ \frac{eAD_{p_n} \exp(\frac{V_{CB}}{V_T}) (v_{cb}/V_T) \cosh \frac{W}{L_{p2}}}{L_{p2} \sinh \frac{W}{L_{p2}}} e^{j2wt} e^{j\phi}$$

$$- \frac{eAD_{p_n} \exp(\frac{V_{EB}}{V_T}) (v_{eb}/V_T)}{L_{p1} \sinh \frac{W}{L_{p1}}} e^{jwt}$$

(VI.61)

Again we see that the expressions (VI.59) and (VI.61) are identical with expressions (VI.14) and (VI.15).

Here, it should be observed that when the applied voltages are pure dc voltages (i.e. $v_{eb} = 0$ and $v_{cb} = 0$) equations (VI.59) and (VI.61)

reduces to the well-known Ebers-Moll equations.

If the more general case 3 is considered the results of the model will again be identical with the theoretical results.

Now the following transient case will be examined.

Let a step voltage be applied to the emitter-base junction at $t=0$ and let the collector-base voltage be zero, and let the excess hole concentration at $t=0^+$ be zero. Then we have the following

$$V_{EB}(t) = c_1 U(t) , \quad V_{CB}(t) = 0$$

$$p(0,t) = p_n \exp \left[\frac{V_{EB}(t)}{V_T} \right]$$

$$p(0,t) = p_n \exp\left(\frac{c_1 t}{V_T}\right) \quad \text{for } t > 0 \quad (\text{VI.62})$$

using the definition $p'(x,t) \triangleq p(x,t) - p_n$ we obtain

$$p'(0,t) = p(0,t) - p_n = p_n \left[\exp\left(\frac{c_1 t}{V_T}\right) - 1 \right] \quad \text{for } t > 0 \quad \text{or}$$

$$p'(0,t) = k_1 U(t) \quad (\text{VI.63})$$

where

$$k_1 = p_n \left[\exp\left(\frac{c_1}{V_T}\right) - 1 \right]$$

$$p'(W,t) = p_n \exp \left[\left(\frac{V_{CB}(t)}{V_T} \right) - 1 \right] = 0 \quad (\text{VI.64})$$

$$p'(x, 0^+) = 0 \quad (\text{VI.65})$$

For these boundary and initial conditions the Laplace transform of the solution of

$$\frac{\partial p'(x, t)}{\partial t} = - \frac{p'(x, t)}{\tau_p} + D_p \frac{\partial^2 p'(x, t)}{\partial x^2} \quad \text{can be found as [24]}$$

$$p'(x, s) = \frac{k_1}{s} \frac{\sinh \frac{W-x}{L_p} \sqrt{1+s\tau_p}}{\sinh \frac{W}{L_p} \sqrt{1+s\tau_p}} \quad (\text{VI.66})$$

Then the Laplace transform of total excess hole charge stored in the base is

$$\begin{aligned} Q_T(s) &= eA \int_0^W p'(x, s) dx \\ &= eA \int_0^W \frac{k_1}{s} \frac{\sinh \frac{W-x}{L_p} \sqrt{1+s\tau_p}}{\sinh \frac{W}{L_p} \sqrt{1+s\tau_p}} dx \end{aligned}$$

$$Q_T(s) = \frac{eAL_p k_1 (\cosh \frac{W}{L_p} \sqrt{1+s\tau_p} - 1)}{s \sqrt{1+s\tau_p} \sinh \frac{W}{L_p} \sqrt{1+s\tau_p}} \quad (\text{VI.67})$$

Before proceeding further consider the currents which are given

as

$$I_E(s) = -eAD_p \left. \frac{\partial p'(x,s)}{\partial x} \right|_{x=0}$$

$$I_E(s) = \frac{eAD_p k_1 \sqrt{1+s\tau_p} \cosh \frac{W}{L_p} \sqrt{1+s\tau_p}}{L_p s \sinh \frac{W}{L_p} \sqrt{1+s\tau_p}} \quad (\text{VI.68})$$

$$I_C(s) = eAD_p \left. \frac{\partial p'(x,s)}{\partial x} \right|_{x=W}$$

$$I_C(s) = - \frac{eD_p A k_1 \sqrt{1+s\tau_p}}{L_p s \sinh \frac{W}{L_p} \sqrt{1+s\tau_p}} \quad (\text{VI.69})$$

Now, going back to the model again, $Q_T(s) = Q_E(s)$, since the collector-base junction voltage is zero implying $Q_C(s) = 0$

If $\beta_F = \frac{1}{\cosh \frac{W}{L_p} \sqrt{1+s\tau_p} - 1}$ is defined, then the model

again gives the same results as shown below.

From the model

$$I_E(t) = \frac{Q_E}{\tau_p} + \dot{Q}_E + \beta_F \left(\frac{Q_E}{\tau_p} + \dot{Q}_E \right)$$

taking the Laplace transform of both sides, assuming $Q_E(0^+) = 0$

$$I_E(s) = \frac{Q_E(s)}{z_p} + sQ_E(s) + \beta_F \left[\frac{Q_E(s)}{z_p} + sQ_E(s) \right]$$

$$= (1+s z_p) \frac{Q_E(s)}{z_p} + (1+s z_p) \beta_F \frac{Q_E(s)}{z_p}$$

$$I_E(s) = (1+\beta_F) \left(\frac{1+s z_p}{z_p} \right) Q_E(s) \tag{VI.70}$$

is obtained. Substituting the above equation which is defined for β_F and equation (VI.67) into (VI.70) we get

$$I_E(s) = \frac{e A k_1 L_p (1+s z_p) \cosh \frac{W}{L_p} \sqrt{1+s z_p}}{z_p s \sqrt{1+s z_p} \sinh \frac{W}{L_p} \sqrt{1+s z_p}}$$

and using $L_p^2 = D z_p$

$$I_E(s) = \frac{e A D k_1 \sqrt{1+s z_p} \cosh \frac{W}{L_p} \sqrt{1+s z_p}}{L_p s \sinh \frac{W}{L_p} \sqrt{1+s z_p}} \tag{VI.71}$$

is obtained.

Similarly for I_c we have

$$I_c = -\beta_F \left(\frac{Q_E}{\tau_p} + \dot{Q}_E \right) \text{ or}$$

$$I_C(s) = -\beta_F \left(\frac{Q_E(s)}{\tau_p} + sQ_E(s) \right) = -(1+s\tau_p) \frac{\beta_F(s)}{\tau_p} Q_E(s)$$

and going through the same algebra as for $I_E(s)$

$$I_c(s) = - \frac{eAD k_1 \sqrt{1+s\tau_p}}{L_p s \sinh \frac{W}{L_p} \sqrt{1+s\tau_p}} \quad (\text{VI.72})$$

is found.

VI.4- REMARKS ON THE MODEL

The model is valid as long as the diffusion equation (VI.1) is satisfied and the collector and emitter currents are given as in equations (VI.4) and (VI.5); otherwise it must be modified. For example, if there exists a contribution of electrons to the collector and emitter currents then the necessary modifications must be done to take into account the charge storage effects due to electrons.

The model is justified by comparing the terminal currents given by model with those given by the diffusion equation (VI.1). Further confirmation of the model has to be done by applying current sources and observing the resulting voltage waveforms. Computer simulated results must be compared with those obtained experimentally.

Another important point is that the small-signal input impedance seen from base-emitter terminals is inductive when the biasing current is relatively high. This behaviour must also be justified.

The model seems to be complex for analytical purposes, but it can be used in computer analysis.

Finally, the model emphasizes the use of memristors in the area of device modeling.

C H A P T E R VII

CONCLUSION

A newly introduced two-terminal nonlinear circuit element, the memristor has been defined, its properties investigated, its realization presented and its use in modeling emphasized. Although the memristor seems to be an hypothetical element, the passivity theorem and the electromagnetic interpretation given in Chapter II have led to the belief that memristors with monotonically increasing ψ - q curves may be produced in a passive physical device form.

In Chapter III the realization of memristors by active circuit elements is considered. The active circuit realization techniques may be used in studies concerning general nonlinear RLCM networks. For example, circuit-theoretic properties of RLCM networks may be justified experimentally using active circuit realization of memristors.

Then, the generalization of memristor into a new class of dynamical systems, namely memristive systems is considered in Chapter IV. Most important characteristics of memristive systems is the zero-crossing property i.e. the output is zero whenever the input is zero. Another one is the dependency of Lissajous figures on the frequency. At low frequencies they behave like nonlinear resistors but at high frequencies they reduce to linear resistors. So, special attention must be paid to the classification of the dissipative systems. Moreover memristive systems exhibit a capacitive or inductive small-signal impedance depending on the operating point which caused some authors to name this property as the anomalous impedance phenomenon [25].

In Chapter V, applications of the memristor is considered. The most important one of these applications is the model given for p-n

junction diodes. The success of this is due mainly to the use of memristor which accounts for the charge storage and conductivity modulation effects. In Chapter VI, a new model for bipolar junction transistor which uses memristors is given to emphasize the use of memristors in the area of device modeling. If we consider this model, first, it seems to be unusual to separate the total excess stored charge into its components. But, once the input voltage is given the components of charge is completely determined and the coefficients are also determined when the input is given. Moreover Ebers-Moll model of transistor is a special case of this model.

REFERENCES

1. L.O.Chua, "Memristor-the missing circuit element" IEEE Trans. Circuit Theory, vol.CT-18, pp.507-519, Sept.1971.
2. R.M.Fano,L.J.Chu, and R.B.Adler, Electromagnetic Fields, Energy, and Forces. New York: Wiley, 1960, Ch.6.
3. G.F.Oster and D.M.Auslander, "The memristor: A new bond graph element", Trans.ASME on Dynamical Syst. Meas. Cont., Vol.94, no.3, pp 249-252, 1972.
4. L.O.Chua, "Synthesis of new nonlinear network elements", Proc.IEEE, vol.56, Aug 1968, pp 1325-1340.
5. L.O.Chua, "Nonlinear circuit theory" lecture notes for EECS 223 and 225, University of California, Berkeley, Winter and Spring 1978.
6. L.O.Chua, S.M.Kang, "Memristive devices and Systems" Proc.IEEE vol.64, pp 209-223, Feb.1976.
7. M.Sapoff and R.M.Oppenheim, "Theory and application of self-heated thermistors", Proc.IEEE, Vol.51, pp 1292-1305 Oct.1963.
8. V.J.Francis, Fundamentals of Discharge Tube Circuits. London, England: Methuen, 1948.
9. A.L.Reenstra, "A low-frequency ascillator using PTC and NTC thermistors", IEEE Trans.Electron Devices, Vol.ED-16, pp 544-554, June 1969.
10. A.L.Hodgkin and A.F.Huxley,"A quantitative description of membrane current and its application to conduction in nerve", J.Physiol, vol.117 pp.500-544, 1952.
11. C.A.Desoer and J.Katzenelson, "Nonlinear RLC networks, Bell Syst. Tech. J., Vol.44 pp.161-198, Jan 1965.

12. J.L.Wyatt, Jr., L.O.Chua, J.W.Gannett, I.C.Göknar and D.Green, "Foundations of nonlinear network theory. PartI: Passivity", Electronic Research Laboratory, College of Engineering, University of California, Berkeley CA 94720, Memo. ERL M78/76, 1978.
13. S.R.Ovshinsky, "Reversible electrical switching phenomena in disordered structures", Phy.Rev.Lett., Vol.21, Nov.11, 1968, pp.1450-1453
14. L.O.Chua and C.W.Tseng, "A memristive circuit model for p-n junction diodes", Int.J.Circuit Theory and Appl., vol.2 pp.367-389, Dec.1974.
15. P.E.Gray, D.DeWitt, A.R.Boothroyd and J.F.Gibbons, Physical Electronics and Circuit Models of Transistors, Wiley, New York, 1964.
16. H.L.Armstrong, "On switching transient in the forward conduction of semiconductor diodes", IRE Trans.Electron Devices, ED-4, pp.111-113, 1957.
17. T.E.Firle and O.E.Hayes, "Some reactive effects in forward biased junctions" IRE Trans. Electron Devices, ED-6, pp.330-334, 1959.
18. I.Ladany, "An analysis of inertia inductance in a junction diode", IRE Trans.Electron Devices, ED-7, pp.303-310, 1960.
19. J.G.Linvill, "Transient response of junction diodes", IEEE Trans. Circuit Theory, CT-10 pp.191-197, 1963.
20. L.O.Chua, "Device modeling via basic nonlinear circuit elements", IEEE Trans. on Circuits and Systems, vol.CAS-27, no.11, Nov.1980.
21. Aldert Van Der Ziel, Solid State Physical Electronics, Prentice-Hall, New Delhi, 1971.
22. R.W.Jensen, "Charge control transistor model for the IBM Electronic Circuit Analysis Program", IEEE Trans.Circuit Theory, Vol.CT-13, pp.428-437, Dec.1966.
23. Ian Getreu, Modeling the Bipolar Transistor, Tektronix, Inc. Beaverton, Oregon, 1976.
24. Gustav Doetsch, Anleitung zum praktischen Gebrauch der Laplace-Transformation, R.Oldenbourg, München, 1956.
25. A.Mauro, "Anomalous impedance, a phenomenological property of time-variant resistance", Biophys.J., Vol.1, pp.353-372, 1961.